CHARACTERIZATION OF VERTICAL INFILTRATION NEAR THE WASTE ISOLATION PILOT PLANT, CARLSBAD, NEW MEXICO

By
Russell J. Vanlandingham

Thesis
Submitted in partial fullfillment of the
requirements for the degree of master of science in geology,
New Mexico Institute of Mining and Technology
Socorro, New Mexico

Geotechnical
Information Center

This thesis is accepted on behalf of the faculty of the Institute by the following committee:

Andrew R Campbell

Adviser

8-30-93

Date

ABSTRACT

The Waste Isolation Pilot Plant (WIPP) in southeastern New Mexico, is a proposed transuranic nuclear waste repository developed by the United States Department of Energy. Federal regulations require transuranic waste be isolated from the accessible human environment for at least 10,000 years. During the performance assessment phase of WIPP construction and licensing, it is necessary to quantify the hydrologic characteristics of the overlying Magenta and Culebra dolomite members of the Rustler formation which could be contaminated with radionuclides. Two previous reports used stable isotopes of oxygen and hydrogen as criteria for evaluating the history of the water within the aquifers. the first report concluded that the water in the Magenta and Culebra dolomite members of the Rustler formation could have a modern component and therefore, there is a risk of rapid migration of radionuclides. Using the same data, a second report suggests that, Magenta and Culebra dolomite member waters are demonstrably different from modern Delaware Basin recharge. Therefore they conclude that the aquifers were recharged some time in the past (>10,000 years ago), indicating the water is relatively stagnant and migration of radionuclides would be extremely slow and is not a risk. Both authors identified the need to better quantify the isotopic composition and rates of infiltration through the vadose zone. The purpose of this project is to use stable isotopes and chloride concentrations from the shallow portions of the sediment profile to determine the isotopic composition, and amount of water infiltrating through the sediment profile.

Continuous soil cores were collected from six shallow hand-augured holes near the WIPP. Water was extracted from the soil samples using a vacuum extraction technique. The resulting water was analyzed to determine its isotopic composition using standard analytical techniques. The data shows steady state $\delta^{18}O$ values ranging from -1.3‰ to -2.9‰, and steady state values for δD are approximately -42 ‰.

The dried soil was analyzed for chloride concentration and a mass balance equation was used to quantify infiltration. The calculated infiltration rates range from 0.23 $^{mm}/_{yr}$ on dune crests to 1.98 $^{mm}/_{yr}$, in dune troughs. These two values provide better defined boundary conditions for hydrologic models of the WIPP site. Another continuity equation was used to calculate the age versus depth profile. The maximum values for age at the bottom of the holes range from 114 years at 199 cm to 575 years at 450 cm.

The stable isotope data from this study leads to two conclusions regarding the two previously published reports. First, the compositional field of modern Delaware Basin recharge should be expanded to include compositions derived from the PPR data. Second, the PPR data suggests that the composition of modern recharge and the Magenta and Culebra dolomite member waters are possibly related. This last conclusion also suggests the need to further examine the hydrologic characteristics in the Magenta and Culebra dolomite members.

ACKNOWLEDGEMENTS

Funding was provided by the Waste Education and Research Consortium (WERC).

Preliminary funding was provided by Sandia National Laboratories and the State of New Mexico, Environmental Evaluation Group (EEG).

Special thanks to Lokesh Chaturvedi for his assistance in starting this project and for access to the EEG library.

TABLE OF CONTENTS

INTRODUCTION

The Waste Isolation Pilot Plant (WIPP) was designed as a transuranic (TRU) nuclear waste repository. One of the factors affecting the site choice for the WIPP is the geologic stability of the region. The WIPP is located 655 meters (2150 feet) below ground level in bedded salt of the Salado formation, approximately 40 kilometers (25 miles) east of Carlsbad, NM (Figures 1 and 2). The bedded salt of the Salado Formation was chosen because it is an indicator of a relatively geologically stable environment. In addition to indicating stability, it behaves plastically. This plasticity is a desirable feature because the salt will anneal itself if a fracture or other type of breach should occur. The Salado is overlain by the Rustler Formation which contain the Magenta and Culebra Members. Because these two units could become contaminated with radionuclides from the repository, it is necessary to quantify their hydrologic characteristics.

During the performance assessment phase of the site evaluation process, it is necessary to consider the local and regional hydrologic characteristics of the WIPP site. The hydrologic characteristics of the overlying Magenta and Culebra aquifers affect the rate of radionuclide migration from the site. The risk of contamination stems from the possibility of 1) seal failure in the shafts which connect the surface facilities with the mine workings, and 2) drilling through the WIPP into the over-pressurized Castile Formation brines. Because the possibility of breaching the facility exists, it must be shown that that any waste which gets into the Magenta and Culebra Members will not migrate any significant lateral distance for at least 10,000 years.

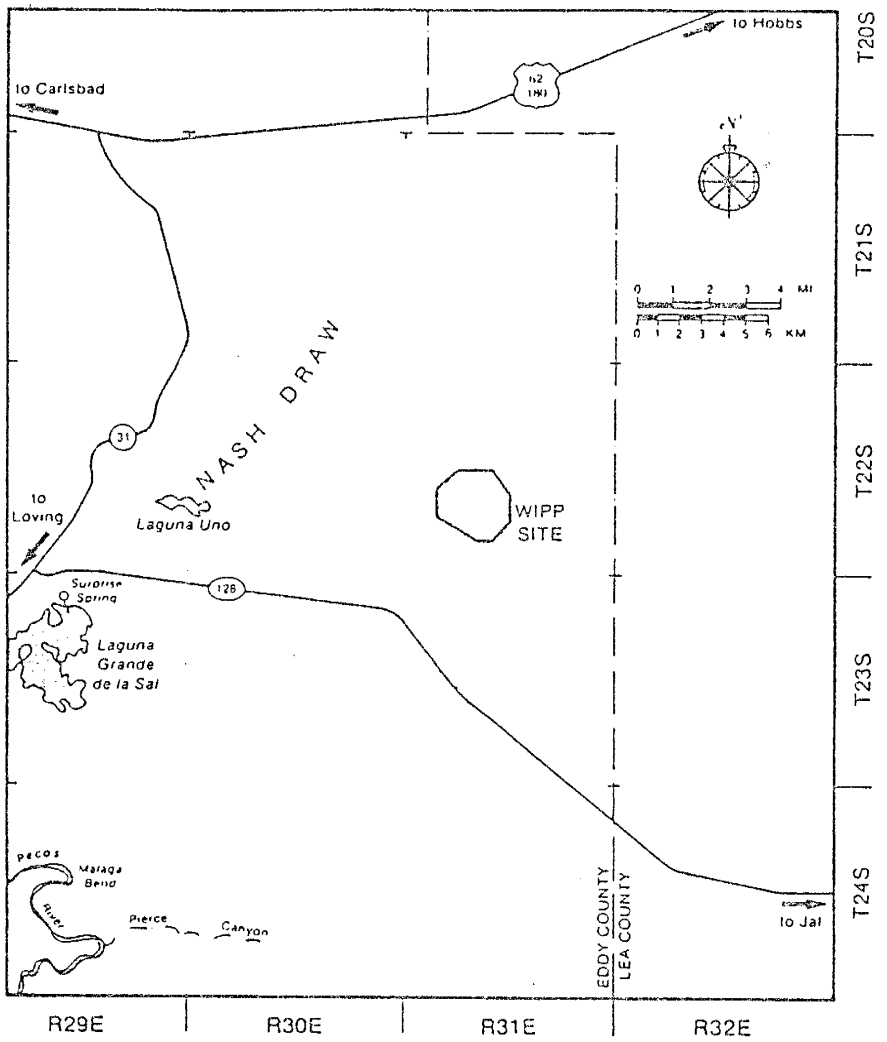

Figure 1: Location of the Waste Isolation Pilot Plant

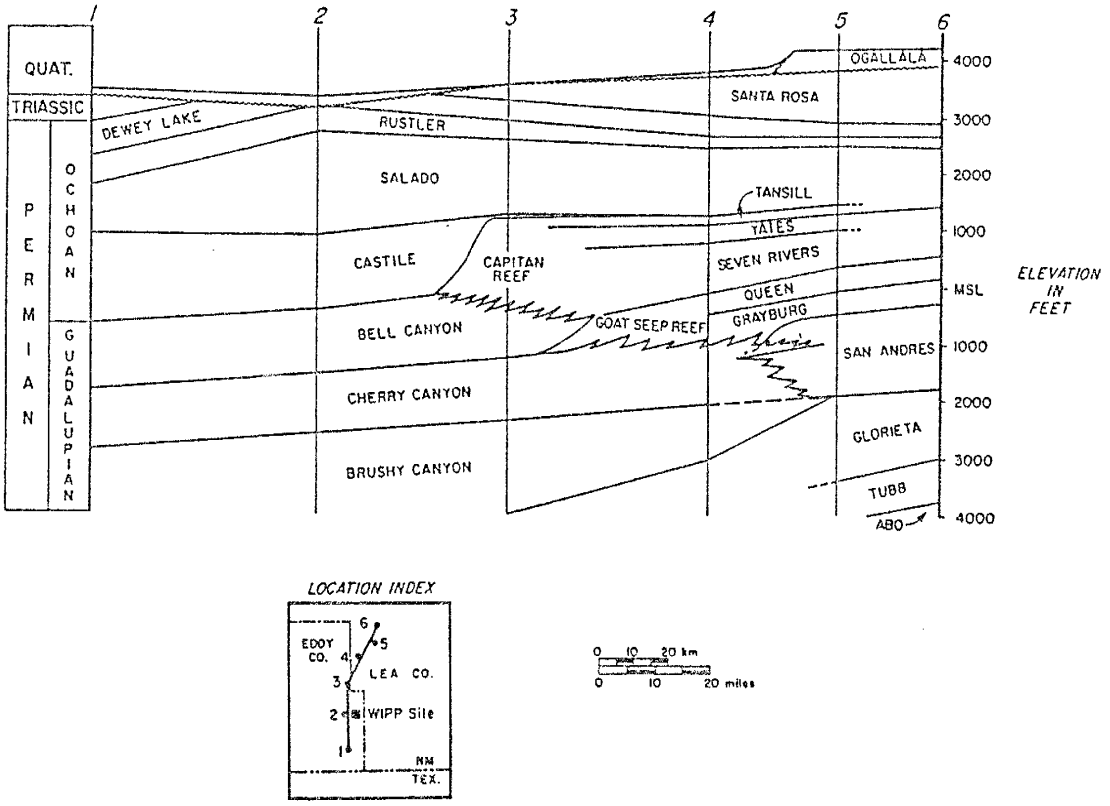

Figure 2: Stratigraphy of the Waste Isolation Pilot Plant

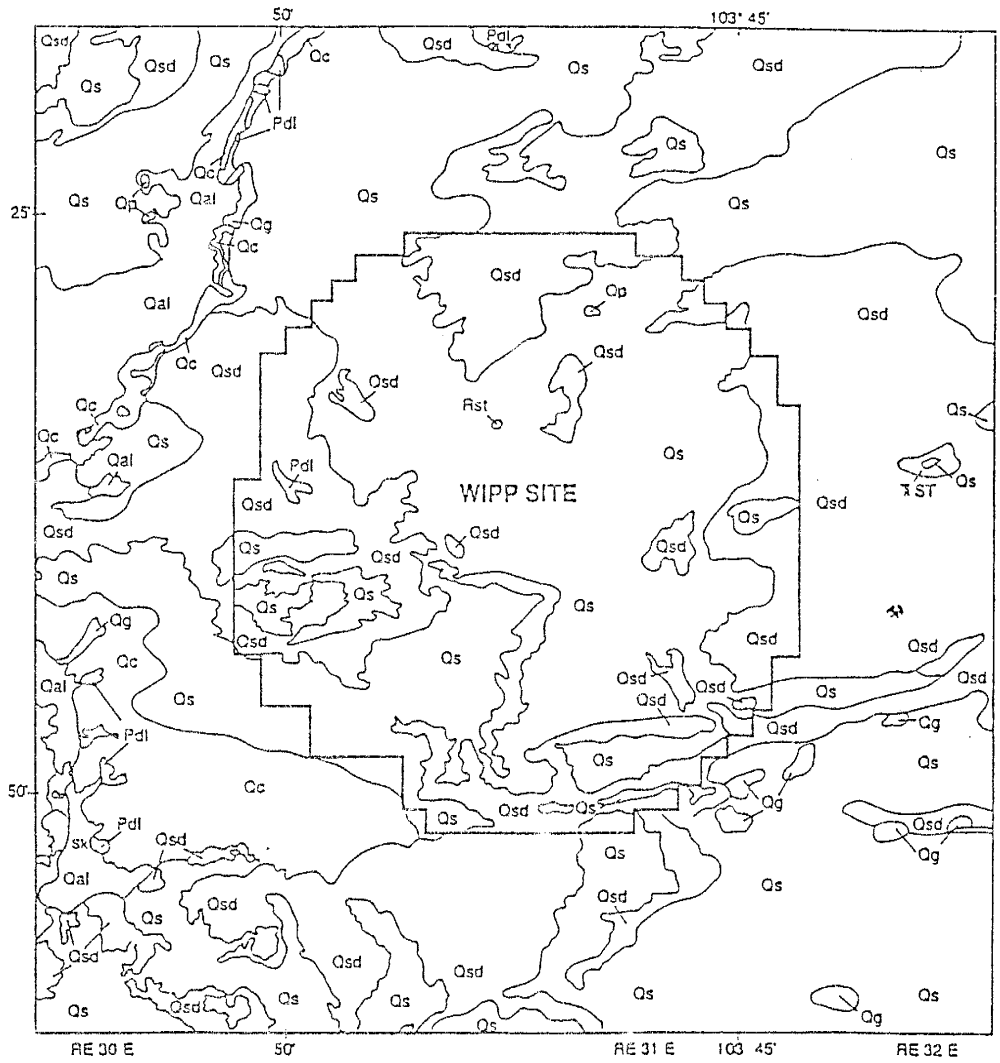

Qal = Quaternary alluvium, Qs = Quaternary sands, Qsd = Quaternary sand dunes, Qc = Quaternary caleche, Qg = Quaternary gatuna, TRST = Tertiary Santa Rosa Pdl = Permian dewey lake

Figure 3: Surface Geology of the Waste Isolation Pilot Plant

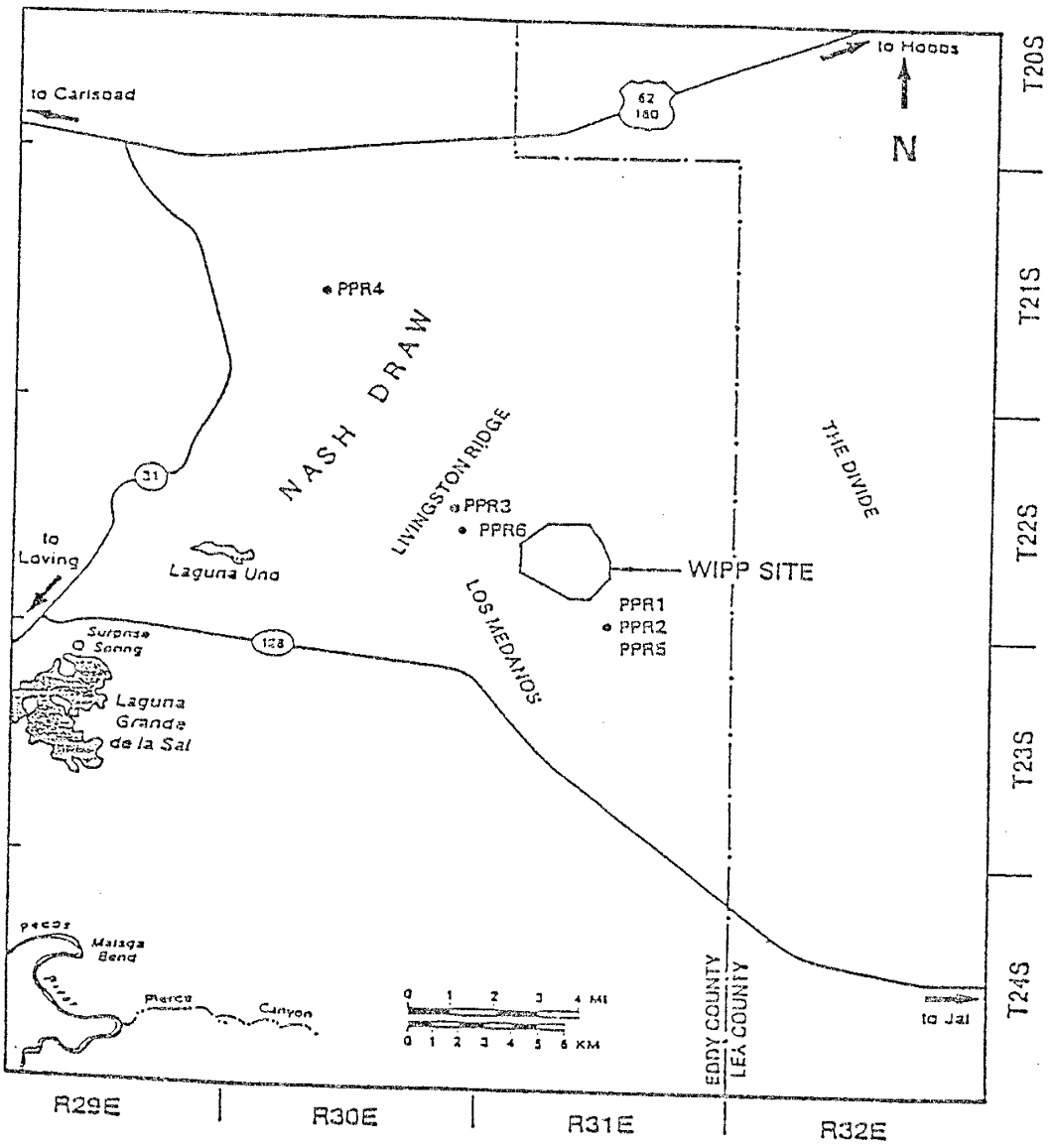

Figure 4: Sampling locations for the PPR data

There are two conflicting ideas regarding the origin of the water from the Magenta and Culebra aquifers. Lambert and Harvey (1987) stated that the water in the Culebra and Magenta aquifers is different than the demonstrably modern Delaware Basin recharge and is "fossil" water, probably recharged during the Pleistocene epoch (>10,000 years ago). The presence of the fossil water indicates the water in the zone of interest has stagnated, thereby suggesting little flow to transport the nuclides. Using the same data set, Chapman (1986) concluded that the composition of "modern Delaware Basin recharge" could be obtained by evaporating modern water in cave pools, at high humidity.

Both reports identify a need to define the composition and quantify the contribution of downward moving water. Quantifying modern recharge will provide better defined boundary conditions for hydrologic models. Defining the isotopic composition of that water will allow a better of comparison of modern recharge with waters from the Magenta and Culebra dolomite members of the Rustler formation.

Research conducted in the Sevilleta National Wildlife Refuge (Knowlton, 1989) and the Chihuahuan desert of Texas (Scanlon, 1991), indicate shallow soil cores can provide the necessary information to identify and quantify modern recharge using stable isotopes and chloride concentrations respectively. The use of soil-chloride profiles from continuous core to determine bottom hole age and quantify recharge has been established by Sharma and Hughes (1985), Allison et al. (1985)and Scanlon (1991). The chloride mass balance method has two advantages over a conventional water balance method for estimating infiltration. These advantages include, a longer

record of precipitation than is possible with historic records and the "smoothing-out" of short-term variations. These advantages allow a better estimation of boundary conditions for modelling flow in an aquifer than traditional water balance methods. Assumptions inherent in the chloride mass balance method include (1) that there is a constant chloride concentration in precipitation (including dry fallout) through time, (2) that precipitation is the only source of chloride, (3) that the precipitation rate remains constant over the time interval, (4) that flow is one dimensional and (5) that piston flow conditions exist below the root zone. The basis of this method is a mass balance between chloride input during precipitation events averaged over a time interval and chloride concentration measured in the soil column. For a precise description of the procedure for determining chloride concentration in soil and use of that data to determine age and recharge rate, see Appendix II.

Barnes and Allison (1983) used a combination of laboratory and field data from Western Australia to explain the characteristic $\delta^{18}O$ and δD profiles for arid environments where the composition of vertically moving water is primarily affected by evaporation. Near the surface, δD and $\delta^{18}O$ values become heavier because of the isotopic fractionation which accompanies evaporation. The profile begins to curve back to lower values, where advective and diffusive mixing of the liquid water from capillary rise and water vapor takes place. Below this mixing zone the profile obtains a steady state value which is considered to be the composition of water which is moving downward and can contribute to recharge.

METHODS

Field sampling

Sites were chosen to represent a variety of the geomorphic environments which exist at the WIPP (Figure 4). Another criteria for site selection was a relatively thick layer of surface sand, from which a relatively long continuous core could be collected for analysis. For the purpose of acquiring water which is undergoing relatively rapid downward motion, the sites were located in dune fields and on eolian sand plains (Figure 3). The first site, containing Past and Present Recharge holes numbers 1 and 2 (PPR1 and PPR2) are located at the top of sand dunes about 3.2 kilometers (2 miles) south of the WIPP. Both holes were augured on the same day and are spaced approximately two meters apart. PPR3 is located adjacent to the WIPP 33 well in a sink hole. This site was selected because personal accounts indicated that large storms can leave standing water at the site which quickly drains, indicating rapid infiltration. PPR4 is next to the WIPP 27 hole which was chosen based on well logs which showed unconsolidated sands to a depth of about 20 meters providing the deepest unconsolidated sediments at this location (Sandia 79-0281). The area around PPR4 is relatively flat and vegetation is sparse in the immediate vicinity. The site for PPR5 is in a trough between dunes adjacent (<10 m) to PPR1 and PPR2 and was selected in an effort to obtain water which might have been focused by the topography. PPR5 samples were processed in duplicate, producing a second set of data labelled PPR5b. The duplicate set was used to test the reproducibility of our procedures using field samples instead of laboratory samples. The location for PPR6 was chosen because it

is near a weather station, which would provide data on precipitation. PPR6 is typical of the eolian sand plain environment near the WIPP, containing grasses and mesquite proximal to the hole.

Field Procedures

From ground level the holes were sampled at 5 cm intervals using a hand trowel. After each sample was taken, the hole was carefully widened. This was repeated until the hole was too deep to continue sampling with the trowel. From that point a hand auger with a three inch diameter by nine inch bucket was inserted into each hole and used to take a continuous core. From the floor of the hole, samples were taken approximately every 10 cm until the auger was no longer able to penetrate the sediments. The sampling interval was somewhat variable depending on the thickness and competency of clay layers and caliche horizons. As sediment was withdrawn from the hole, each sample was immediately placed in an air-tight jar, sealed with silicon vacuum grease and labeled with hole designation and depth interval. The core was logged qualitatively for relative root density, sediment texture and compositional variations such as caliche, large amounts of clay or biogenic products.

Laboratory Procedures

The method utilized to extract water from the soil samples was non-aezeotropic vacuum-distillation, which was developed and tested at the New Mexico Institute of Mining and Technology (NMIMT) Stable Isotope Laboratory. This method has been tested several times and has been shown to be adequate if most of the water (>99.5%)

is extracted (Knowlton et al., 1989). Due to the typically low volumetric-water-content of the samples (<0.10), the PPR samples required between 150-250 grams of soil in order to extract usable volumes of water.

After distillation was complete, the water and soil were carefully stored. The dried soil was stored in air-tight bags for chloride analysis. The extracted water was placed in air-tight glass jars. The jars which are used to store water for isotopic analysis used one of two types of lids, (1) paper gasketed, phenolic, threaded lids sealed with paraffin wax or parafilm, or (2) polyseal, phenolic, threaded lids. Subsequently, it was discovered that the paper gaskets do not adequately seal the jars, therefore, the isotope data from PPR1, PPR2, PPR3 and part of PPR5 may be inaccurate. Since rates of leakage are variable, there is no systematic way to correct the data.

The isotopic composition of the extracted water was determined using standard methods of analysis for hydrogen and oxygen. The CO_2/H_2O equilibration technique as described by Roether (1970) was used to process the early samples. During the data collection phase for the PPR samples, previously undiscussed problems were discovered. Although there is no theoretical justification for the volume of water having an effect on the time required for equilibration, our testing showed the minimum time to reach equilibration increases as the volume of water decreases. This effect was discovered after processing PPR1, PPR2, and parts of PPR3. A new method (Socki et al., 1989) which was tested for small water samples was used to process PPR4, PPR5, PPR5b and PPR6. This method involved the use of pre-

evacuated glass vials and worked well. Details of the procedure and testing results are summarized in appendix IV. Hydrogen analysis was performed using the zinc reduction method outlined by Kendall and Coplen (1985). Although this lab has tested several ratios of zinc to water, we used $0.3g_{(Zn\ reagent)}$ to $3\ \mu l_{(water)}$ as suggested by Kendall and Coplen (1985).

Each dried soil sample from the distillation procedure was analyzed for its chloride concentration. The first three holes (PPR1, PPR2 and PPR3) were analyzed here at NMIMT using an ion-specific electrode to determine concentration of chloride in parts per million (ppm). The rest of the samples were analyzed at the WERC-SWAT lab in Las Cruces, NM.

DATA PRESENTATION

Field Data

PPR1 The core for PPR1 consists primarily of medium- to fine-grained sand. The first few samples near the surface contain roots, twigs and animal pellets. The roots are present down to a depth of 76 cm and at 254 cm the water content of the soil increased notably. At approximately 350 cm the first clay layer was encountered and auguring temporarily slowed. Auguring was stopped for PPR1 at 403 cm after encountering an impenetrable clay layer. Sixty samples were collected and analyzed.

PPR2 is composed mostly of medium- to fine-grained sand, and samples near the surface had roots, twigs and animal pellets. Overall, PPR2 is very similar to PPR1. Sixty samples were collected, but only the top 32 samples have been analyzed (204 cm).

PPR3 The stratigraphy consists primarily of medium and fine sand. Again, the upper sections of core contain roots and twigs. Some minor clay is encountered at 35.5 cm and the auguring ended at 585 cm when a layer of caliche was struck. A total of 70 samples were collected and analyzed from PPR3.

PPR4 Roots and twigs are in the near surface samples and the core was dominated by fine sand throughout its length. Caliche was found at 412 cm and the core ended at 443 cm. Forty-seven samples were collected and analyzed from PPR4.

PPR5 extended to a depth of 199 cm which is dominated by fine sand. Roots and twigs were present to only 60 cm and the first occurrence of clay was at 117 cm. A screw bit was used to break through the clay layer which extends from 117 to 155 cm.

At 199 cm caliche was encountered and the auger was no longer able the penetrate the soil. A total of 32 samples were collected and analyzed from PPR5.

PPR6 The upper-most samples have fine roots, twigs and thorns. The core consists primarily of medium sand and is relatively homogeneous throughout its length. Thirty-two samples were collected to a depth of 213 cm.

Laboratory Data

PPR1 Examining the graphs for PPR1 shows that the volumetric-water-content (θ) gradually increased to about 350 cm, and then increased sharply between 350 cm and the bottom of the hole (Figure 5a). This increase in θ corresponds to the occurrence of clay toward the bottom of the hole and would indicate that the clay has a higher matric suction causing the water to accumulate over that interval. Chloride concentration varies from 165 $^{mg}/_{l}$ to 1500 $^{mg}/_{l}$ and does not appear to exhibit any systematic variation (Figure 5b). Using chloride accumulation, the water at the bottom of the hole exhibits an age of 403 years (Figure 6a).

By graphing cumulative water (cm) versus cumulative chloride (mg/cm^2) we can calculate average chloride concentration which can be used to estimate average recharge (Figure 6b). In PPR1 the line can be broken into approximately two sections. Cumulative water content increases from 0 cm to 0.75 cm across the root zone, which extracts water and increases the chloride concentration and results in a slightly steeper slope across the 0.0-0.75 cm interval. Beyond 0.75 cm the slope flattens reflecting conditions below the root zone. Presumably, further downward movement is under piston flow conditions. By calculating the slope of the deeper segment of the

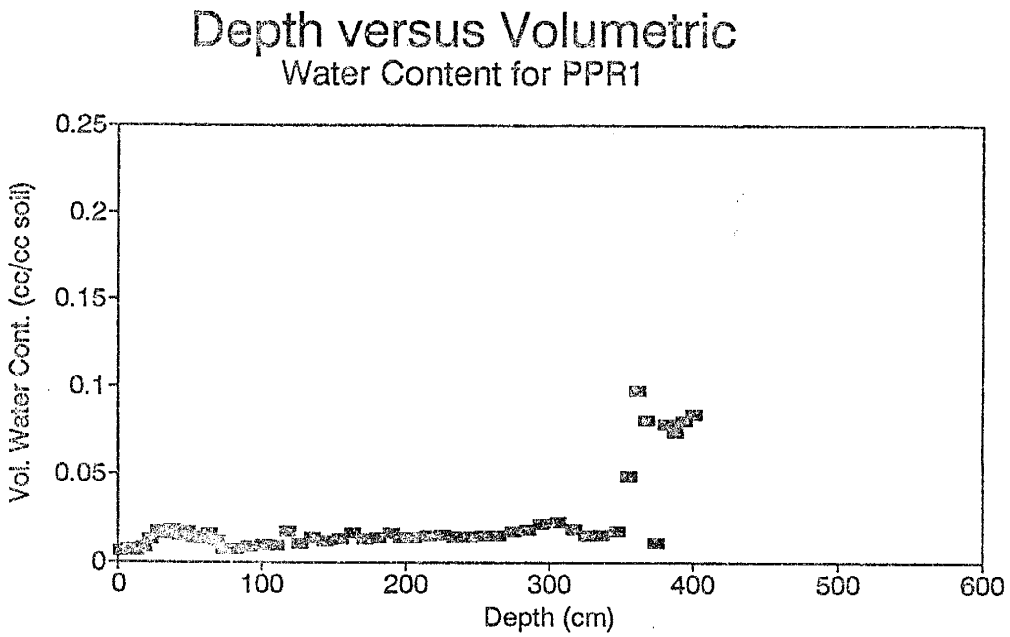

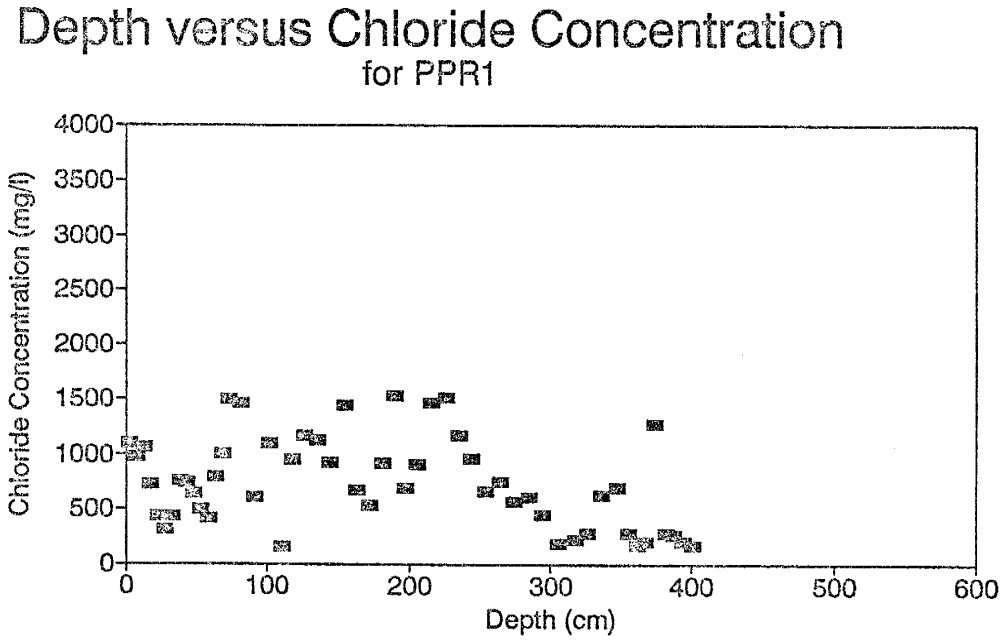

Figure 5: a) Depth versus volumetric water content for PPR1
b) Depth versus chloride concentration for PPR1

(a)

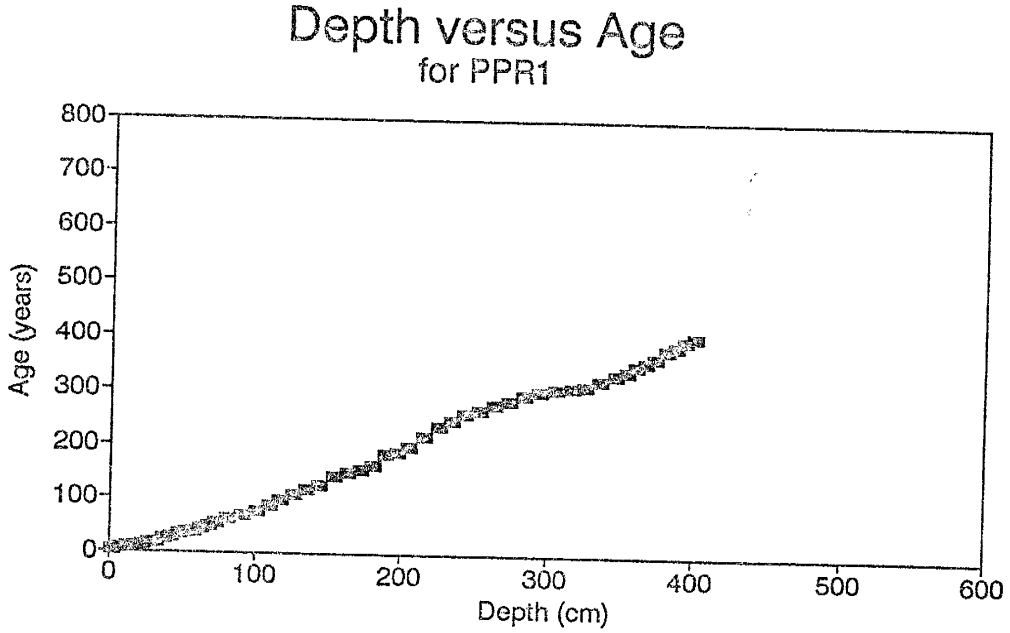

(b)

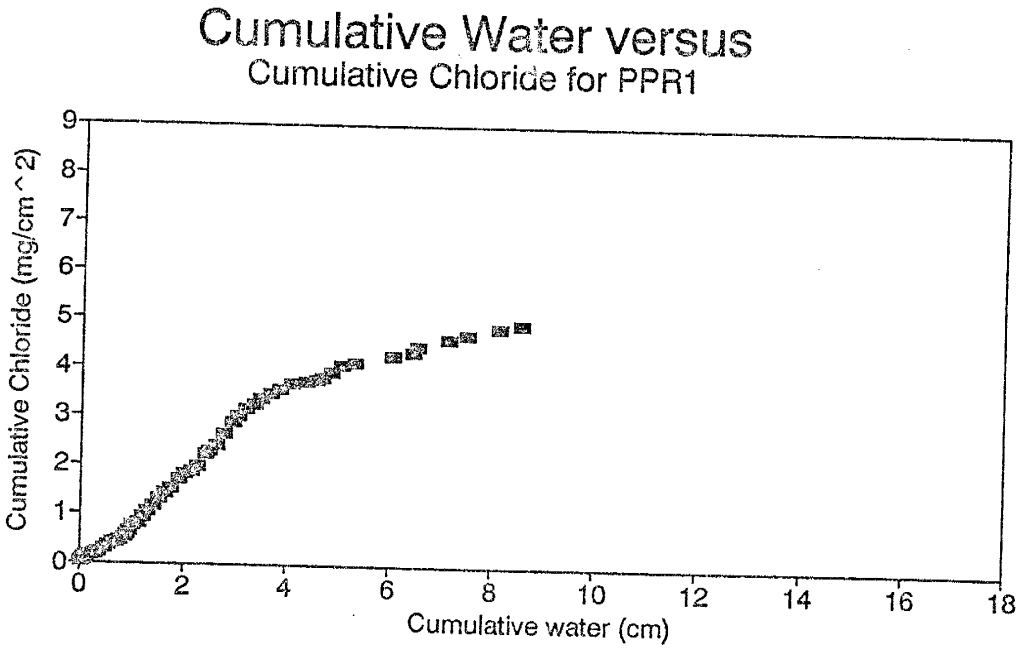

Figure 6: a) Depth versus age for PPR1
b) Cumulative water versus cumulative chloride for PPR1

line and using mass balance equations, a recharge value of .23 $^{mm}/_{yr}$ can be calculated (Figure 6b).

The $\delta^{18}O$ data for PPR1 shows two distinct populations from the surface to approximately 250 cm (Figure 7a). One of the profiles is offset from the other by about 3‰ more negative than the other. As discussed in the methods section, these parallel profiles are the result of an incomplete equilibration. A correction factor of approximately 3 ‰ was determined from testing (Appendix V) and applied to the appropriate points. Unfortunately this correction still does not sufficiently adjust the data (Figure 7b). Therefore, any estimation of a steady state value is probably not valid and was not done.

The δD profile exhibits a shape which corresponds well with the shape defined by Allison et al., (1984) as characteristic for an arid environment (Figure 8a). At the top of the profile there is an evaporation zone from 0 to about 25 cm. The general shape of this curve suggests that the steady state value for downward moving soil water is continually getting lighter. This continued change of the δD values suggests there is an additional control on δD which has no effect on $\delta^{18}O$.

A common way to express the composition of water is to plot it in δD/δO space (Figure 8b). Values for PPR1 in this space, range from -20‰δD to -60‰δD and -10‰δO to 3‰δO.

PPR2 In general, the curve for depth versus volumetric water content agrees with the same curve for PPR1 (Figure 9a). The slopes for both PPR1 and PPR2 show a steady increase in volumetric water content with depth but a slight water bulge is observed

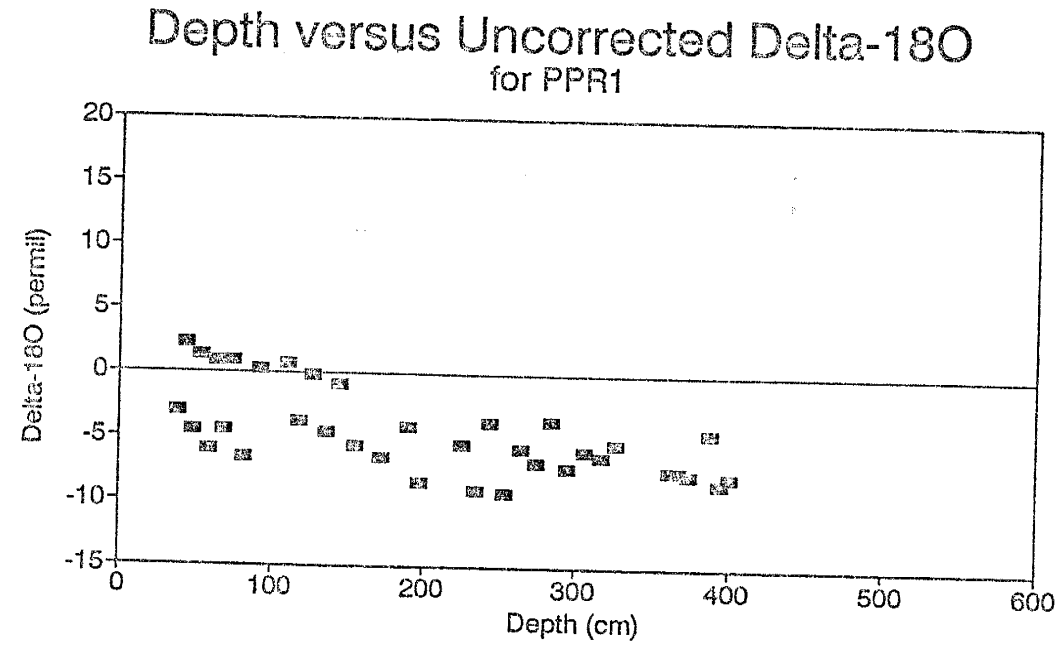

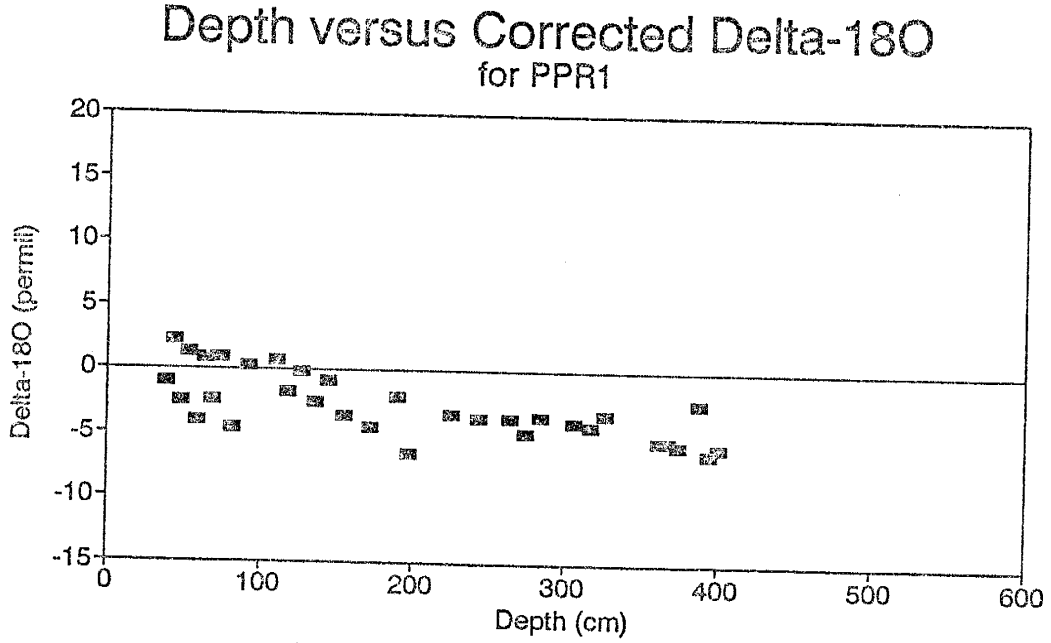

Figure 7: a) Depth versus uncorrected δ180 for PPR1
b) Depth versus δ180 corrected for small volumes of water for PPR1

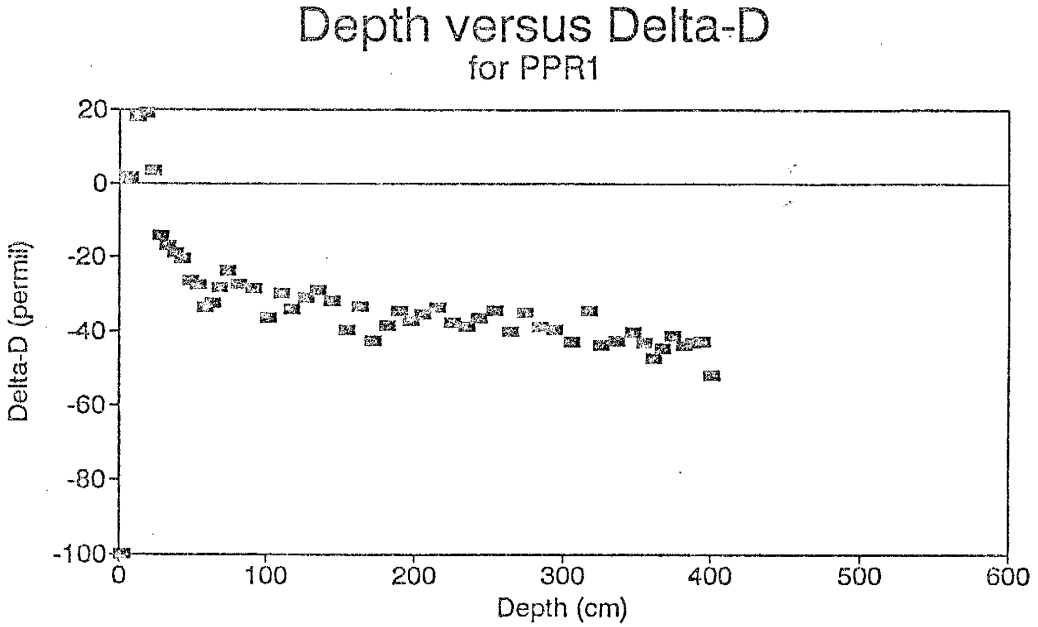

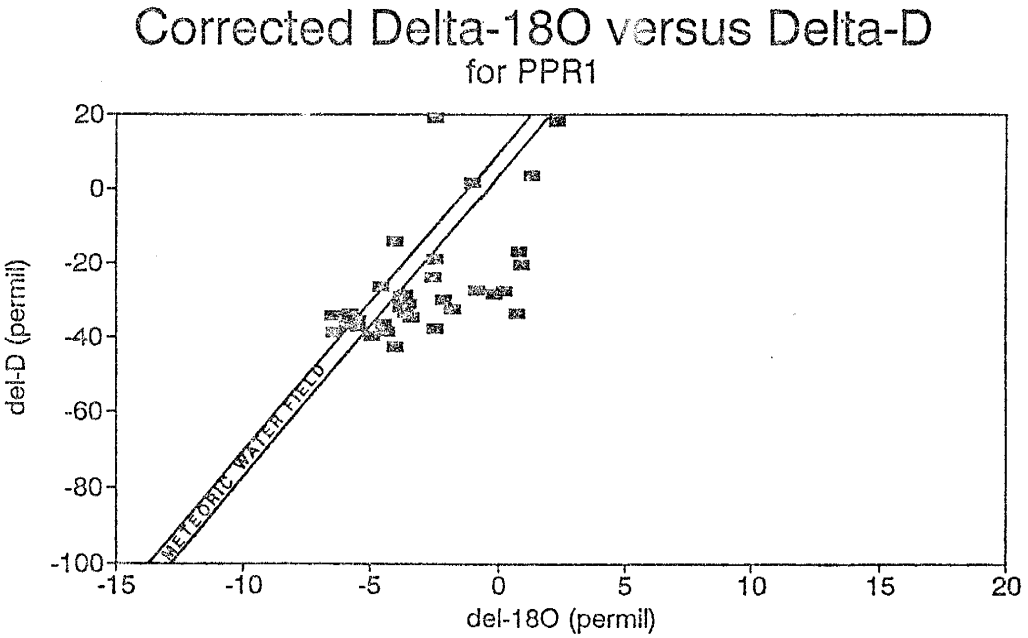

Figure 8: a) Depth versus δD for PPR1
b) Corrected δ18O versus δD for PPR1

(a)

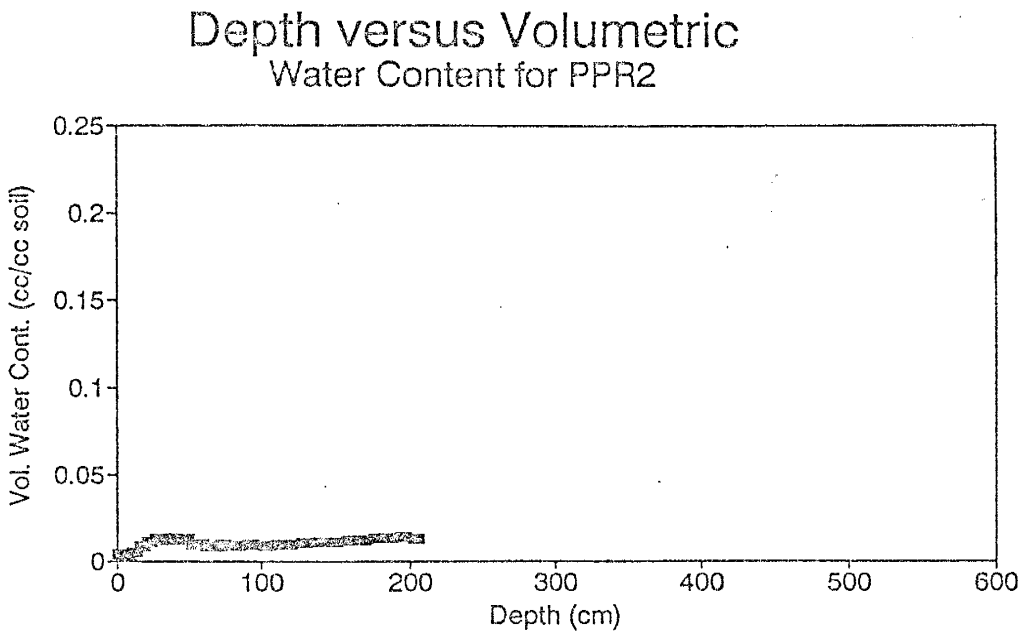

(b)

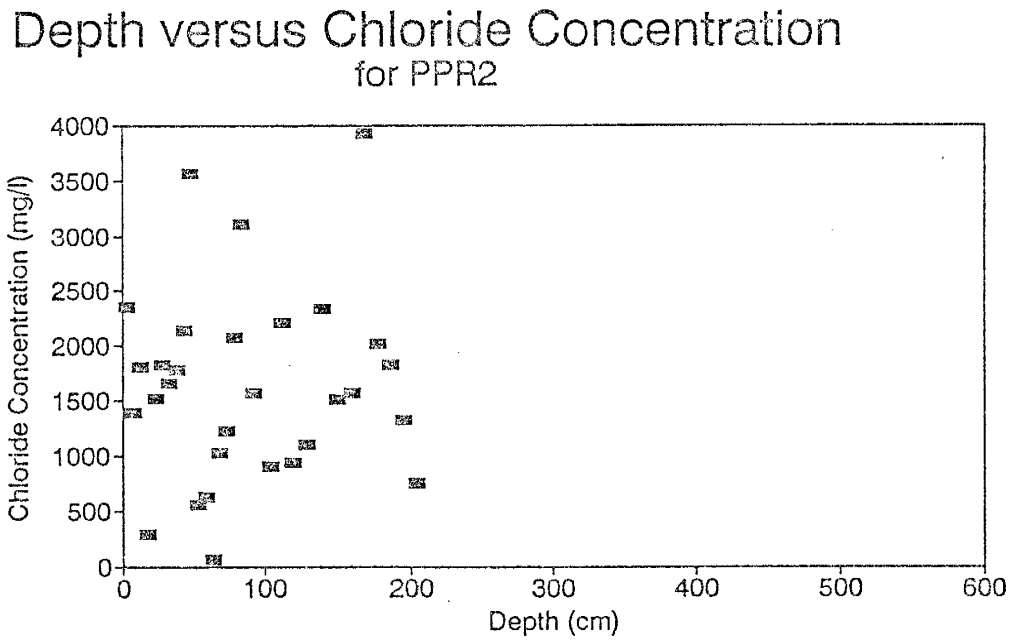

Figure 9: a) Depth versus volumetric water content for PPR2
b) Depth versus chloride concentration for PPR2

between 25 cm and 60 cm on both. The chloride concentration curve for PPR2 shows a variation between 295 $^{mg}/_{l}$ and 4000 $^{mg}/_{l}$(Figure 9b). At least half of these points are more concentrated than PPR1 over the same interval. This set of higher concentrations results in an age of 300 years at 200 cm compared to 200 years at the same depth for PPR1 (Figure 10a). The difference in age estimates probably reflect lateral heterogeneity within the dune. The cumulative water versus cumulative chloride curve for PPR2 gives us information for samples in and above the root zone, therefore no calculation of recharge can be made (Figure 10b).

The $\delta^{18}O$ curve shows a typical arid environment profile (Figure 11a). There is an enrichment in $\delta^{18}O$ from 0 to 25 cm. This shape is the result of evaporation as discussed previously. Below 25 cm the curve begins to swing back and more or less achieves a steady value of -2.5‰.

The δD profile shows the some shape as the $\delta^{18}O$ profile (Figure 11b). The lower portion of this curve defines a steady state value of approximately -42 ‰. When these two data sets are plotted $\delta D/\delta^{18}O$ space, most of the points fall within a range of -40 $‰_{\delta D}$ to -60 $‰_{\delta D}$ and -4 $‰_{\delta O}$ to 3 $‰_{\delta O}$ (Figure 12). However, there are some points outside this range which plot almost as a line with an approximate slope of 2.3. This slope corresponds well to the estimated slope of evaporation for arid environments. the evaporation slope in arid environments ranges from about 2 to 3.

PPR3 Depth versus volumetric water content for PPR3 shows a similar profile to the two previous holes but the volumetric water contents are generally higher by about 0.01 (Figure 13a). The chloride concentration varies from approximately 68 $^{mg}/_{l}$ to

(a)

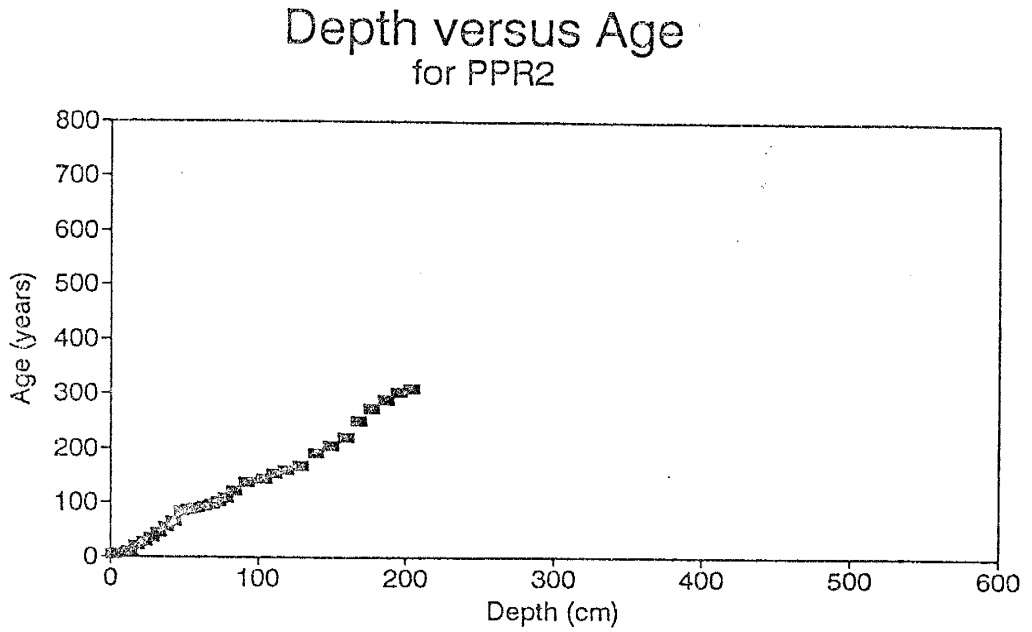

(b)

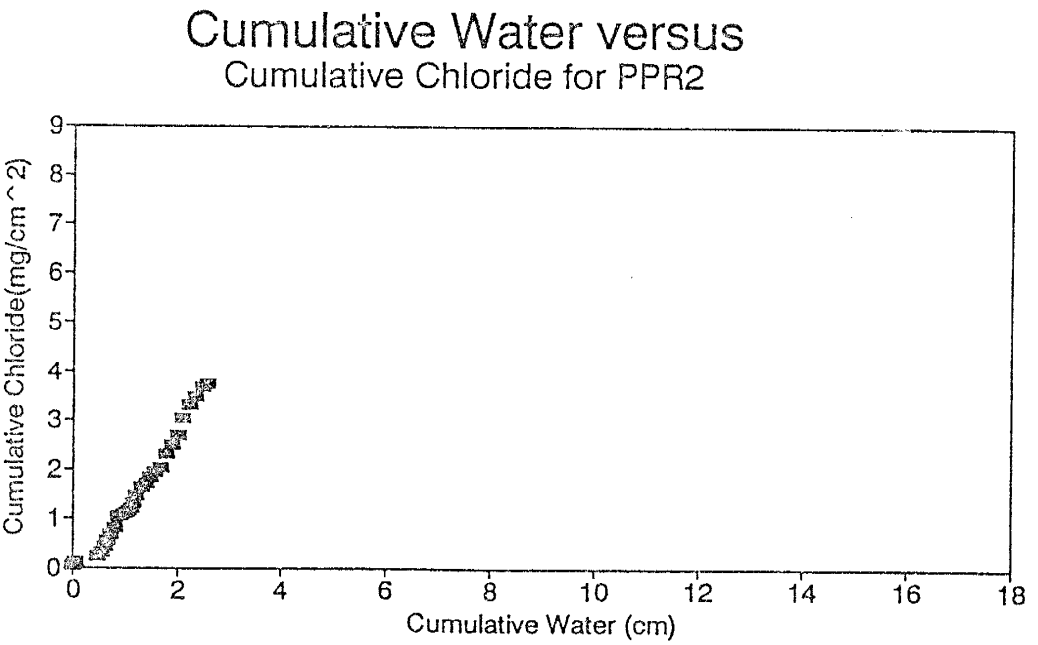

Figure 10: a) Depth versus age for PPR2
b) Cumulative water versus cumulative chloride for PPR2

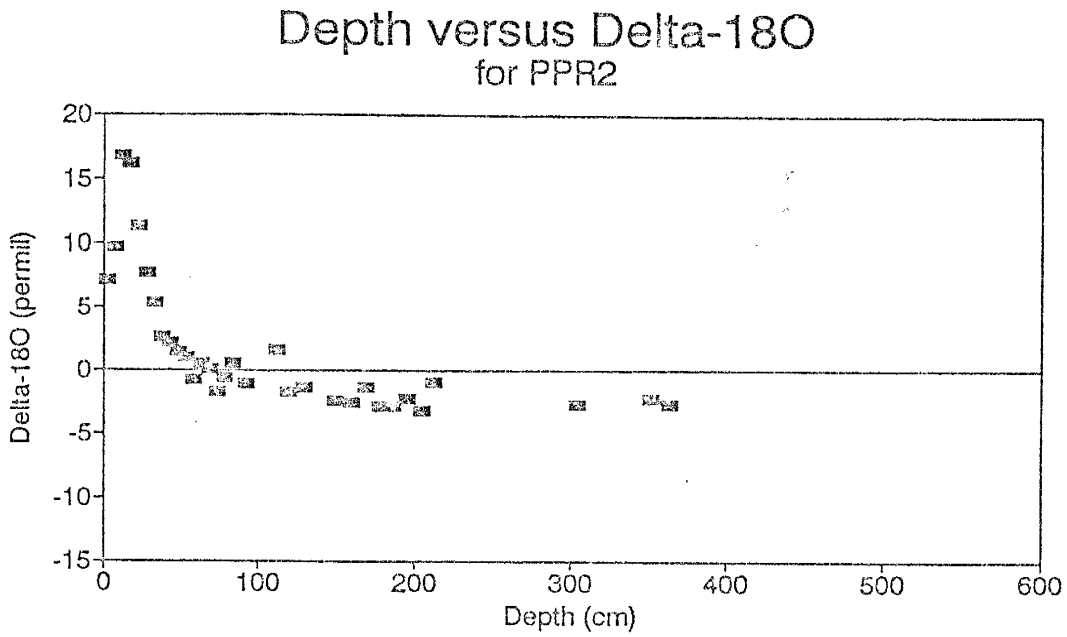

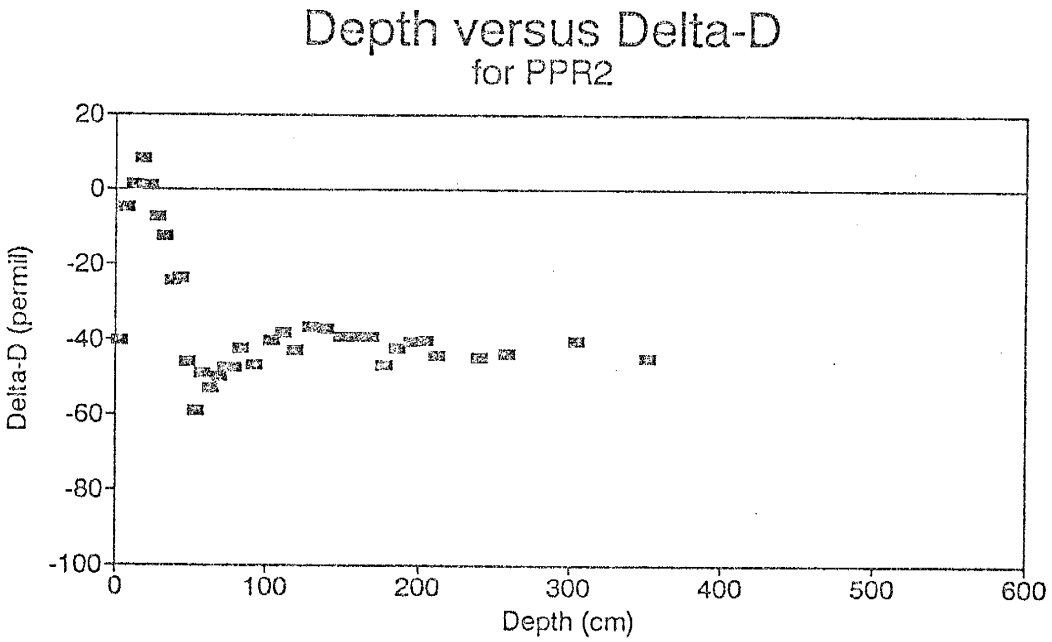

Figure 11: a) Depth versus δ18O for PPR2
b) Depth versus δD for PPR2

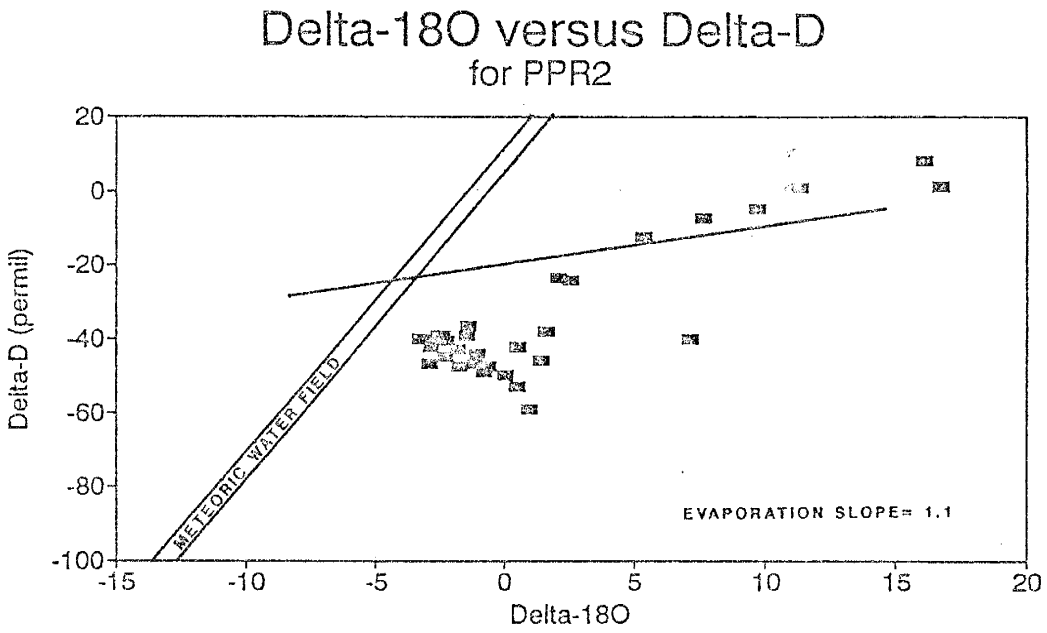

Figure 12: a) δ18O versus δD for PPR2

(a)

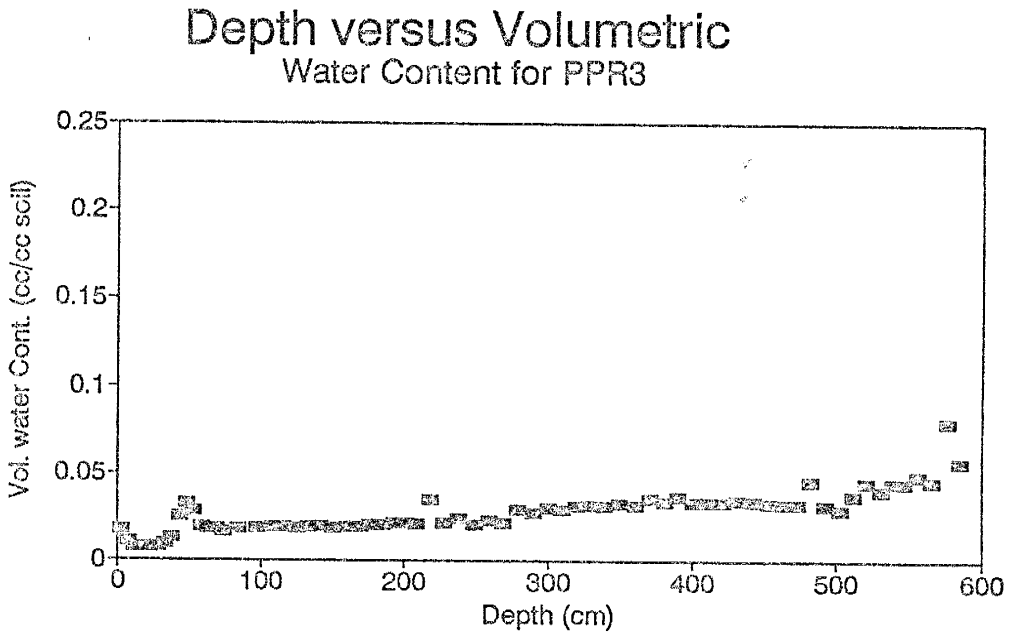

(b)

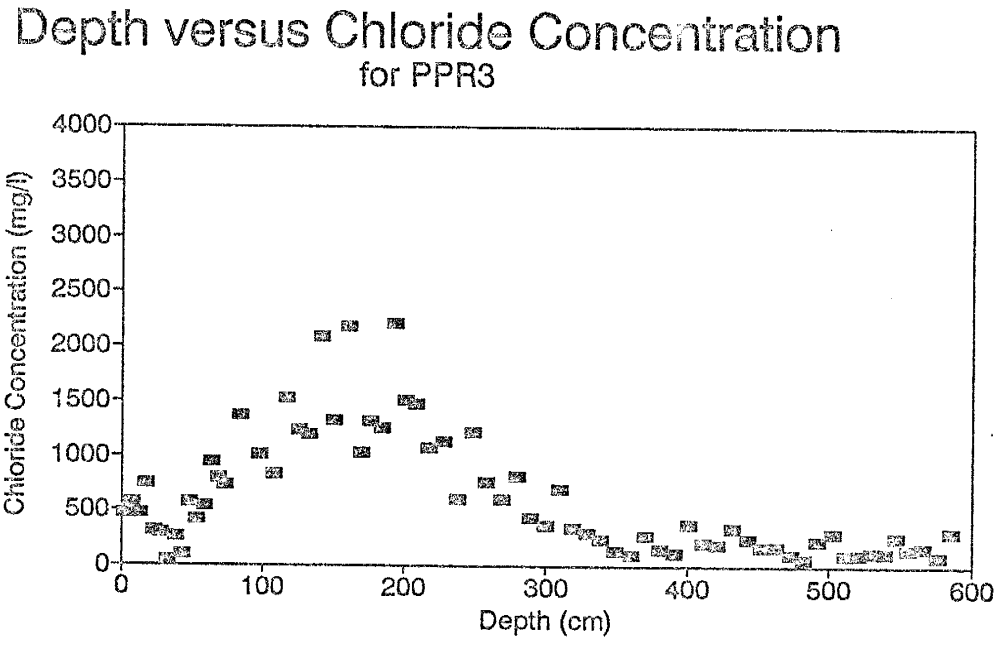

Figure 13: a) Depth vesus volumetric water content for PPR3
b) Depth versus chloride concentration for PPR3

2250 $^{mg}/_{l}$ with a distinct bulge at approximately 200 cm (Figure 13b). Chloride mass balance calculations show the bottom hole age to be 575 years (Figure 14a). The lower portion of the curve (0-80 cm), shows a very shallow slope then a steeper slope beginning at 80 cm. The cumulative water versus cumulative chloride graph yields a recharge rate of 0.67 $^{mm}/_{yr}$(Figure 14b). Similar to PPR1, the effect of the root zone on the cumulative water versus cumulative chloride can be seen from 0 to 1 cm cumulative water.

$\delta^{18}O$ values for PPR3 show the effects of evaporation near the surface (Figure 15a). The steady state value is approximately -7 ‰ but the value never really seems to reach an actual steady state. The δD profile shows the same evaporation front as $\delta^{18}O$, and once again, the profile never achieves a steady state value (Figure 15b). The profile seems to oscillate between 35 ‰ and 40 ‰. The $\delta D/\delta^{18}O$ plot shows two sets of points similar to PPR2. The majority of the points fall from -35 $‰_{\delta D}$ to -60 $‰_{\delta D}$ and -10 $‰_{\delta O}$ to 0 $‰_{\delta O}$ (Figure 16). Another group of points sort of trail off defining a line similar to the trailing points of PPR2 but with a slope of approximately 2.

PPR4 The values for volumetric water content range from 0.02 to 0.05 for PPR4 (Figure 17a). The chloride data shows a well defined profile with depth (Figure 17b). Near the top of the profile there is an increase in chloride concentration because water is extracted by the roots of plants, and a relatively steady state value of 100 $^{mg}/_{l}$ is achieved by 200 cm. The age profile shows the same general relationship with depth as in PPR3 (Figure 18a). The bottom hole age is 575 years at 443 cm. The

(a)

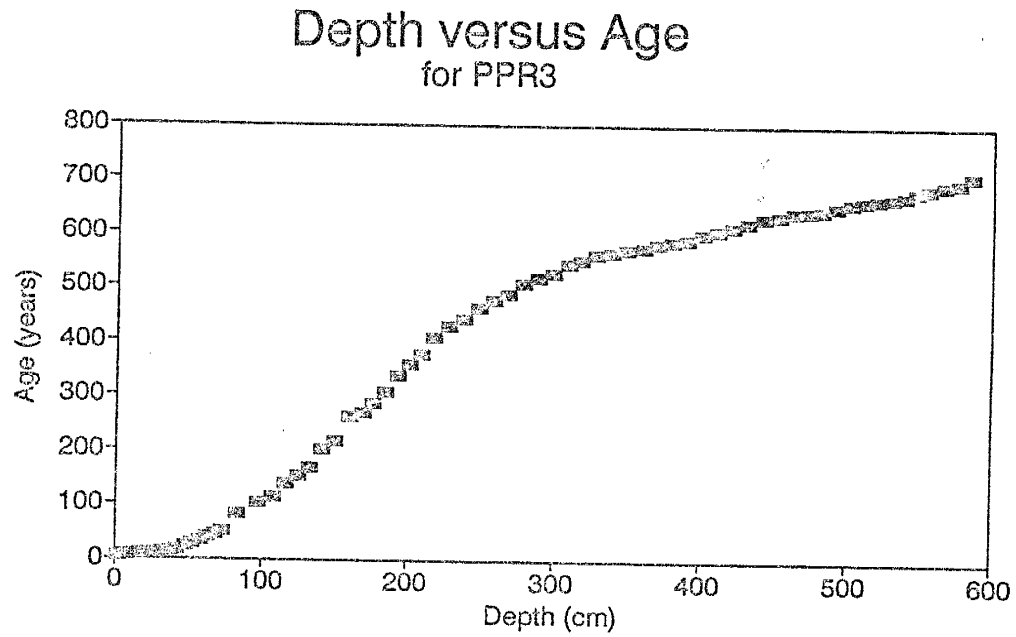

(b)

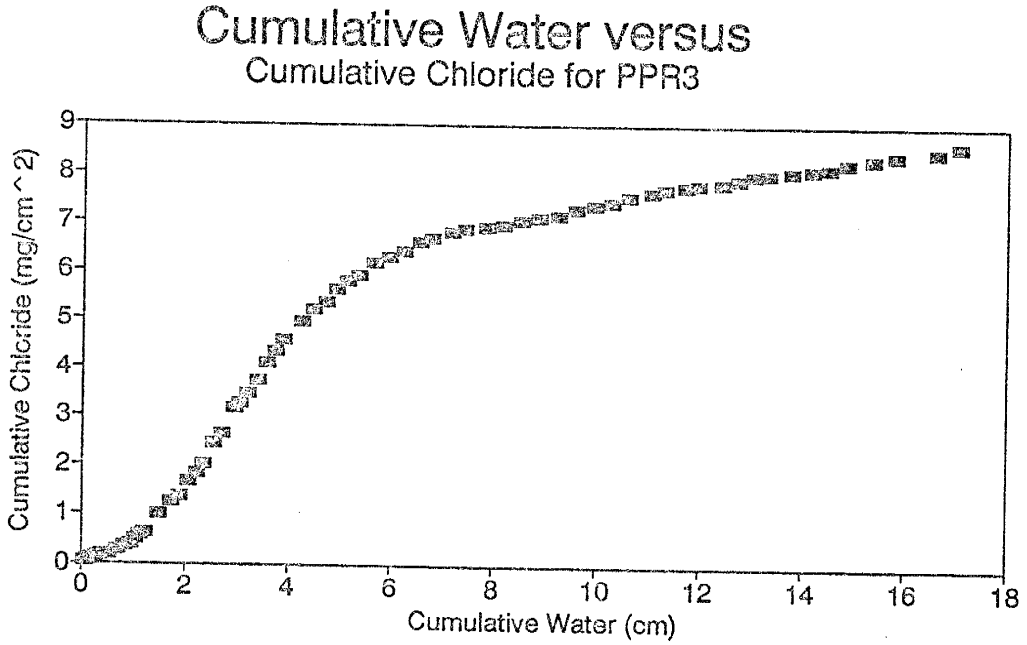

Figure 14: a) Depth versus age for PPR3
b) Cumulative water versus cumulative chloride for PPR3

(a)

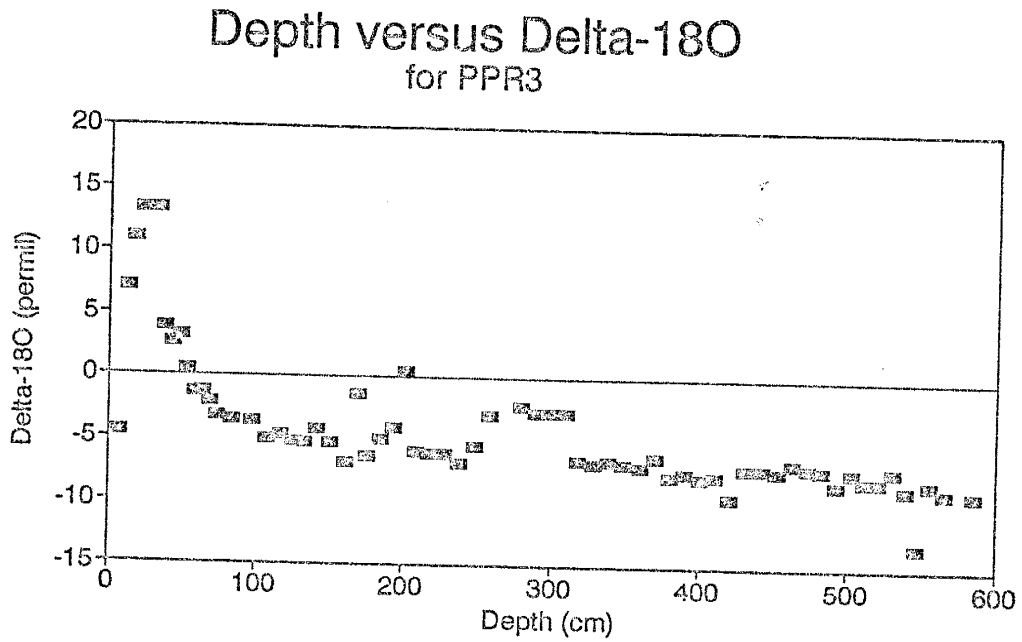

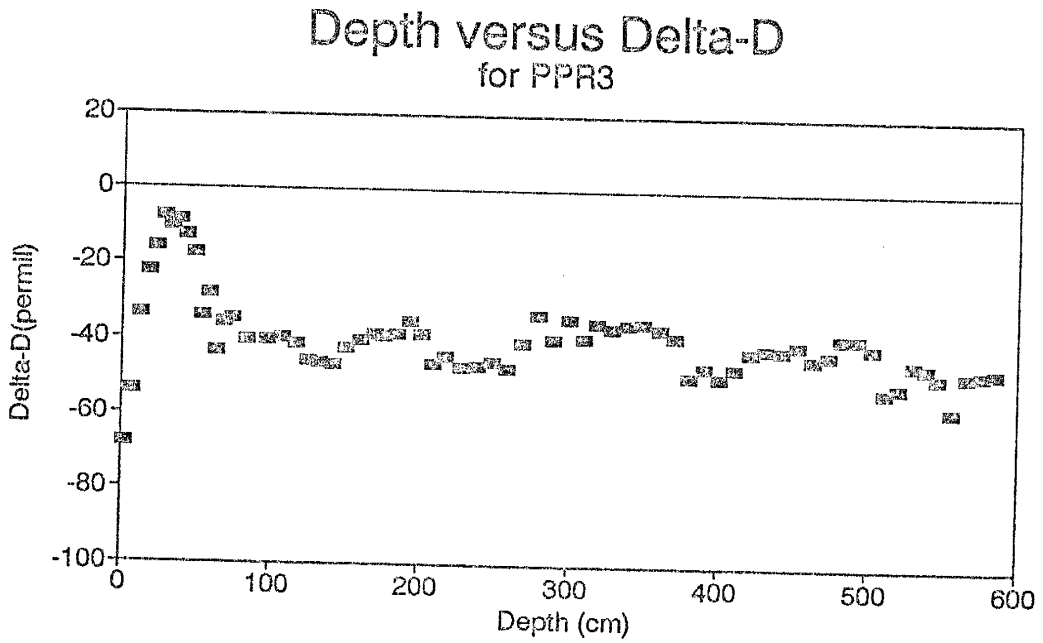

Figure 15: a) Depth versus δ18O for PPR3
b) Depth versus δD for PPR3

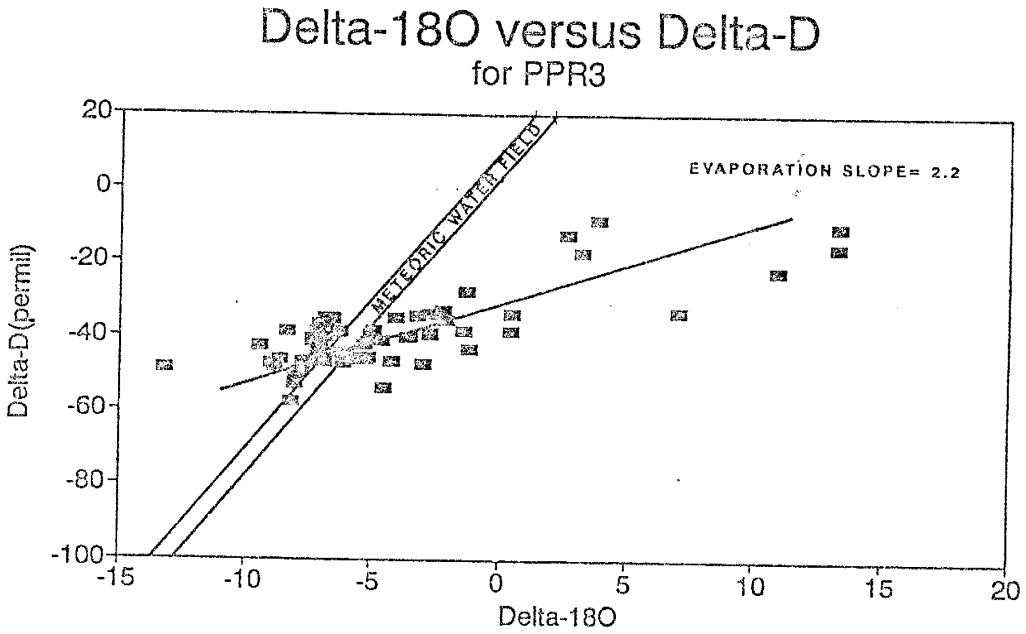

Figure 16: δ18O versus δD

(a)

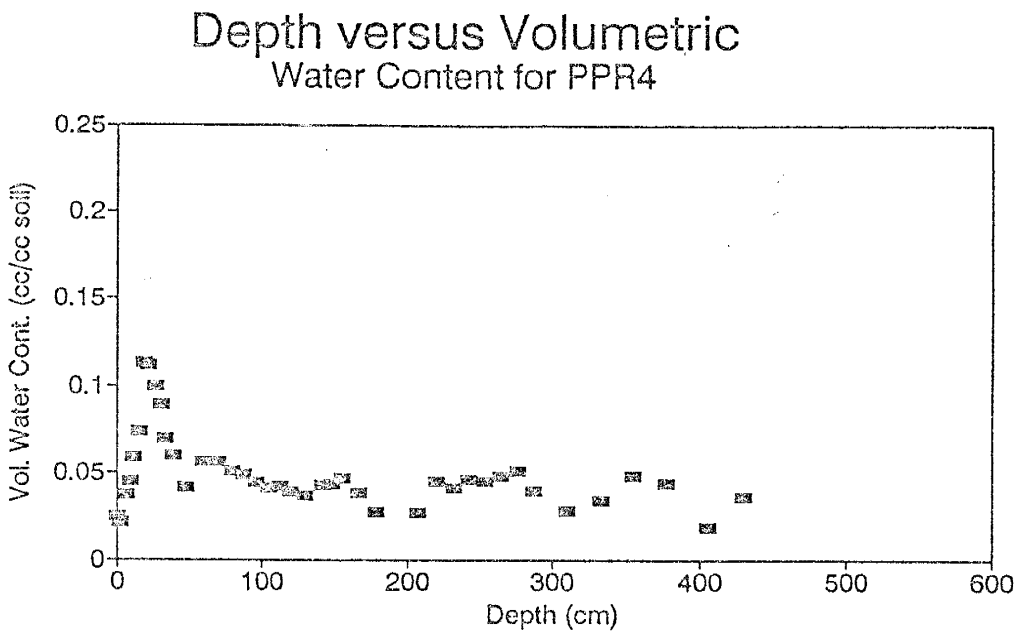

(b)

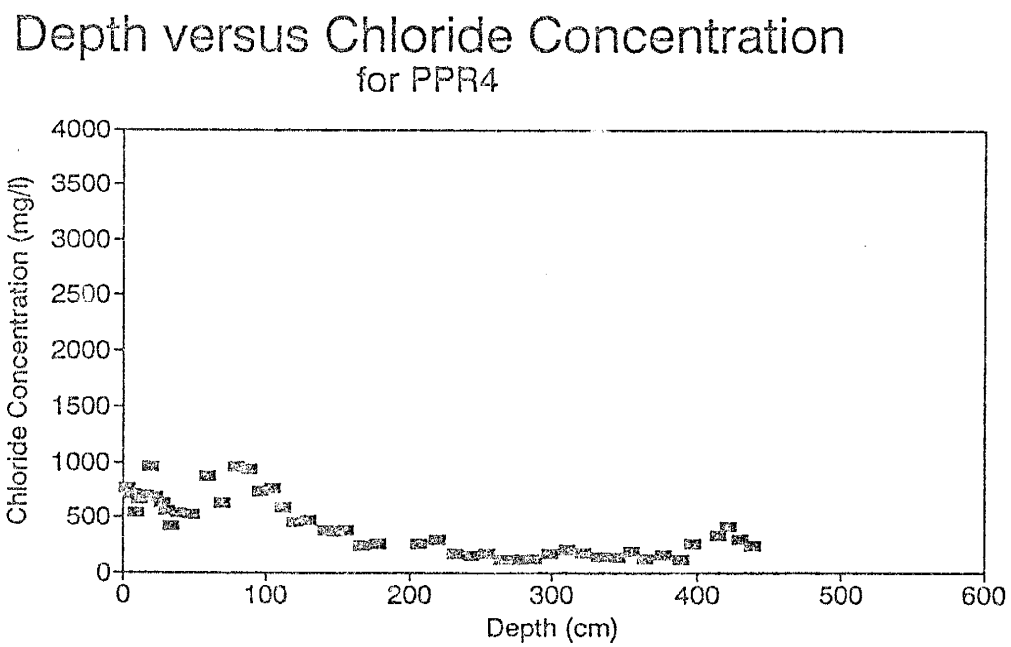

Figure 17: a) Depth versus volumetric water content for PPR4
b) Depth versus chloride concentration for PPR4

(a)

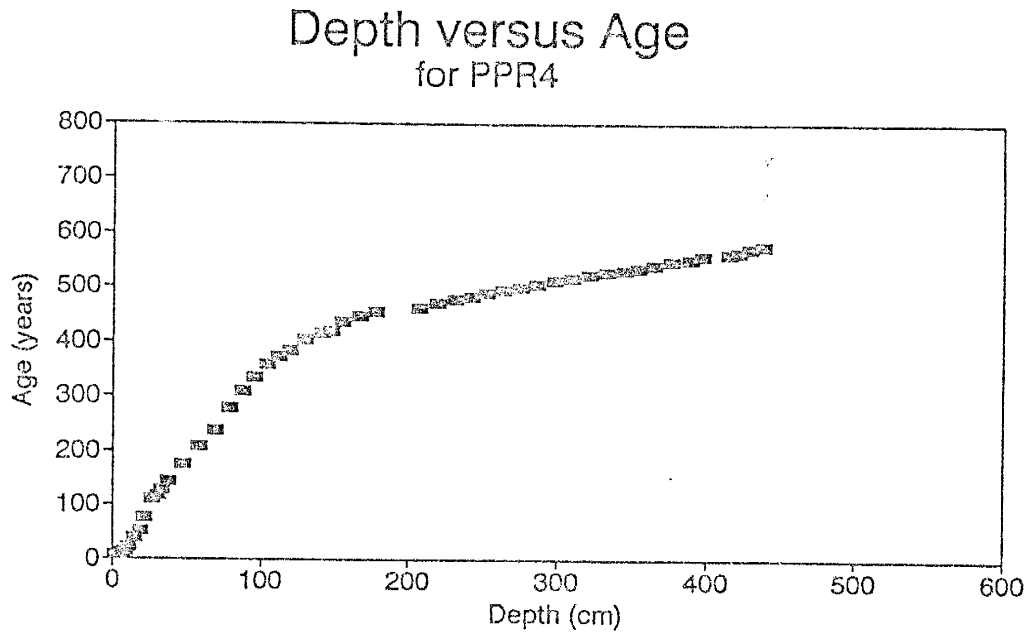

(b)

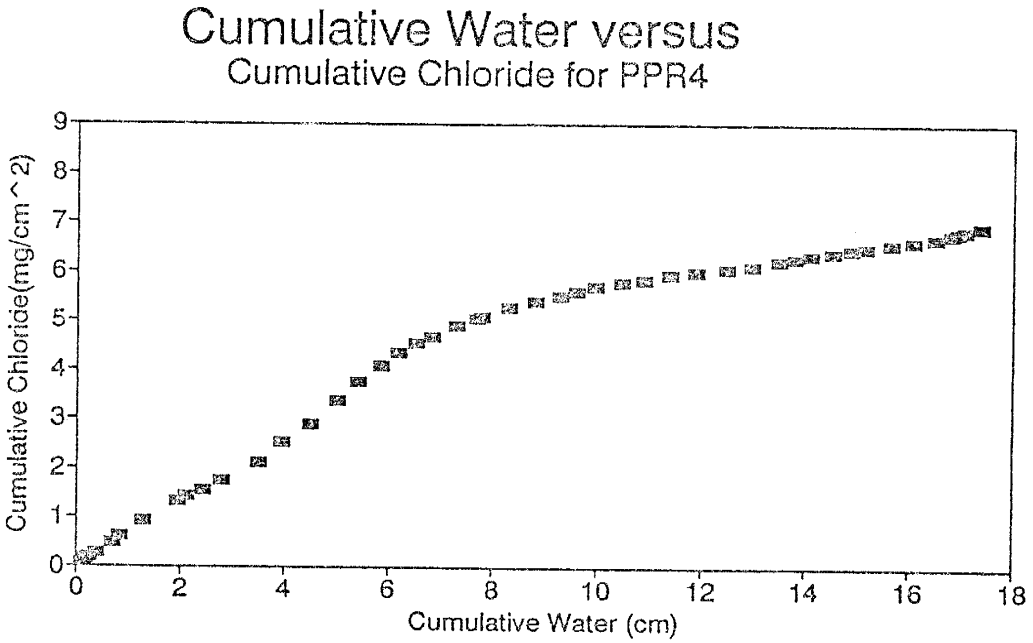

Figure 18: a) Depth vesus age for PPR4
b) cumulative water vesus cumulative chloride for PPR4

cumulative water versus cumulative chloride yields a recharge rate of 0.77 $^{mm}/_{yr}$ (Figure 18b). The effect of evaporation on the profile is not as noticeable.

Depth versus $\delta^{18}O$ shows a very well developed evaporation front and a steady state value of -1.38‰ is reached at approximately 140 cm (Figure 19a). In the δD profile the evaporation zone is from 0 to approximately 30 cm and a steady state value of approximately -42 ‰ is obtained (Figure 19b). In $\delta D/\delta^{18}O$ space the range of most points is from -40 $‰_{\delta D}$ to -60 $‰_{\delta D}$ and -2 $‰_{\delta O}$ to 0 $‰_{\delta O}$ (Figure 20). Again a tail of points define an evaporation line with a slope of approximately 2.

PPR5 The volumetric water content curve for PPR5 shows a steady increase with depth until about 40 cm where it achieves a steady state value of 0.04 (Figure 21a). At 100 cm the values begin to increase again and continue increasing until the bottom of the hole. The low conductivity, high porosity clay at the bottom of the hole is probably the cause of the moisture spike which can be observed from 125 cm to 199 cm. An interesting feature of this curve is the significant increase in moisture to 0.20 which is the highest volumetric water content observed from the PPR series. The high matric suction clay layer is the best explanation for this. Near the top of the hole there is an increase in chloride concentrations due to evaporation of soil water in that zone (Figure 21b). The depth versus age profile for PPR5 shows a monoclinal shape resulting in an age of approximately 150 years at 200 cm (Figure 22a). The cumulative water versus cumulative chloride graph yields a recharge rate of 1.98 $^{mm}/_{year}$ (Figure 22b). Since two sets of extractions were run on PPR5 a second set of data,

(a)

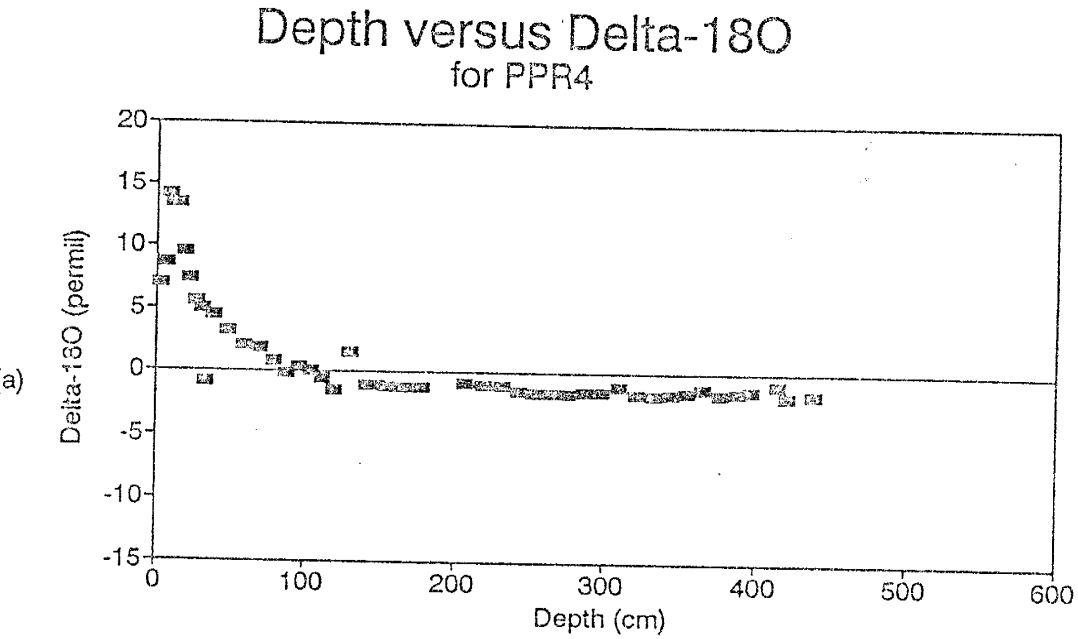

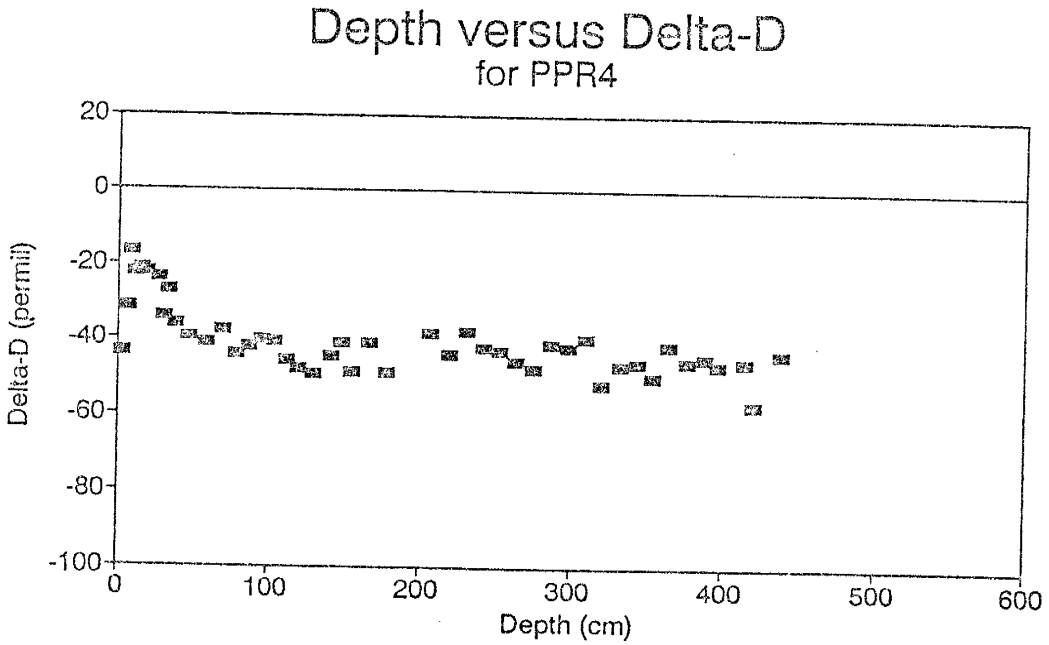

Figure 19: a) Depth vesus δ18O for PPR4
b) Depth versus δD for PPR4

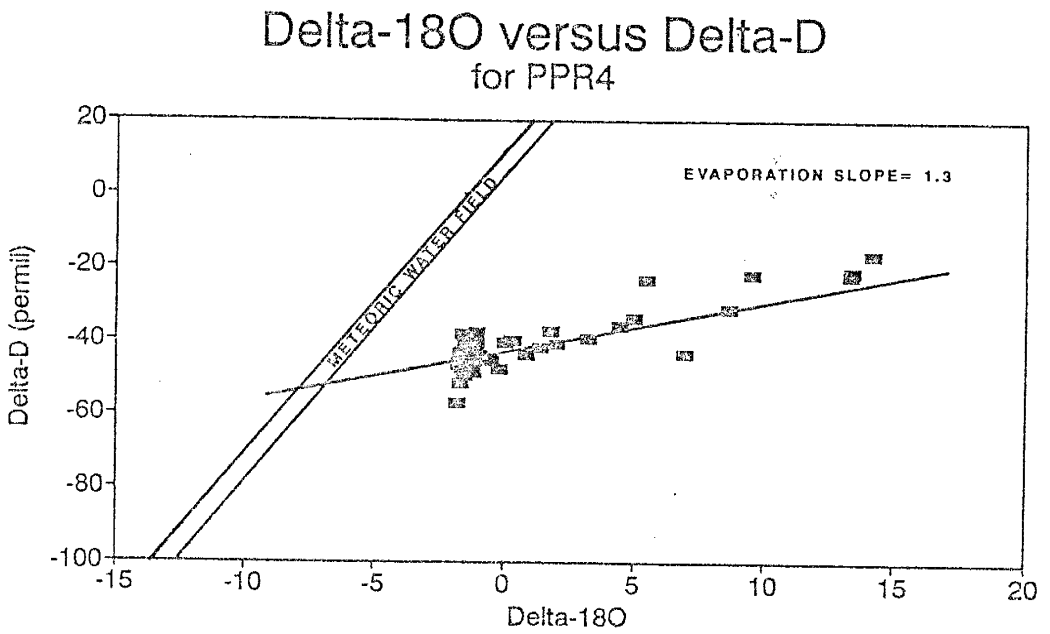

Figure 20: δ18O versus δD for PPR4

(a)

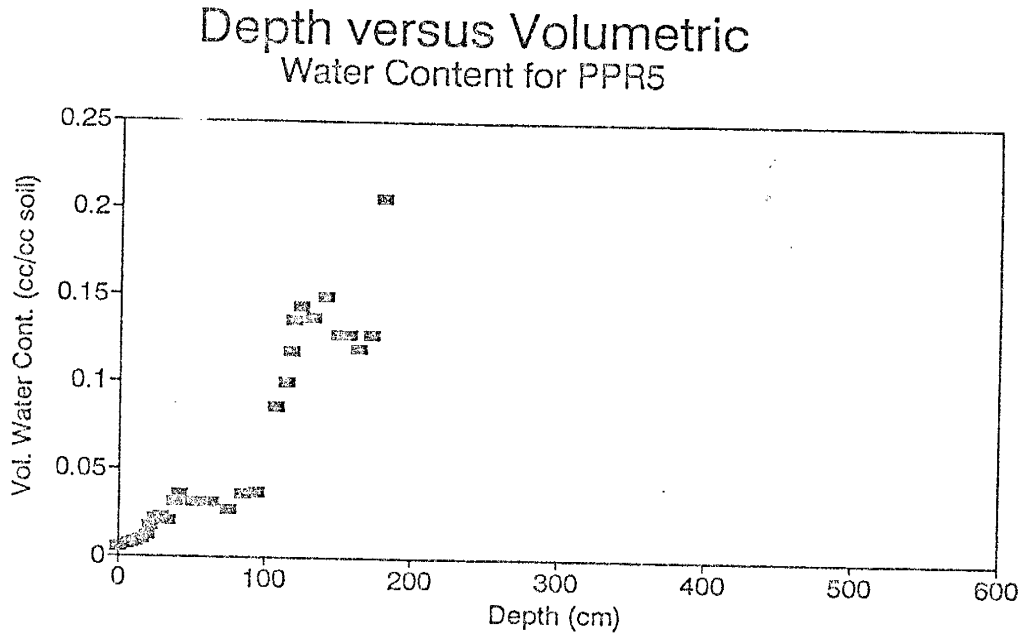

(b)

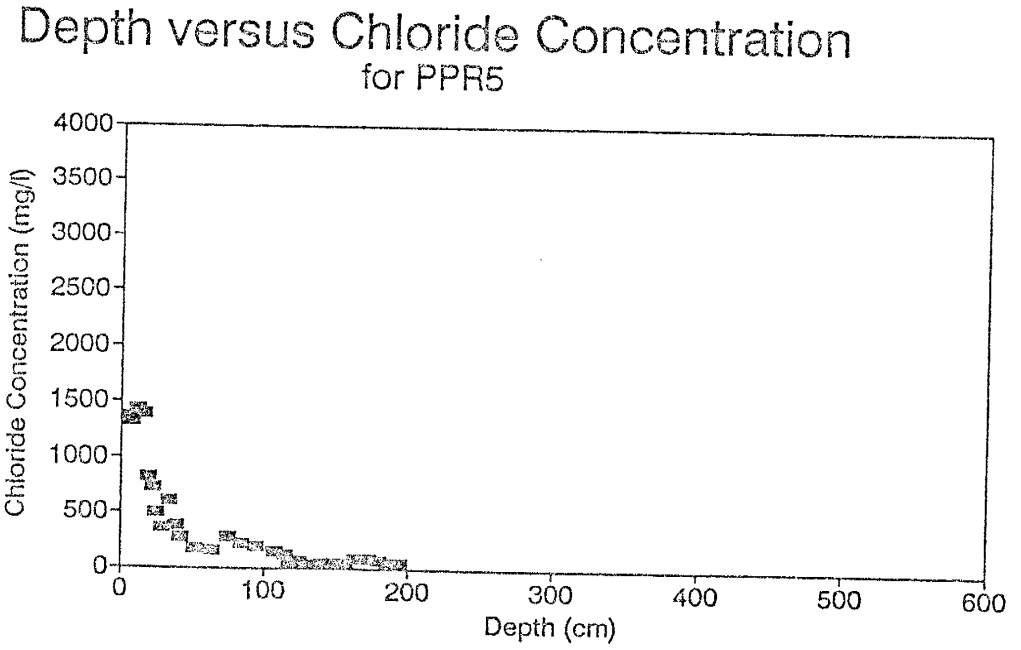

Figure 21: a) Depth versus volumetric water content for PPR5
b) Depth versus chloride concentration for PPR5

(a)

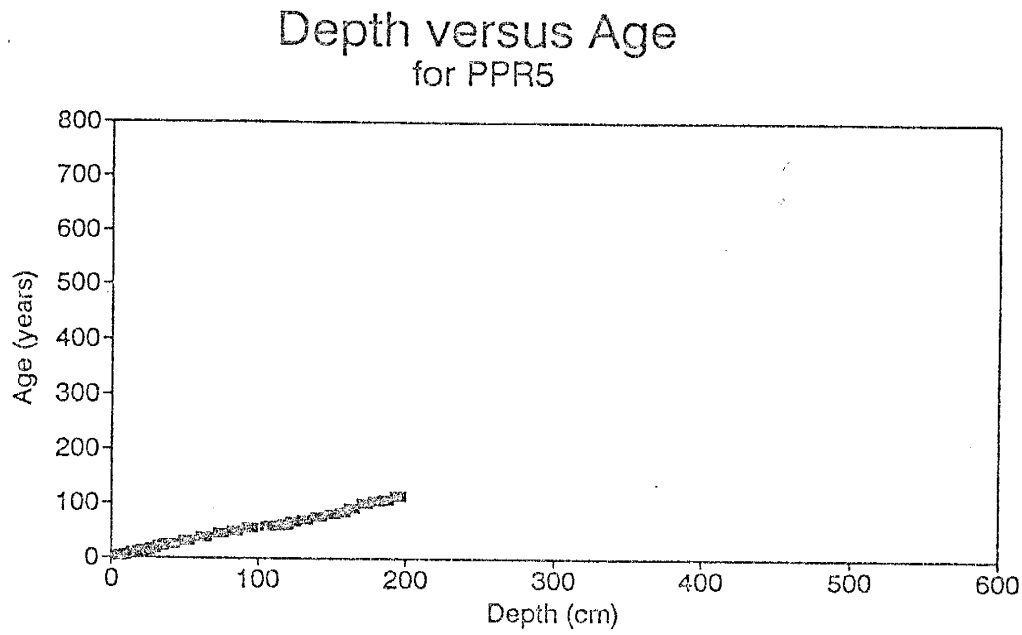

(b)

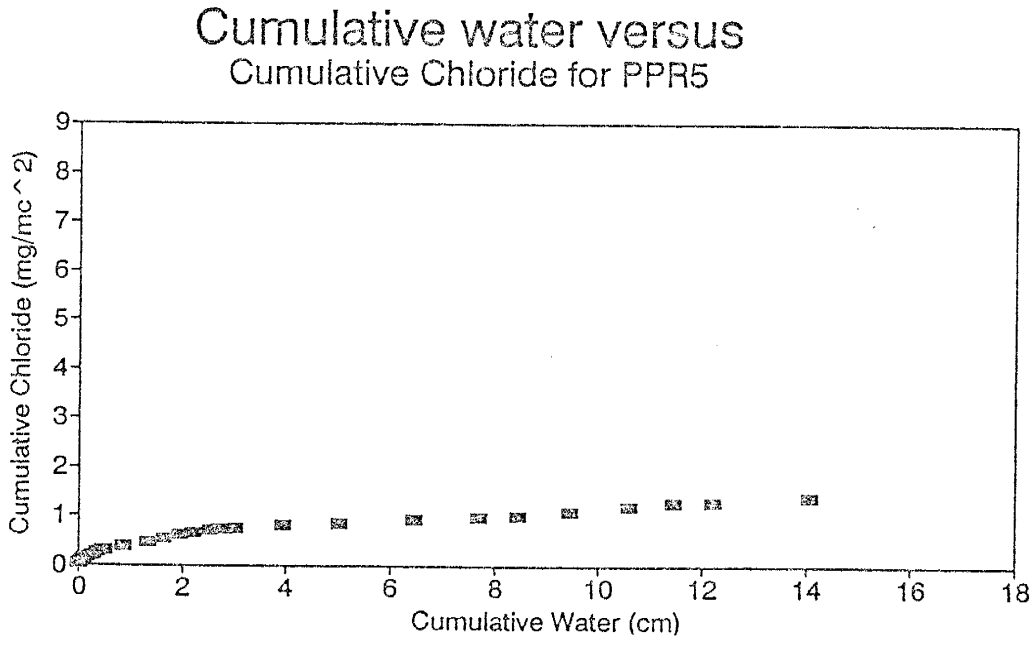

Figure 22: a) Depth vesus age for PPR5
b) Cumulative water versus cumulative chloride for PPR5

PPR5b, was collected. However, at this time this only oxygen and hydrogen data is available for analysis, chloride data has not been received.

PPR5 and PPR5b exhibit the effects of evaporation and obtain steady state $\delta^{18}O$ values of -2.8‰ (Figure 23a) and -2.9‰ (Figure 23b) respectively. Both curves also show a slight isotopic enrichment bulge between 100 cm and 150 cm. With respect to hydrogen, both profiles exhibit an evaporation front. No steady state δD value can be independently estimated for PPR5 because difficulties with sample storage and limited availability of water lead to an incomplete profile for PPR5 (Figure 24a) but a steady state value of approximately -42 ‰ can be estimated for PPR5b (Figure 24b). Both δD/δO profiles are remarkably similar to the previous profiles. In the case of PPR5, values range from -30 $‰_{\delta D}$ to -55 $‰_{\delta D}$ and cluster between -4$‰_{\delta O}$ and -2$‰_{\delta O}$ (Figure 25a). There are so few points from above the evaporation front, that an evaporation slope for PPR5 cannot be reasonably estimated. The range of values for PPR5b are slightly more restricted with respect to δD, ranging from -35 $‰_{\delta D}$ to -52 $‰_{\delta D}$ (Figure 25b). The range of oxygen values is the same as for PPR5. In this case there are enough points to estimate an evaporation slope for PPR5b of about 3.

PPR6 Depth versus volumetric water content for PPR6 shows an increase with depth and a water bulge between 50 and 110 cm (Figure 26a). The volumetric water content values are as high as 0.10 at approximately 80 cm. The chloride concentration profile for PPR6 exhibits a steady state value of approximately 1500 $^{mg}/_{kg}$ (Figure 26b). Root zone effects are relatively obvious between 0 cm and 40 cm.

(a)

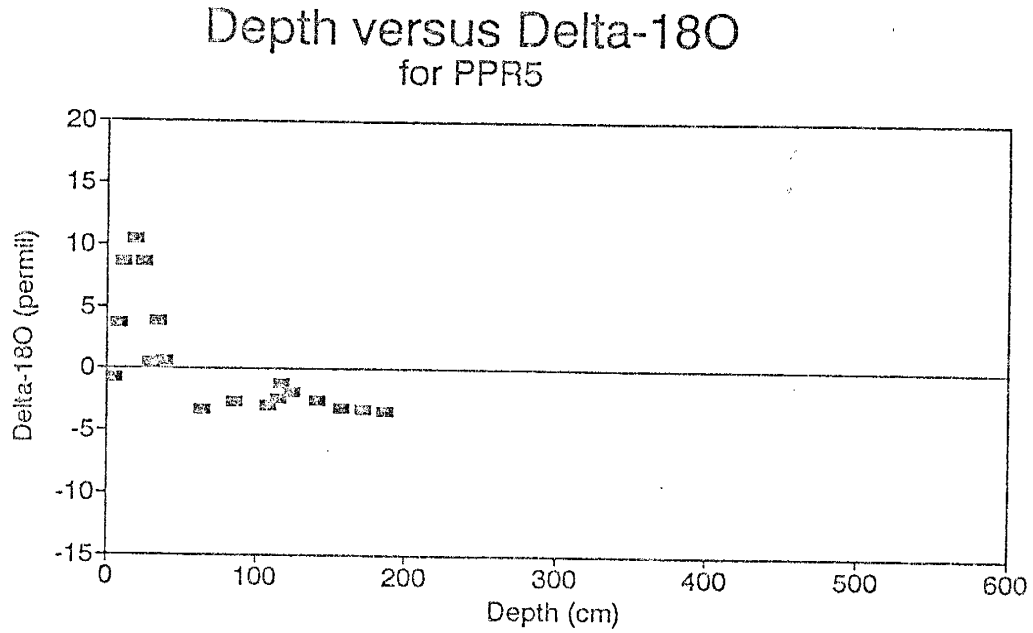

(a)

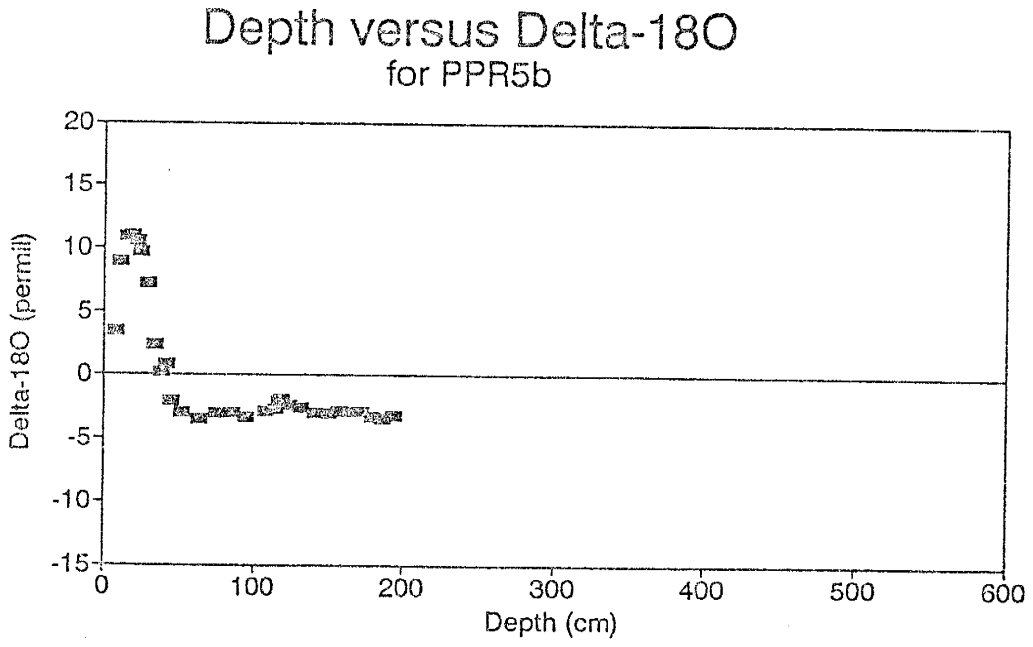

Figure 23: a) Depth versus $\delta 18\overline{O}$ for PPR5
b) Depth versus $\delta 18O$ for PPR5b

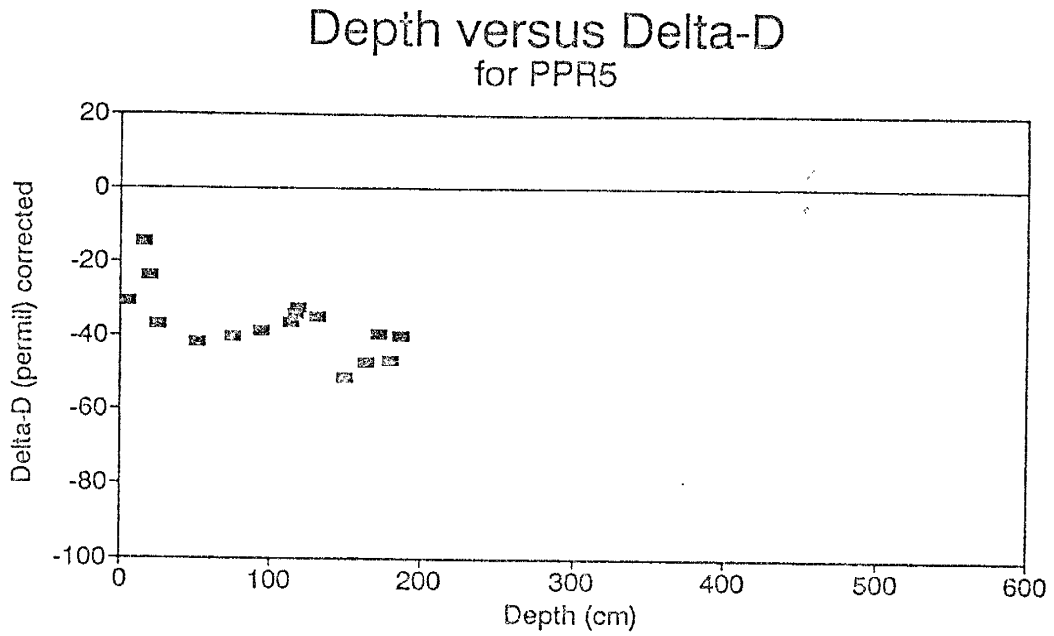

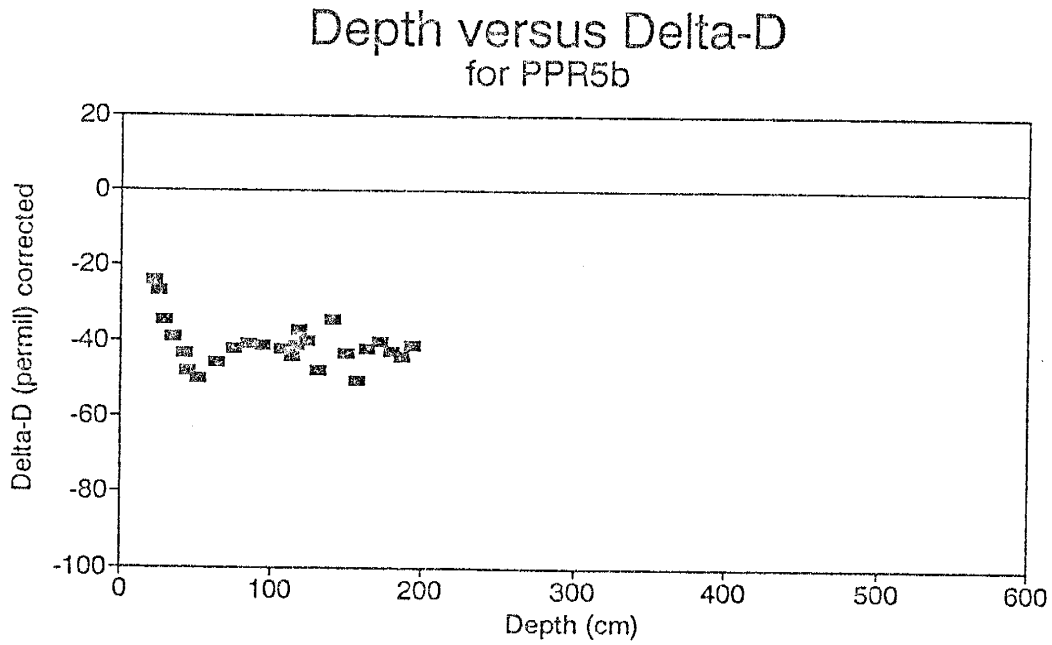

Figure 24: a) Depth versus δDfor PPR5
b) Depth versus δD for PPR5b

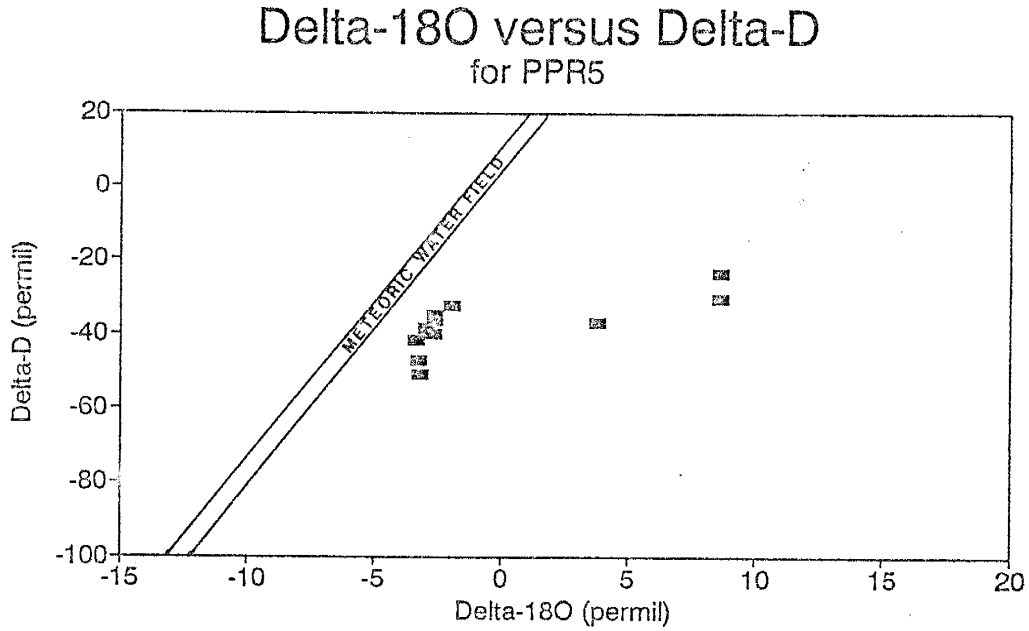

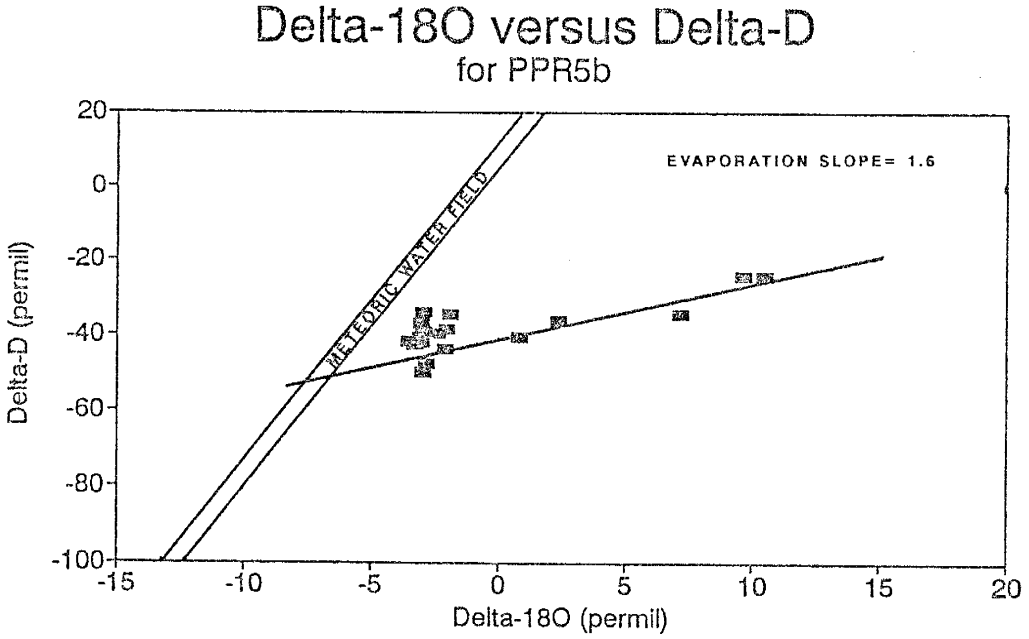

Figure 25: a) δ18O versus δD for PPR5
b) δ18O versus δD for PPR5b

(a)

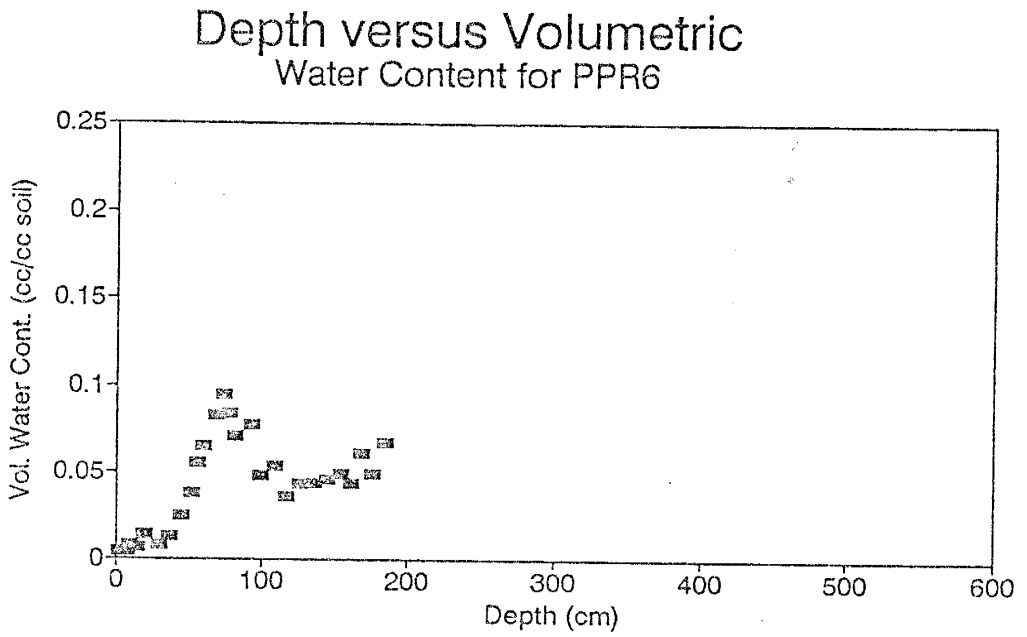

(b)

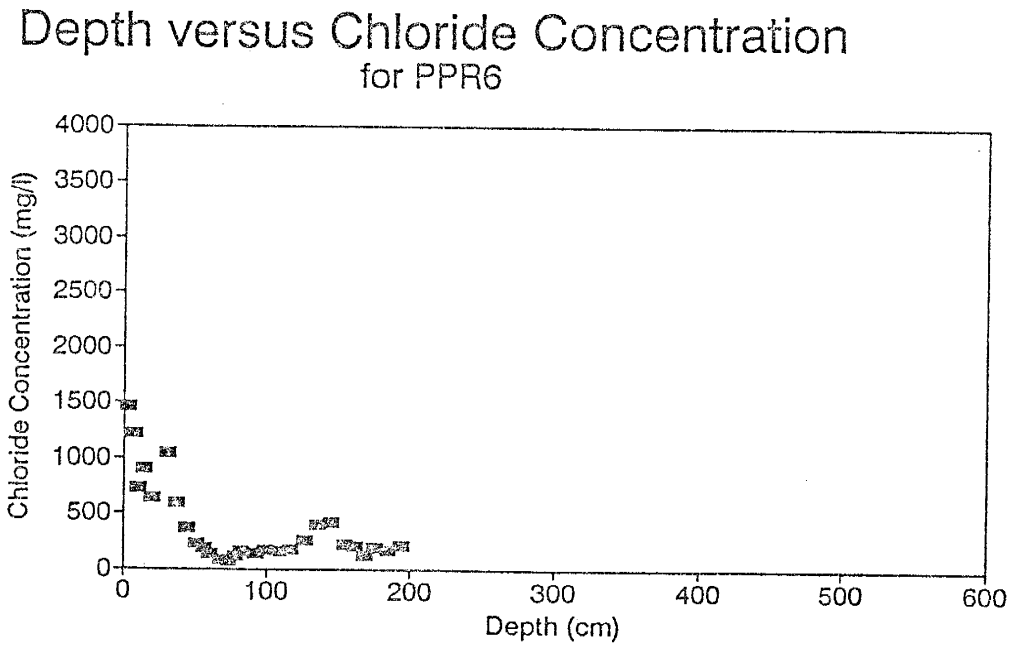

Figure 26: a) Depth versus volumetric water content for PPR6
b) Depth versus chloride concentratin for PPR6

(a)

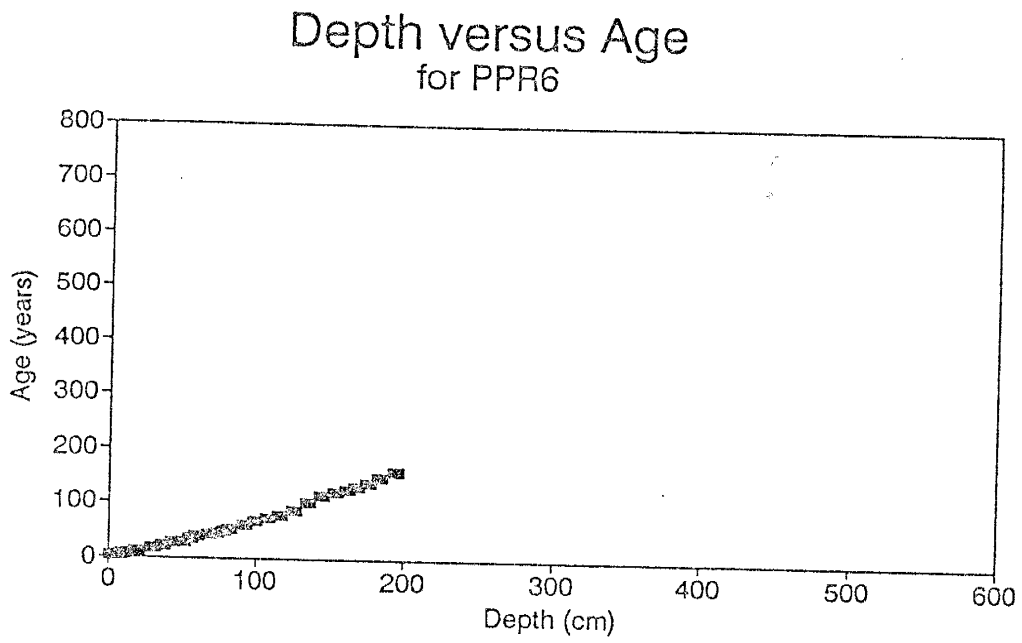

(b)

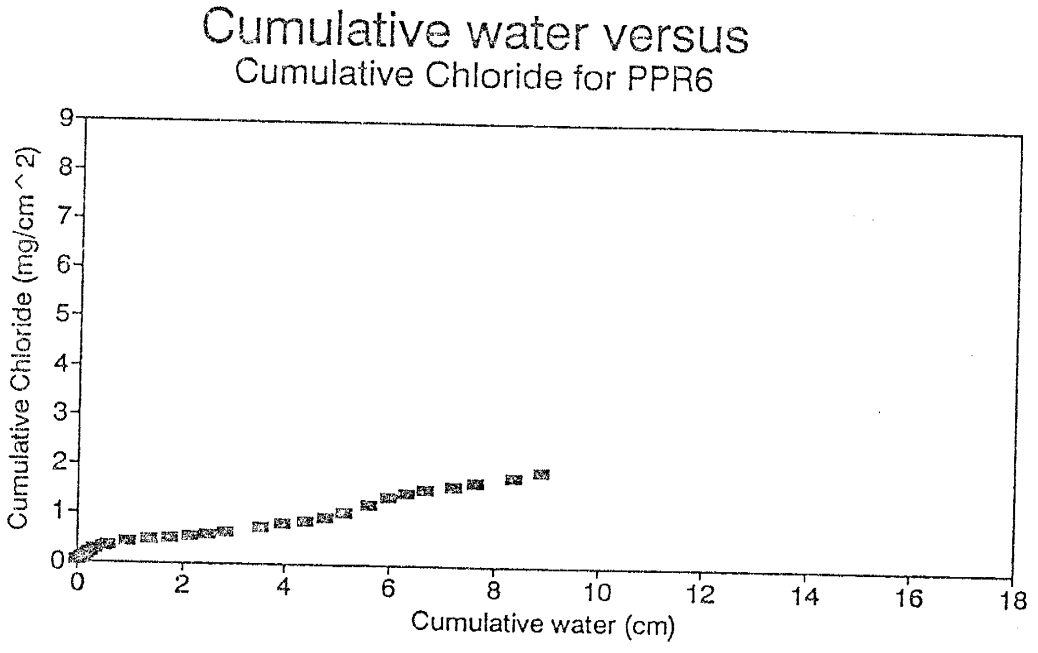

Figure 27: a) Depth versus age for PPPR6
b) cumulative water versus cumulative chloride for PPR6

(a)

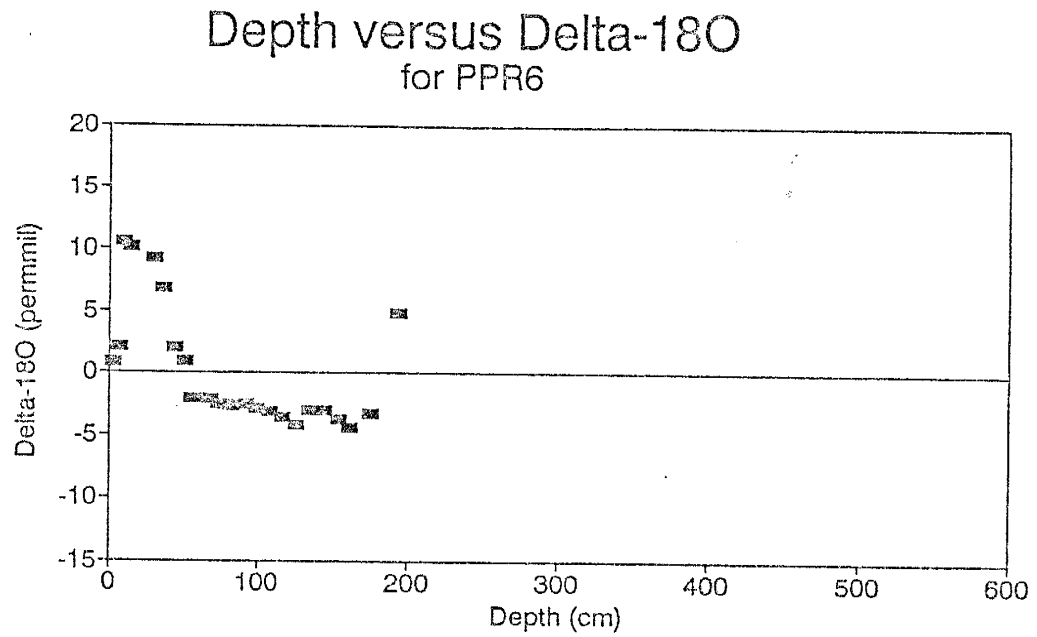

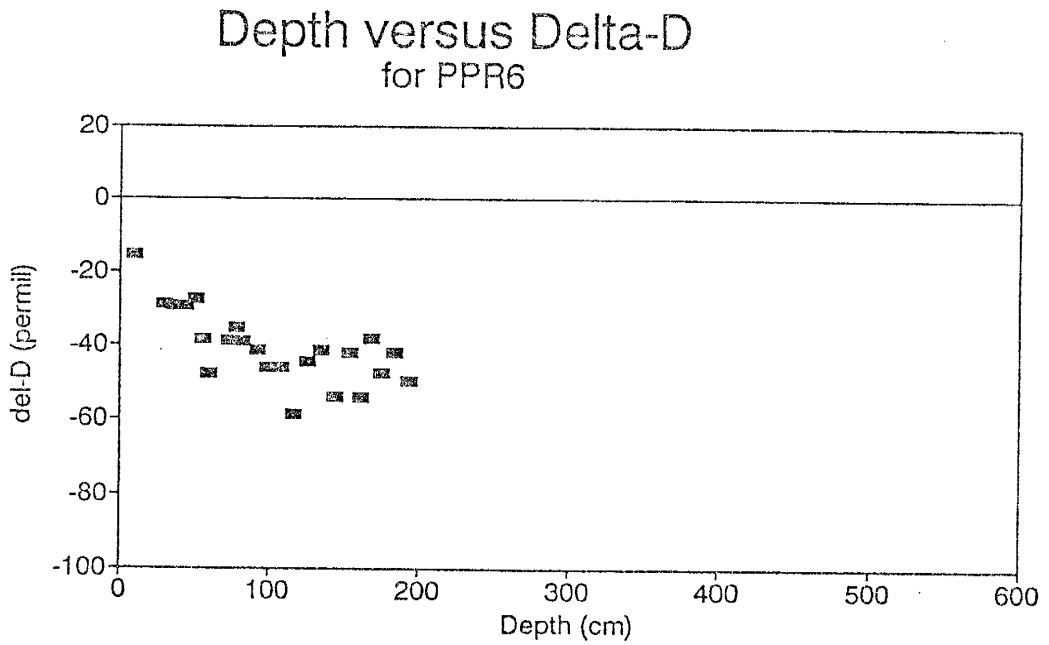

Figure 28: a) Depth versus δ18O for PPR6
b) Depth versus δD for PPR6

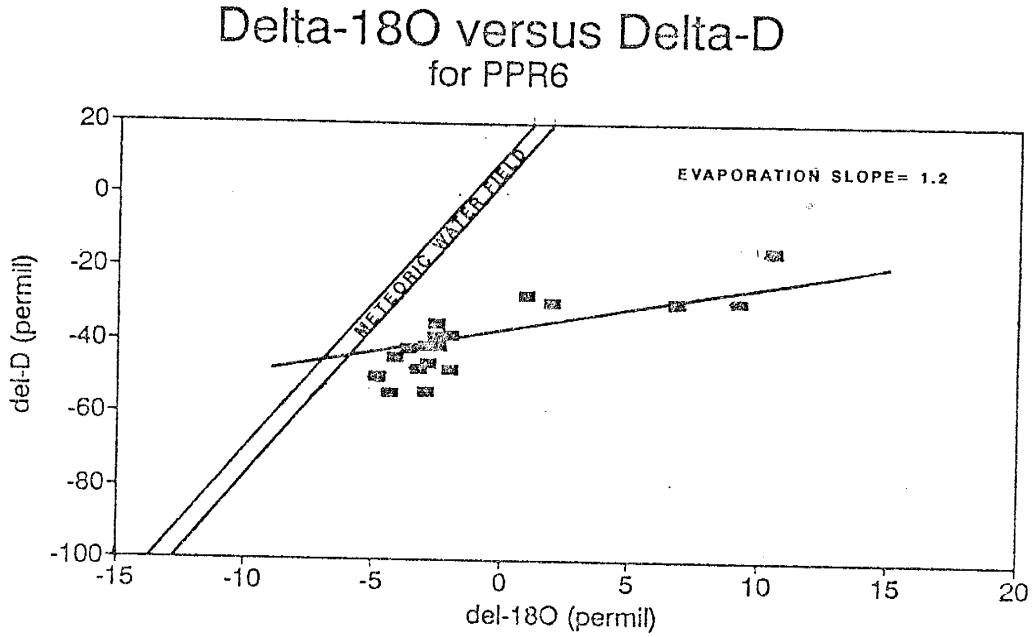

Figure 29: a) δ18O versus δD for PPR6

Further evaluation of the chloride data estimate a bottom hole age of 158 years at 213 cm (Figure 27a). Cumulative water versus cumulative chloride shows a slightly different curve than the other PPR data sets (Figure 27b). The graph shows the steepest part of the line is near the surface indicating a rapid increase in chloride concentration, probably due to root zone effects. The deepest segments of the curve show recharge to be about 0.56 $^{mm}/_{year}$ (Figure 27b).

Oxygen data exhibits a well developed evaporation front and a steady state value of -2.9‰ (Figure 28a) which correlates well with the data from PPR5 and PPR5b. With respect to δD, the profile for PPR6 is not well defined (Figure 28b). Near the surface, data suggest the presence of an evaporation front but scatter obscures any definite determination. Also, no steady state value can be estimated, because scatter obscures that determination as well. In spite of the scatter observed in the data, a well defined compositional field and evaporation slope can be determined when the data is plotted in $\delta D/\delta^{18}O$ space (Figure 29). The field ranges from approximately -5 to -2 with respect to $\delta^{18}O$ and -35 to -60 with respect to δD. An evaporation slope of 1.2 is estimated for PPR6.

INTERPRETATION

This section uses chloride concentrations and stable isotopes to identify the physical processes that affect infiltration as it moves down through the sediment profile. Among the processes discussed are evaporation, transpiration and topographic effects on the isotopic composition and rates of vertical recharge.

Chloride Concentration and Related Variables

Chloride concentrations in soil can be used to determine depth versus age profiles, bottom hole age and recharge rates. In order to evaluate these results, it is necessary to first examine physical processes which affect the chloride and water movement. The calculation to determine age profiles and recharge rates are based on moisture content and chloride concentrations in the sediments. Therefore it is necessary to examine these independent variables to understand the physical processes that affect them and how they affect infilration and age determinations.

The first variable, volumetric water content (θ), is controlled by (1) soil texture, (2) evaporation, (3) transpiration and (4) time since the last precipitation event. The effect of soil texture can be observed in PPR1, PPR3, PPR5 and PPR6 at 350 cm, 500 cm, 100 cm and 75 cm respectively. At each of these depths, in their respective holes, a clay layer was encountered. In the case of PPR3 the contact between the clay layer and sand was gradational. The gradational transition from sand to clay results in an attenuated increase in θ, whereas the θ increase is obvious in the other three.

Evaporation and transpiration affect all of the profiles similarly. These effects simply result in reduced water contents throughout the length of the hole.

The final controlling factor is the time since the last precipitation event. In PPR1, PPR2, PPR3 and PPR4 a θ spike is observed near the surface. The spike in PPR1 and PPR2 is at 50 cm and is the same magnitude in each of the profiles. The flatness of the spike is probably due to a relatively long time period between the event and when the samples were collected. In PPR3 the spike is better defined. It occurs at 50 cm, similar to PPR1 and PPR2 but is of greater magnitude. The depth of the spike suggests it is the same or similar event as at PPR1 and PPR2. The difference in magnitude is probably a result of increased water input due to the topographic effect of the sink-hole in which PPR3 is located. The exact amount of the excess water is uncertain, however personal accounts indicate that large storms leave standing water in the sink-hole, sometimes covering the hole to a depth of about 200 cm. PPR4 was collected the following summer and exhibits a severe θ spike at approximately 30 cm. The intensity of the spike suggests very little time had elapsed from the event to the collection date although weather station data has not been examined to definitively prove the relationship. If there was a storm which showed up as a peak in θ values in PPR4, the same or similar peak would be expected in PPR5 and PPR6, however, this is not the case. The presence of the clay layers near the surface are probably masking the presence of a peak in PPR5, PPR5b and PPR6.

Since infiltration calculations are based on a cumulative water versus cumulative chloride graph, it is obvious the θ values will affect the calculation of

infiltration. If θ values increase and chloride concentrations remain constant, the effect will be a reduction in the slope of the graph which will increase the infiltration estimate. This effect will be discussed in later paragraphs.

All of the factors that affect moisture content also affect chloride concentration. These factors affect chloride concentration because chloride is only transported through the soil by liquid water. There also seems to be other controls on chloride concentration which contribute to the scatter and are not understood. One interesting feature of the chloride profiles is that they seem to fall into one of two general groupings. PPR1, PPR2 and PPR3 define the first group which exhibits a relatively large amount of scatter and only PPR3 shows an identifiable pattern. PPR1 and PPR2 exhibit a significant amount of scatter, PPR2 more so than PPR1. One possible explanation for the scatter is a contribution of biogenic chloride. PPR1 and PPR2 had notably more fecal matter in the surface samples suggesting more faunal activity in this area and therefore a biogenic influx of chloride from small animals. Also PPR2 was located closer to plants where there is more cover for small animals. As there is a higher concentration of fecal matter at PPR1 and PPR2, it would be reasonable to suggest that there is also more urine present, which would affect chloride input rates and possibly result in a highly variable chloride profile. PPR3 also exhibits some variability but a definite trend can be distinguished from the profile. Chloride concentrations in PPR3 show a bulge from approximately 100 cm to 300 cm. The exact cause of this bulge is unclear. It is possible that roots are penetrating the interval and extracting water, thereby increasing chloride concentration. Below 300

cm, the chloride concentrations stabilize somewhat. Variability is still present, but it is not as significant. By examining PPR3 carefully and comparing it to PPR1, it is possible to suggest a matching profile exists at PPR1, however, more scatter is present. This first group has an additinal feature in common that the second group does not. All of the points in PPR1, PPR2 and PPR3 were processed here at the NMIMT. This common factor suggests a more likely cause of scatter is analytical error. However, this interpretation is in question because each value was arrived at by averaging multiple analyses and in many cases, duplicate samples were reproducible. Therefore, the cause of the scatter is still unclear.

The second group of profiles (PPR4, PPR5 and PPR6) exhibit well defined trends. PPR4 shows a spike chloride concentration near the surface. The cause of this spike is probably the combined effects of evaporation and transpiration. These two effects reduce the amount of liquid water available to transport chloride further downward, resulting in an increase in concentration. The peak for PPR5 and PPR6, like the peak in PPR4 is probably due to evaporation and transpiration. In the case of PPR6, transpiration is probably dominant because large plants are nearby. However, in the case of PPR5, evaporation is most likely dominant because there are very few plants nearby and PPR5 is in a bowl shaped trough between dune crests which collects heat from incident solar radiation more readily.

In a similar way to volumetric water content, chloride concentration affects infiltration and age determinations. In the case of age, there is a linear relationship between chloride concentration and the age contribution of any one sample. For

recharge rates the chloride concentration is inversely proportional to recharge. For example, if θ is held constant and chloride concentration is reduced the calculated recharge will increase. As stated earlier the relationship of recharge to θ and chloride concentration will be saved for examination in later paragraphs.

One of the goals of this study is to determine the stable isotopic composition of modern infiltration through the vadose zone. Because the area around the WIPP site has a very deep water table and low rates of infiltration, it is possible that water deep in the vadose zone is quite old (>10,000 years). For this part of the study only the shallow portions of the soil profile are sampled to look at the recently infiltrated water. The residence time of this water can be calculated using a chloride accumulation rate which yields an apparent "age" for the water at any given depth. Age relationships do in fact, verify the modern nature of the water samples. Estimates of age range from 114 years at PPR5 to 575 years at PPR4. PPR3 shows an age of 708 years, however this is probably not accurate. Since PPR3 is in a sink-hole and receiving additional chloride contributions, the calculation yields a false age.

Recharge estimates are perhaps the most interesting aspect of chloride usage to deal with. There is evidence that strongly suggests topography affects recharge estimations. The most pronounced effect of topography is observed in the profiles from the dune fields. PPR1, which is located on a dune crest, has the smallest estimate of recharge at .23 mm/yr. This reduced value of recharge is probably the result of locally divergent flow conditions that exist at dune crests. A recharge rate from PPR2 was not calculated because only samples from the evaporation front were

processed originally and therefore the estimate would be meaningless. PPR5 which is located in the dune trough immediately adjacent to PPR1 provides an estimate of 1.98 mm/yr. This estimate is high compared to other sites due to the locally convergent flow conditions of a dune trough. PPR3 and PPR4 , which estimate vertical recharge rates of 0.67 mm/year and 0.77 mm/year respectively, are probably overestimating recharge slightly, similar to PPR5. As indicated earlier PPR3 is in a sink-hole which receives not only it's share of direct precipitation but also runoff from the surrounding slopes. This runoff component would increase not just the amount of chloride input but also water which would result in the over estimation of regional recharge. Evidence for over estimation of recharge by the PPR4 profile is also present. PPR4 is located on a flat area where mudcracks were observed. The presence of mudcracks suggests occasional standing water in the area. The sediment profile for PPR4 was very well sorted. This sorting of the sand and lack of silts and clays could result in rapid infiltration of the water at this point leading to the overestimation of recharge on a regional scale. The final hole, PPR6, estimates recharge at 0.56 mm/yr. This value is probably the most representative value for regional application. Unlike all of the previous holes, no topographic extremes exist at this site. The area is a semi-vegetated, sand-plain. Although the estimates for recharge from each of the holes are variable, they all fall within ranges determined by previous workers for arid regions(0.1 to 3 mm/year; Phillips et al., 1984; Allison et al., 1985; Phillips and Stone, 1985; Mattick et al.,1987; Stone, 1990; and Scanlon, 1991).

Stable Isotope Profiles

In arid environments, the profiles for δD and $\delta^{18}O$ versus depth have a characteristic shape. This shape is directly related to the physical processes that affect the isotopic composition of water as it passes through the unsaturated zone. Near the ground surface, the values for δD and $\delta^{18}O$ exhibit a shift towards heavier compositions, this is caused by the fractionation of the light isotope into the vapor phase during evaporation. As this heavy water moves downward, it mixes with upward moving lighter vapor such that the overall composition begins to return to lighter values. The composition further down hole begins to stabilize and achieves a steady state. This steady state composition is considered representative of water moving downward through the unsaturated zone to become recharge.

The PPR series data support the assertion of a characteristic and predictable shape for arid soil profiles. All of the profiles exhibit the characteristic shape with respect to $\delta^{18}O$ except for PPR1. Profiles for PPR2, PPR3, PPR4, PPR5, PPR5b and PPR6 all exhibit a reasonably well defined curve, consisting of 1) an evaporation front, 2) mixing zone and 3) a steady state value. PPR1 does not show the characteristic profile due to the analytical difficulties mentioned in the methods sections. The data from PPR1 groups itself into two distinct vertically oriented populations and there is no data in the region near the surface. The lack of data near the surface is due to analytical difficulties experienced at the start of this project. The two distinct populations can be attributed to analytical difficulties related to volume versus equilibration time effects as described in Appendix IV.

A similar statement may be made concerning δD profiles for each of the holes. All of the holes exhibit the characteristic profile for arid environments. Aberrations from the expected curves are due to missing data points, from insufficient amounts of water to process or values obtained from improperly sealed storage bottles.

A common way to compare water compositions is to plot them in $\delta D/\delta^{18}O$ space. The result is a set of points which characterize a field of compositions for a particular population of water samples. The plots usually consist of a relatively well defined group of compositions usually samples taken from below the evaporation front. A second set of points form a line which corresponds to samples taken from above the evaporation front. This line is defined by the change in isotopic composition as water evaporates from the soil profile. The slope of this line is called the evaporation slope. The evaporation slope is most dependent on the relative humidity. In addition to plotting all of the PPR data on a $\delta D/\delta^{18}O$ graph the following features were included, Meteoric Water Field, Modern Delaware Basing Recharge, Culebra and Magenta water compositions, water from pools in the Carlsbad Caverns and water from ceiling seeps in the Carlsbad Caverns.

The compositional field of each of the PPR series can be used to determine the composition of the source precipitation. By measuring the slope of the evaporation

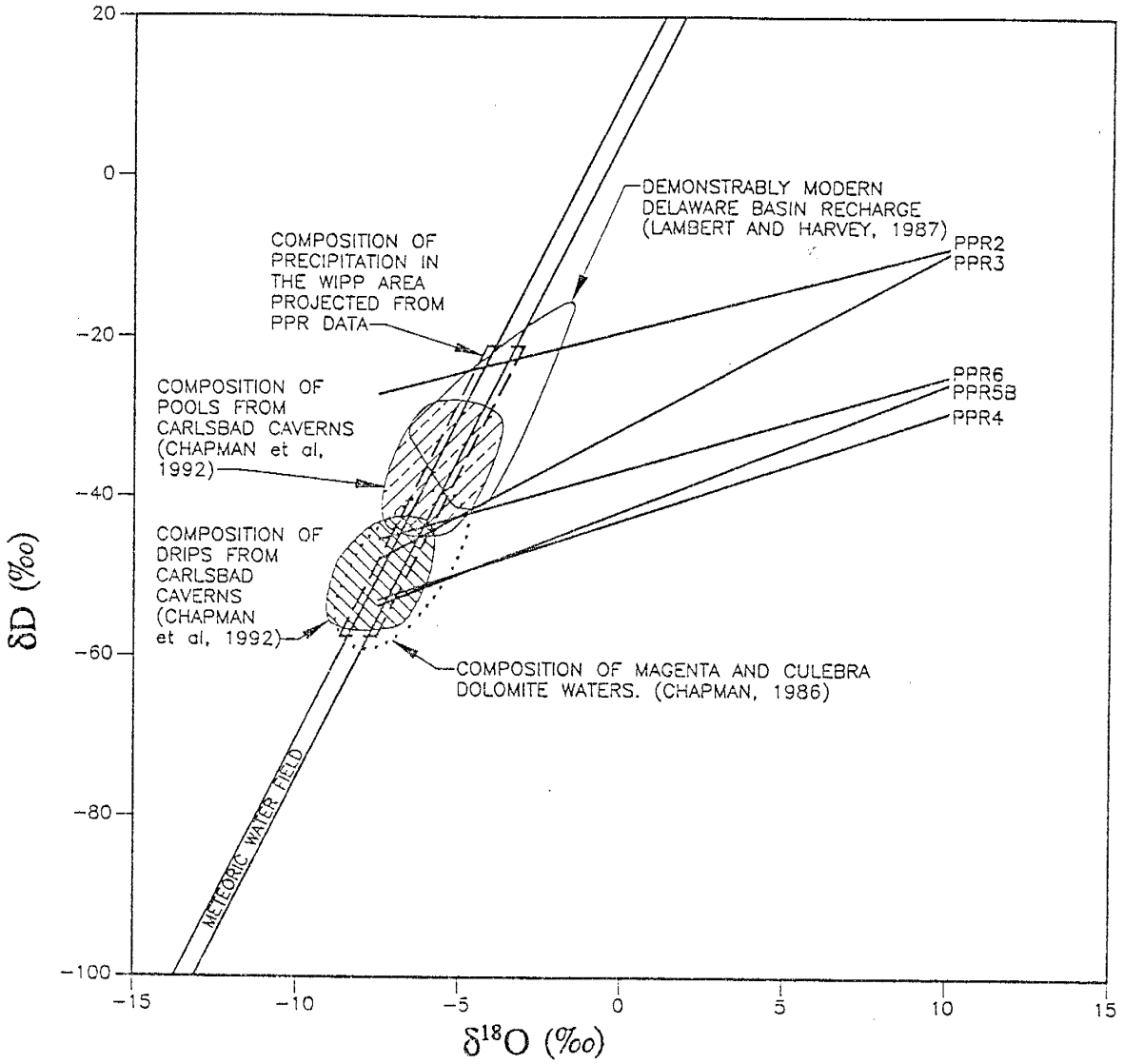

Figure 30: Compositions of source precipitation calculated from PPR data, Magenta and Culebra aquifers, ceiling drips and pools from Carlsbad Caverns compared to the Demonstrably Modern Delaware Basin Recharge composition.

line and projecting the recharge composition along that line to the meteoric water field (Epstein et.al., 1965; Epstein et. al., 1970 and Craig 1961) the pre-evaporation composition can be estimated. The meteoric water field is the region between the following curves:

$$\delta D = 8\delta^{18}O + 5 \qquad \text{(Epstein et al., 1965:1970)}$$

$$\delta D = 8\delta^{18}O + 10 \qquad \text{(Craig, 1961)}$$

Data sets PPR2, PPR3, PPR4 PPR5b and PPR6 have evaporation slopes ranging from 1.1 to 2.2, which is a reasonable range for an arid environment. By projecting the compositional fields for each of the PPR data sets along their respective evaporation slopes to the meteoric water field, an overlap between the, Culebra/Magenta waters, the water from ceiling seeps in the Carlsbad Caverns and the PPR-derived precipitation is observed (Figure 30). Culebra and Magenta water compositions were obtained from previous research (Cooper et al., 1971; Mercer et al.,1979; and Lambert et al., 1984). The compositions of ceiling seeps and pools were determined by Chapman et.al. (1992).These shared fields indicate the Culebra/Magenta waters and the ceiling seep waters could be the direct result of modern precipitation infiltrating through some process which does not cause significant evaporation such as quick recharge through karst. Furthermore, by evaporating these compositions in a humid environment such as the caverns themselves, the compositions would shift along a line with a steep slope (possibly 7 or 8) to produce the Modern Delaware Basin Recharge field (Lambert and Harvey, 1987). It is important to note that the composition of water taken from the pools in the Carlsbad Caverns share a significant area with the

water defined as Demonstrably Modern Delaware Basin Recharge. Since the water in the pools is the product of evaporation the ceiling seep composition in high humidity, it is reasonable to say that both waters are the result of modern processes. The following table summarizes the data obtained from the PPR series.

Summary of PPR Data:
Including Total Depth (TD), Age (A), Recharge (R),
and steady state values for $\delta^{18}O$ and δD

Hole	TD (cm)	A (yr)	R (mm/yr)	$\delta^{18}O$ (‰)	δD (‰)
PPR1	403	403	0.23	****	****
PPR2	208	308	****	-2.5	-42
PPR3	589	708	0.67	-7.8	****
PPR4	443	575	0.77	-1.4	-42
PPR5	199	114	1.98	-2.9	****
PPR5b	199	****	****	-2.8	-42
PPR6	213	158	0.56	-2.9	****

**** Values are indeterminate due to missing data and/or analytical errors.

CONCLUSIONS

Individual estimates of vertical recharge from the chloride mass balance method cannot be used as regional values. The estimate of vertical flux varies significantly from one point to another within a relatively small area. An example of this variability is observed in the dune field, where an estimate from a trough (PPR5) is an order of magnitude larger than estimates from the adjacent crest (PPR1). Therefore, in order to develop a better estimate of regional vertical recharge through shallow soils it is necessary to attempt a weighted average of point estimates. The average must account for the areal distribution of sediment types, topography and floral density.

The data obtained from the PPR series ceiling seeps from the Carlsbad Caverns and the Culebra and Magenta waters have similar compositions. This similarity suggests stable isotopes cannot be used to rule out a modern component of recharge. The projected composition of source precipitation for the PPR samples shares a significant portion of the $\delta D/\delta^{18}O$ space with the Culebra and Magenta water and ceiling seep fields, indicating the Modern Delaware Basin Recharge field defined by Lambert and Harvey (1987) should be expanded to include these compositions. Therefore, the PPR data suggests Chapmans' (1986) assertion of a modern component of recharge in the Magenta and Culebra Dolomite aquifers is possible.

REFERENCES

Allison, G.B., Barnes, C.J., Hughes, M.W., and Leany, F.W., 1984. Effect of Climate and Vegetation on Oxygen-18 and Deuterium Profiles in Soils. *Isotope Hydrology*. IAEA, Vienna, 105-124.

Allison, G.B., Stone, W.J., and Hughes,M.W., 1985, Recharge in Karst and Dune Elements of a Semi-Arid Landscape as Indicated by Natural Isotopes and Chloride, *Journal of Hydrology* 76:1-26

Barnes, C.J. and Allison, G.B., 1983. Distribution of D and ^{18}O in Dry Soils: *Journal of Hydrology*. 60:141-156

Chapman, J. (1986). Stable Isotopes In southeastern New Mexico Groundwater: Implications for Dating Recharge in the WIPP Area. *EEG Report #35*, 76p.

Chapman, J., Ingraham, N., and Hess, J., (1992), Isotopic Investigation of Infiltration and Unsaturated Zone Flow Processes at Carlsbad Caverns, New Mexico. *Journal of Hydrology*., 133, p. 343-363.

Cooper, J.B. and Glanzman, 1971, Geohydrology of Project Gnome Site, Eddy County, New Mexico, *U.S. Geol. Surv. Prof Paper* 712-A, pp A1-A24

Craig,H., 1961, Standard for Reporting Concentrations of Deuterium and Oxygen-18 in Natural Waters, *Science*, V. 133 pp 1833-1834

Epstein,S., Sharp, R.P., and Gow, A.J., 1965, Six-year Record of Oxygen and Hydrogen Isotope Variations in South Pole Firn., *Journal of Geophysical Research*, V. 70, pp 1809-1814

Epstein, S., Sharp, R.P., and Gow, A.J., 1970, Antarctic Ice Sheet: Stable Isotope Analyses of Byrd Station Cores and Interhemispheric Climatic Implications, *Science*, V. 168, pp 1570-1572

Kendall, C. and Coplen, T.B. (1985). Multisample Conversion of Water to Hydrogen by Zinc Reduction for Stable Isotope Determination. *Analytical Chemistry*, June, p. 1437-1446.

Knowlton, R.G. Jr., Phillips, F.M. and Campbell, A.R. (1989). *Technical Completion Report No. 237, New Mexico Water Resources Research Institute*, New Mexico State University, Las Cruces, NM, 88p.

Lambert, S. and Harvey, D. (1987), Stable-Isotope Geochemistry of Groundwaters in the Delaware basin of Southeastern New Mexico. *Sandia Report SAND87-0138*, 218p.

Lambert, S., and Robinson, K.L., 1984, Field Geochemical Studies of Groundwaters in Nash Draw, Southeastern, New Mexico, Sandia National Laboratories, *SAND83-1122*, pp 1-38

Mattick, J.L., Duval, T.A. Phillips F.M., 1987. Quantification of Groundwater Recharge rates in New Mexico Using Bomb ^{36}Cl, Bomb ^{3}H and Chloride as Soil-water Tracers. *Water Resources Research Institute, Report 220* Las Cruces, New Mexico

Mercer, J.W.,1983, Geohydrology of the Proposed Waste Isolation Pilot Plant site, Los Maddens area, Southeastern, New Mexico, *U.S. Geol. Surv. Water-Resources Investigation 83-4016*, pp 1-113

Mercer, J.W. and Oar, B.R., 1979, Interim Data report on the Geohydrology of the Proposed Waste Isolation Pilot Plant site, Southeastern, New Mexico, *U.S. Geol. Surv. Water-Resources Investigation 79-98*, pp 1-178

Phillips, F.M., Trotman, K.N., Bentley, H.W. and Davis, S.N., 1984. The Bomb 36Cl Pulse as a Tracer for Soil-water Movement near Socorro, New Mexico. *New Mexico Bureau of Mines and Mineral Resources. Water Quality Pollution in New Mexico. Hydrologic Report 7* pp 270-280

Phillips, F.M., and Stone, W.J., 1985. Chemical Considerations in Groundwater Recharge, Socorro New Mexico, Symposium of Water and Science, New Mexico Water Resources Research Institute, Las Cruces, New Mexico 109-125

Roether, W. (1970). Water-CO_2 Exchange Set-up for the Routine ^{18}O Assay of Natural Water. *International Journal of Applied Radiation and Isotopes*, **21**, 379-387.

Scanlon, B. (1991). Evaluation of Moisture Flux From Chloride Data in Desert Soils. *Journal of Hydrology*, **128**, 137-156.

Sharma, M.L. and Hughes, M.W., (1985). Groundwater Recharge Estimation Using Chloride, Deuterium and Oxygen-18 Profiles in the Deep Coastal Sands of Western Australia. *Journal of Hydrology*, 81, 93-109 (1985).

Socki, R., Karlsson, H. and Gibson, E., (1992), Extraction Technique for the Determination of Owygen-18 in Water Using Peevacuated Glass Vials, *Analytical Chemistry, 64,829-831*.

Sandia National Laboratories and United States Geological Survey, 1979. Basic Data Report for Drillhole WIPP27 (Waste Isolation Pilot Plant-WIPP), *Sand 79-0281*

Stone, W.J., 1990. Natural Recharge of the Ogallala Aquifer Through Playas and Other Non-Streamchannel Settings, Eastern New Mexico. In T.C. Gustovson (editor); Geologic Framework and Regional hydrology; Upper Cenozoic Blackwater Draw and Ogallala Formations, Great Plains. University of Texas Austin, Bureau of Economic Geology pp 180-192

APPENDICES

APPENDIX I

Volumetric Water Content (VWC)

Volumetric water content is a measure of the volume of water per volume of soil, therefore it is unitless and is calculated using the following equation:

$$\theta = \frac{V_w}{V_t} = \frac{V_w}{V_w + M_s * \frac{1}{\rho_{sb}}}$$

θ = VWC (cm^3 water/100cm^3 soil)
V_w = volume of water (cm^3)
V_t = volume of soil (cm^3)
M_s = mass of soil (g)
ρ_b = soil bulk density (g/cm^3)

* ρ_b for the PPR sands was experimentally determined to be 1.39 g/cm^3.

Sample VWC Calculation

Sample designation: PPR5 (184-190)
$V_w = 9.55cm^3$
$M_s = 91.1g$
$\rho_{sb} = 1.39g/cm^3$

Therefore,

$$\theta = \frac{9.55}{9.55 + 91.1 * \frac{1}{1.39}} = .1272$$

APPENDIX II
CHLORIDE CONCENTRATION AND EVALUATION

Chloride Concentration

After soil distillation is complete, chloride is leached from the distilled soil. A ion-specific electrode is used to measure the electrical potential (mv) of the leachate. Distilled soils are prepared by combining them with an Ionic Strength Adjuster (ISA) solution in Nalgene Oak Ridge centrifuge tubes. The mixtures are shaken a minimum of 6 hours. Standards are prepared each day to develop a daily calibration curve for the electrode. The procedure is performed in triplicate on each soil and the values are averaged to determine a final value.

Procedure

1. Mix ISA with HNO3. (2 ml ISA/100 ml water)
2. Mix approximately equal masses (10 g) of soil and ISA solution.
3. Prepare 3 mixtures of each soil.
4. Shake mixtures for a minimum of 6 hours.
5. Centrifuge the mixtures.
6. Prepare standards by serial dilution of solutions with known chloride concentrations and ISA solution. Use 100, 50, 10, 5, 3 and 1 ppm standards.
7. Put electrode in ISA for 30 Minutes to stabilize.
8. Measure the standards beginning with the lowest concentration.
9. develop a semi-logarithmic calibration curve
   X = millivolts.
   Y = log [concentration] (ppm)
10. Measure each mixture and compare with the calibration curve to obtain the concentration n.

Evaluation

Time/Age

After the chloride concentration has been determined for each soil sample, the data is used to determine age versus depth profiles and vertical recharge rates. Since the concentration is given in ppm of the soil, we can use the following equation to determine the time interval represented by each depth interval.

$$T = \frac{C_i * d_i * \rho_b * X}{C_o * P}$$

T	=	Age (years)
C	=	Chloride concentration (mg/kg)
d_i	=	Depth interval (cm)
ρ_b	=	Dry bulk density (g/cm^3)
X	=	Conversion factor (1kg/1000g)
C_i	=	Chloride input (mg/cm^3)
P	=	Precipitation (cm/yr)

$\rho_b = 1.39\ g/cm^3$

(ρ_b for fine sand was determined experimentally in the Stable Isotope Laboratory here at NMIMT)

$C_o = 0.32*10^{-3}\ mg/cm^3$

(C_o was determined by interpolation from chloride concentration in precipitation data from Las Cruces, Socorro and the Chihuahuan desert of Texas (Scanlon, 1991). The value was substantiated by Bomb-pulse ^{36}Cl calculations performed by Dr. Fred Phillips.)

P = 38 cm/yr

(This value was calculated from 1970-1987 precipitation records)

therefore we can rewrite the equation as:

$$T = C * d_i * \frac{1.39}{(1000)*(.32*10^{-3})*(38)}$$

simplifying to:

$$T=.1143*C*d_i$$

Where:
T = Time represented by the interval i (yr)
C_i = Chloride concentration in the interval i (mg/Kg)
d_i = Depth interval (cm)

To calculate the time at any point in the soil column (T_i),

$$T_i=\sum(.1143)*C_i*d_i$$

Where: C_i = Chloride Concentration for interval i ($^{mg}/_{Kg}$)
d_i = Depth interval (cm)

Recharge

To calculate the recharge rate using chloride data, the volume of water present in each interval (cm) must be determined and chloride concentration must be put into units of mg/cm^2. Therefore the following calculations must be made:

(1) Volume of water in cm

Since θ is unitless, we must take into account the length of the depth interval, therefore we must multiply θ by the depth interval.

$$V=\theta*d_i$$

(2) Conversion of mg/kg to mg/cm^2

$$C_{i_b}=C_{i_a}*X*\rho_b*d_i$$

Where: C_{ib} = Chloride concentration ($^{mg}/_{cm2}$)
C_{ia} = Chloride concentration ($^{mg}/_{kg}$)
X = Conversion factor (1kg/1000g)
ρ_b = Bulk density ($1.39\ ^{g}/_{cm^3}$)
d_i = Depth interval (cm)

After conversion of the above values recharge can be calculated by plotting the cumulative water versus cumulative chloride and using the following equation:

$$R = P * \frac{m}{C_o}$$

Where: R = Recharge ($^{cm}/_{yr}$)
P = Precipitation ($^{cm}/_{yr}$)
m = Slope of line for cumulative water versus cumulative chloride ($^{mg}/_{cm3}$)
C_o= Concentration of chloride in precipitation ($^{mg}/_{cm3}$)

APPENDIX III

DAILY CORRECTIONS FOR OXYGEN AND HYDROGEN

Oxygen Correction

After processing the Oxygen from each of the samples, a correction must be applied to the values obtained from mass spectrometry because these values represent the equilibrated composition of the CO_2 with the liquid H_2O. The Following equation is used to correct the values:

$$\delta^{18}O^{i}_{H_2O} = \frac{Y}{X}\left(\delta^{18}O^{f}_{CO_2} - \delta^{18}O^{i}_{CO_2}\right) + \alpha\left(\delta^{f}_{CO_2} + 10^3\right) - 10^3$$

Where:

δ18OiH2O	=	Initial composition of the water (‰)
δ18OfCO2	=	Final composition of equilibrated CO2 (‰)
δ18OiCO2	=	Initial composition of CO2 (‰)
Y	=	Quantity of CO2 used in equilibration (μmol)
X	=	Quantity of H2O used in equilibration (μmol)
α	=	fractionation constant (= 0.96)

The data was corrected using a computer program written by Robert Knowlton (1989) which performs the calculation automatically.

Hydrogen Correction

Using a commercially available spreadsheet program (*Quattro® Pro*), the measured values for the gas standards are plotted against the accepted values and a linear regression was done. The resulting equation:

$$Y = m_{hd} * X + b_{hd}$$

where: Y = $\delta D_{corrected}$ (‰)
$*m_{hd}$ = daily constant (X Coefficient)
X = $\delta D_{measured}$ (‰)
$*b_{hd}$ = daily constant

* Constants are obtained from the gas standard regression output data for each day on the following pages.

was used to correct the procedural standard data. The procedural standard data was plotted similar to the gas standard data and the resulting equation:

$$Y=m_{ce}*X+b_{ce}$$

where:

Y	=	$\delta D_{corrected}$ (‰)
* m_{ce}	=	daily constant (X Coefficient)
x	=	$\delta D_{measured}$ (‰)
* b_{ce}	=	daily constant

* Constants are obtained from the procedural standard regression output data for each day on the following pages.

we used to correct the PPR data collected on the referenced day.

Sample Calculation for data collected on 9-19-91

On 9-18-91, three reactions each of SMOW,SLAP and GISP were performed and measured. The following data was obtained:

SMOW	SLAP	GISP
-26.807	-430.142	-197.710
-24.724	-427.033	-200.486
-19.349	-430.651	-201.787
* 0.000	* -423.500	* -190.000

On 9-19-91, the mass spectrometer was prepared for analysis of hydrogen gases using gas standards. The following calibration data was obtained:

hd-1	hd-2	hd-3
-53.219	-109.767	-232.823
* -53.167	* -110.991	* -229.015

(*) indicates accepted values

the regression equation for the gas standards is as follows:

$$Y=.975856*X-2.30685$$

Putting the data from 9-18-91 into the above equation yields the following data:

SMOW measured/corrected	SLAP measured/corrected	GISP measured/corrected
-26.80/-28.47	-430.14/-422.06	-197.71/-195.24
-24.72/-26.43	-427.03/-419.03	-200.48/-197.95
-19.34/-21.19	-430.65/-422.56	-201.78/-199.22
* 0.00	* -423.50	* -190.00

By plotting the corrected data for 9-19-91 against the accepted values for SMOW, SLAP and GISP, the resulting linear regression yields the following correction equation for 9-19-91

$$Y=.975856*X-2.30685$$

APPENDIX IV

TESTING OF CO_2/H_2O EQUILIBRATION PROCEDURE

The testing of CO_2/H_2O equilibration procedures for small volumes of water discovered previously undiscussed problems. After processing PPR1, PPR2 and parts of PPR3 the data shows unexpected shifts and scatter in $\delta^{18}O$ compositions. After reviewing the laboratory log books, a relationship between the volume of water available for equilibration and the time required to reach equilibrium was hypothesized. Experiments were designed to (1) test the hypothesis and (2) possibly develop a correction factor for the data.

Samples were processed ranging from 0.25 ml to 2.0 ml and varying the equilibration time, reaction vessel volume, shaking speed. The procedure for equilibrating water and carbon dioxide follows Roether (1970). Test 1 and 2 used an in lab standard called Standard Distilled Water (SDW, $\delta^{18}O$= -9.366‰) and a CO_2 gas with a known isotope composition ($\delta^{18}O$= -14.212‰). In an effort to increase the efficiency of our laboratory procedures a modified CO_2/H_2O equilibration procedure developed by Socki et al. (1989) was tested using small volumes of water (Test 3). This procedure proved reliable, reduced the expenditure for materials and increased our daily production.

Test 1

Standard reaction vessels
Two hours of equilibration
300 cycles per minute (cpm)
Variable volumes of water

Volume (ml)	$\delta^{18}O$ (‰)
$CO_{2(unequilibrated)}$	-14.21
0.5	-11.35
0.5	-11.57
0.5	-11.37
0.5	-11.64
1.0	-10.58
1.0	-10.53
1.0	-10.47
1.0	-10.57
2.0	- 9.53
2.0	- 9.35

The data shows a well defined curvelinear approach to the known value for SDW (Figure IV-1). The duplicate points exhibit excellent reproducibility and show the optimum time for equilibration of 2.0 ml of water at 300 cpm to be 2.0 hours

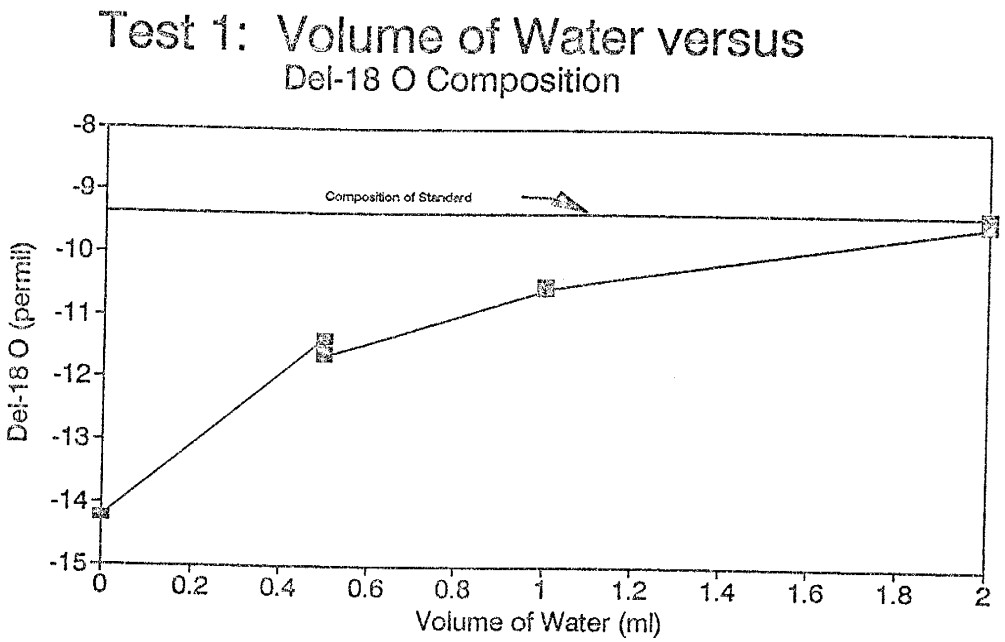

Figure IV-1: Data from equilibrium test 1

Test 2 This testing section actually four sub-sections.

- Test 2(a)
  Standard reaction vessels
  0.5ml of water,
  300 cpm.
  Variable equilibration time (1-5 hr/ 1 hr increments)

Equilibration Time (hour)	$\delta^{18}O$ (‰)
1.0	-13.46
2.0	-13.24
3.0	-11.78
4.0	-11.10
5.0	-10.47

The data for 2(a) shows a very well defined trend (Figure 38). The trend has a moderate, positive slope and all data falls within a reasonable range defining the trend. It may also be noticed that the $\delta^{18}O$ value of the data is approaching the SDW value but never quite reaches it.

- Test 2(b)
  Standard reaction vessels
  1.0 ml of water
  300 cpm
  Variable equilibration (0.5-3.0 hr)

Equilibration Time (hour)	$\delta^{18}O$ (‰)
0.5	-12.87
1.5	-11.40
2.5	-11.11
3.0	- 9.84

2(b) reinforces the conclusions in 2(a), however the change of volume results in a curve which has a more positive slope than 2(a) indicating that 1.0 ml will equilibrate faster than 0.5 mL assuming all other variables are held constant (Figure 38).

- Test 2(c)
  Standard reaction vessels
  1.0 ml of water
  No shaking
  Variable equilibration time

Equilibration time (hour)	$\delta^{18}O$ (‰)
0.00	-14.21
0.75	-13.94
3.00	-14.04

The data from 2(c) shows almost no equilibration with time (Figure 38). The vessels were allowed to set undisturbed. The points which were obtained showed us that shaking is indeed a very important portion of the procedure. It is important to note that the values vary from the known gas value of -14.212 ‰by only 0.27 ‰.

- Test 2(d)
  Hydrogen reaction vessels (small volume)
  0.25 ml of water
  310-320 cpm
  Variable equilibration time (4-7 hr/ 1 hr increments)

Equilibration time (hour)	$\delta^{18}O$ (‰)
4.0	- 9.21
5.0	- 9.11
6.0	- 8.97
7.0	- 9.10

Data from 2(d) shows a faster equilibration time than would be expected if the only variable changed was the volume of water (Figure IV-2). It appears, the time required for equilibration is strongly related to the shaking of the samples, as is evidenced by 2(c) as well. As the samples get smaller, the surface tension is not broken as easily and the effect of the shaking is decreased. By changing the size of the vessel, the area in which the sample was able to move around was reduced and the result was the physical overlapping of the sample thus breaking the surface tensionand increasing the kinetic energy of the system.

The increased shaking speed also affects the kinetic energy of the system. Since an increase in speed results in a rise in the kinetic energy, the surface tension is reduced and equilibrium is more rapidly facilitated. The fact that it reached equilibrium is evidenced by the slope of a line defined by the $\delta^{18}O$ values being almost equal to zero (Figure IV-2). The problem with the values come from their relative position on the graph. They all plot heavier than expected. This is probably due to evaporation of the standard. It was discovered improperly sealed prior to test 2(d).

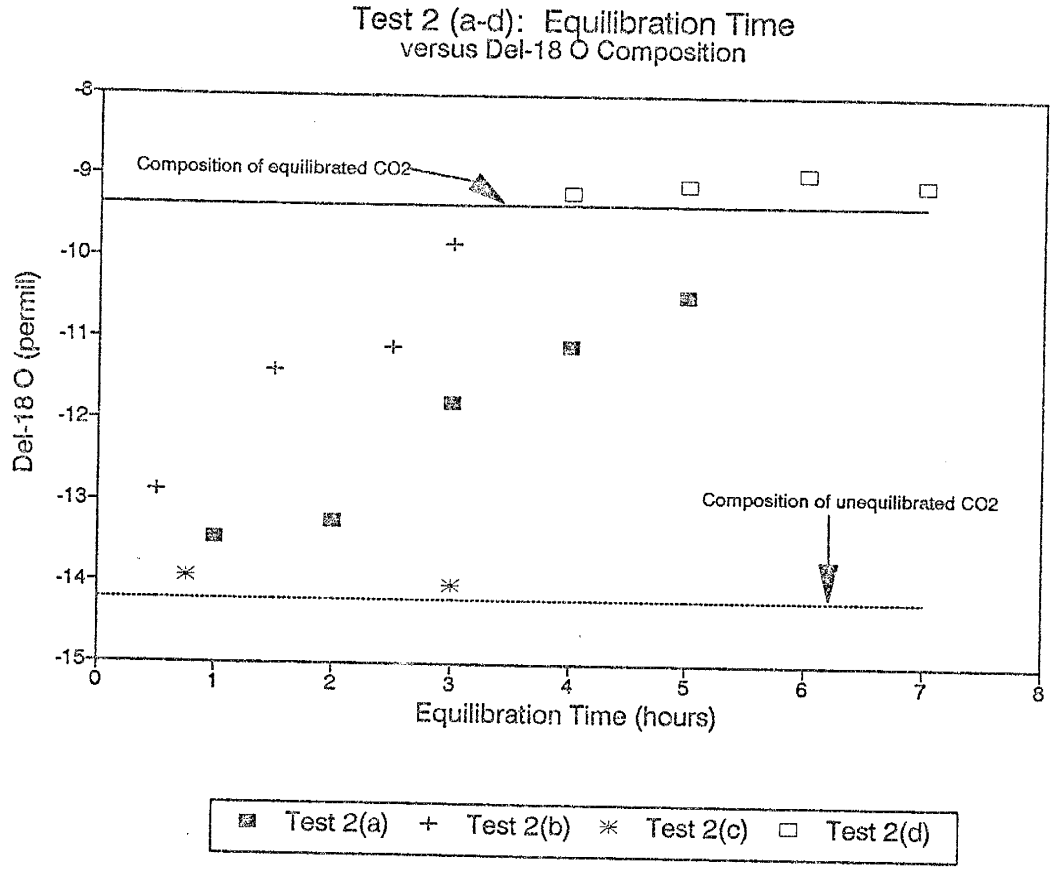

Figure IV-2: Data from equilibration test 2

TEST 3 The method developed by Socki et al. (1989) was tested using an in laboratory standard, Socorro Late October Precipitation (SLOP). The experiment was run under the following conditions:

10 ml *Vacutainer*™ reaction vessels
0.5 ml of water
300 cpm
Variable equilibration time (30-420 min)

Equilibration time (min)	$\delta^{18}O$ (‰)
30	- 5.965
60	- 3.995
120	- 1.739
150	- 1.083
180	- 0.964
240	- 0.765
270	- 0.631
300	- 0.619
360	- 0.702
420	- 0.693

Our testing showed equilibrium is obtained at 240 min. PPR4, PPR5, PPR5b and PPR6 were processed using this method (Figure IV-3).

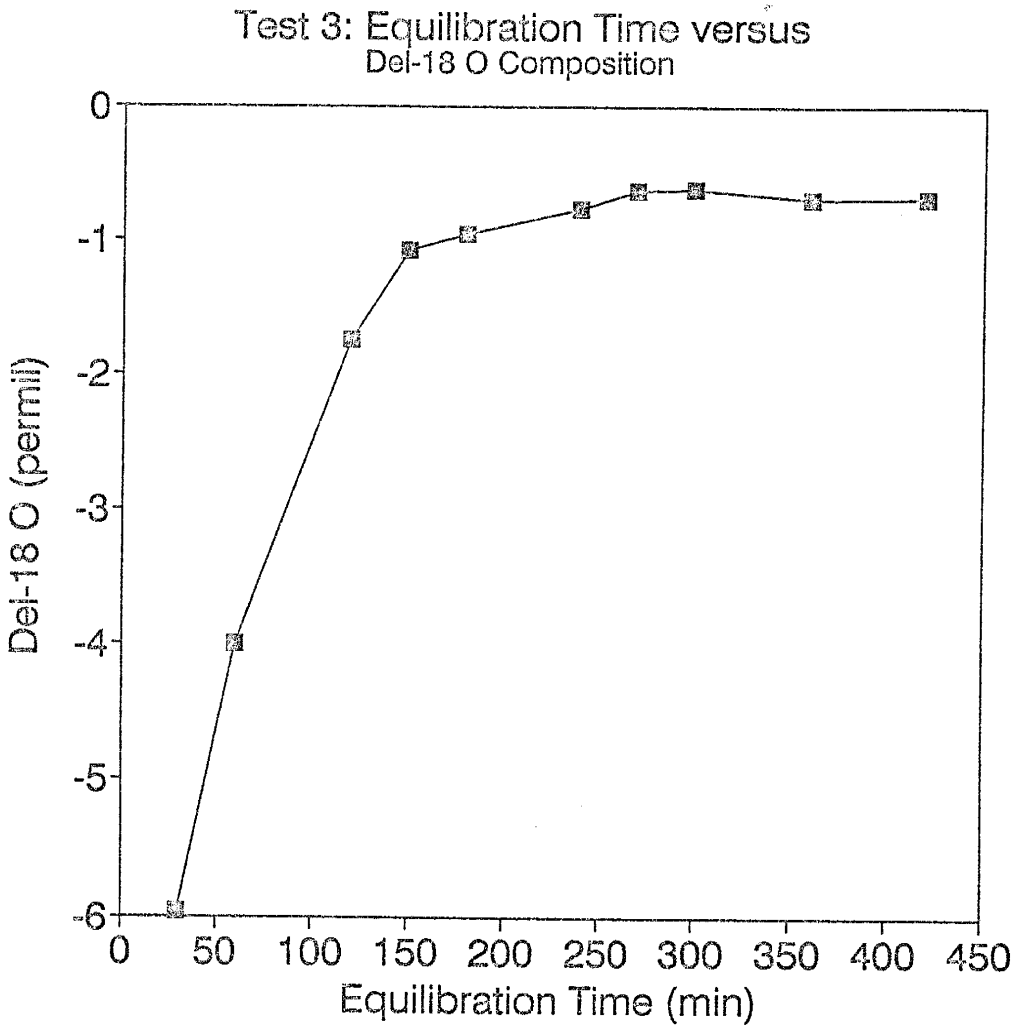

Figure IV-3: Data from equilibration test 3

CONCLUSIONS

It was determined that several factors affect the equilibration of the samples. Among these are, volume of sample, volume of reaction vessel, equilibration time and shaking speed.

Generally, the larger the sample volume, the faster equilibration will take place as evidenced by tests 2(a) and 2(b). One way to decrease the equilibration time is to increase the shaking speed as shown in test 2(d). The time scale which we used to conduct test 2(c) was too short to allow complete equilibration.

The method developed by Socki et al. (1989) seems to work very well. This method reduces the overall cost of processing by increasing the daily production of samples from a maximum of 18 to 36+ and by reducing the quantity of costly materials ($N_{2(l)}$, $CO_{2(s)}$, alcohol etc.) per sample. This method was used to process PPR4, PPR5, PPR5b and PPR6.

CORRECTIONS TO DATA

Samples for which less than 1 ml of water was available for equilibration can be divided into two groups. For the first group had only 1 ml pipettes available. Therefore, all we noted was that less than 1 ml was run. Later we obtained an adjustable automatic pipet, with this we could measure one half ml easily. For this second group we feel that a correction factor can be applied from figure X. Although the corrected values should not be considered as accurate as a good equilibration, it at least allows better interpretation of the data. The samples which were corrected will eventually be reanalyzed with the new procedures to obtain a more trustworthy analysis.

APPENDIX V
DATA FOR PPR SERIES

HEADER DEFINITIONS FOR PPR1

$\delta D(‰)$	=	Isotopic composition of water with respect to H^2/H^1 ratio
$\delta^{18}O(‰)$	=	Isotopic composition of water with respect to O^{18}/O^{16} ratio
$\delta^{18}O$ (‰)	=	isotopic composition corrected for laboratory error
d_i(cm)	=	depth intervals
θ	=	volumetric water content
$\theta * d_i$	=	contribution of water per depth interval
[Cl] (mg/kg)	=	chloride concentration by mass
[Cl] mg/cm^2	=	chloride concentration per unit area

DATA FROM PPR1

Depth (cm)	δD (‰)	$\delta^{18}O$ (‰)	d_i (cm)	θ	θ * d_i	[Cl] (mg/kg)	[Cl] mg/cm²	Cumulative				
								Time (years)	Time (years)	θ	[Cl] mg/kg	[Cl] mg/cm²
2.54	-100		5.08	0.006	0.032	5.00	0.035	3	3	0.03	5.0	0.035
7.62	2		5.08	0.007	0.036	5.00	0.035	3	6	0.07	10.0	0.071
12.70	18		5.08	0.007	0.033	5.00	0.035	3	9	0.10	15.0	0.106
17.78	19		5.08	0.009	0.044	4.50	0.032	3	11	0.15	19.5	0.138
22.86	3		5.08	0.013	0.064	4.00	0.028	2	14	0.21	23.5	0.166
27.94	-14		5.08	0.018	0.089	4.00	0.028	2	16	0.30	27.5	0.194
33.02	-17		5.08	0.016	0.081	5.00	0.035	3	19	0.38	32.5	0.229
38.10	-19	-2.99	5.08	0.018	0.092	10.00	0.071	6	25	0.47	42.5	0.300
43.18	-21	2.35	5.08	0.015	0.076	8.00	0.056	5	30	0.05	50.5	0.357
48.26	-26	-4.43	5.08	0.017	0.087	8.00	0.056	5	34	0.63	58.5	0.413
53.34	-28	1.37	5.08	0.014	0.071	5.00	0.035	3	37	0.70	63.5	0.448
58.42	-34	-5.98	5.08	0.013	0.067	4.00	0.028	2	40	0.77	67.5	0.477
63.50	-33	0.88	5.08	0.016	0.080	9.00	0.064	5	45	0.85	76.5	0.540
68.58	-28	-4.39	5.08	0.013	0.064	9.00	0.064	5	50	0.92	85.5	0.604
73.66	-24	0.99	5.08	0.007	0.038	8.00	0.056	5	55	0.95	93.5	0.660
81.28	-27	-6.52	10.16	0.008	0.077	8.00	0.113	9	64	1.03	101.5	0.773
91.44	-29	0.28	10.16	0.009	0.092	4.00	0.056	5	69	1.12	105.5	0.830
101.60	-37		10.16	0.010	0.103	8.00	0.113	9	79	1.23	113.5	0.943

Depth (cm)	δD (‰)	$\delta^{18}O$ (‰)	d_i (cm)	θ	θ * d_i	[Cl] (mg/kg)	[Cl] mg/cm²	Cumulative				
								Time (years)	Time (years)	θ	[Cl] mg/kg	[Cl] mg/cm²
110.49	-30	0.78	7.62	0.010	0.074	11.00	0.117	10	88	1.30	124.5	1.059
118.11	-34	-3.74	7.62	0.018	0.133	12.00	0.127	11	99	1.43	136.5	1.186
127.00	-31	-0.11	10.16	0.011	0.109	9.00	0.127	11	109	1.54	145.5	1.313
135.89	-29	-4.52	7.62	0.014	0.104	11.00	0.117	10	119	1.64	156.5	1.430
144.78	-32	-0.81	10.16	0.012	0.122	8.00	0.113	9	129	1.77	164.5	1.543
154.94	-40	-5.56	10.16	0.014	0.137	14.00	0.198	16	145	1.90	178.5	1.741
163.83	-33		7.62	0.016	0.125	8.00	0.085	7	152	2.03	186.5	1.825
172.72	-43	-6.45	10.16	0.013	0.133	5.00	0.071	6	158	2.16	191.5	1.896
181.61	-39		7.62	0.014	0.104	9.00	0.095	8	166	2.27	200.5	1.991
190.50	-35	-4.08	10.16	0.016	0.167	18.00	0.254	21	187	2.43	218.5	2.245
198.12	-37	-8.44	5.08	0.014	0.071	7.00	0.049	4	191	2.50	225.5	2.295
205.74	-36		10.16	0.014	0.140	9.00	0.127	11	202	2.64	234.5	2.422
215.90	-39		10.16	0.015	0.154	16.00	0.226	19	221	2.80	250.5	2.648
226.06	-38	-5.45	10.16	0.016	0.159	17.00	0.240	20	241	2.96	267.5	2.888
234.95	-39	-9.03	7.62	0.014	0.109	12.00	0.127	11	251	3.07	279.5	3.015
243.84	-37	-3.73	10.16	0.015	0.147	10.00	0.141	12	263	3.21	289.5	3.156
254.00	-34	-9.24	10.16	0.015	0.149	7.00	0.099	8	271	3.36	296.5	3.255
264.16	-40	-5.74	10.16	0.015	0.149	8.00	0.113	9	281	3.51	304.5	3.368
274.32	-35	-6.87	10.16	0.017	0.175	7.00	0.099	8	289	3.69	311.5	3.467

Depth (cm)	δD (‰)	$\delta^{18}O$ (‰)	d_i (cm)	θ	θ * d_i	[Cl] (mg/kg)	[Cl] mg/cm²	Cumulative				
								Time (years)	Time (years)	θ	[Cl] mg/kg	[Cl] mg/cm²
284.48	-39	-3.60	10.16	0.018	0.185	8.00	0.113	9	298	3.87	319.5	3.580
294.64	-40	-7.25	10.16	0.022	0.220	7.00	0.099	8	307	4.09	326.5	3.679
306.07	-43	-5.98	12.7	0.023	0.290	3.00	0.053	4	211	4.38	329.5	3.732
317.50	-35	-6.30	10.16	0.019	0.189	3.00	0.042	4	315	4.57	332.5	3.774
326.39	-44	-5.34	7.62	0.015	0.114	3.00	0.032	3	317	4.68	335.5	3.806
365.55	-43		12.7	0.015	0.196	7.00	0.124	10	327	4.88	342.5	3.930
347.98	-40		10.16	0.018	0.181	9.00	0.127	11	338	5.06	351.5	4.057
355.60	-43		5.08	0.049	0.247	10.00	0.071	6	344	5.31	361.5	4.127
361.95	-47	-7.45	7.62	0.097	0.742	12.00	0.127	11	355	6.05	373.5	4.254
368.30	-45	-7.42	5.08	0.081	0.410	12.00	0.085	7	362	6.46	385.5	4.339
374.65	-41	-7.74	7.62	0.011	0.083	10.00	0.106	9	370	6.54	395.5	4.445
382.27	-44		7.62	0.079	0.598	16.00	0.169	14	385	7.14	411.5	4.614
388.62	-43	-4.43	5.08	0.074	0.375	14.00	0.099	8	393	7.52	425.5	4.713
394.97	-43	-8.38	7.62	0.080	0.612	12.00	0.127	11	403	7.13	437.5	4.840
401.32	-52	-7.87	5.08	0.084	0.427	10.00	0.071	6	409	8.56	447.5	4.911

PPR1 DEPTH VERSUS $\delta^{18}O$
CORRECTED FOR SMALL VOLUME OF WATER USED DURING EQUILIBRATION - SEE APPENDIX VI

Depth (cm)	Corrected $\delta^{18}O$ (‰)
38.10	-0.99
43.18	2.35
48.26	-2.43
53.34	1.37
58.42	-3.98
63.50	0.88
68.58	-2.39
73.66	0.99
81.28	-4.52
91.44	0.28
110.49	0.78
118.11	-1.74
127.00	-0.11
135.89	-2.52
144.78	-0.81
154.94	-3.56
172.72	-4.45
190.50	-2.08
198.12	-6.44
226.06	-3.45
243.84	-3.73
264.16	-3.74
274.32	-4.87
284.48	-3.60
306.07	-3.98
317.50	-4.30
326.39	-3.34
361.95	-5.45
368.30	-5.42
374.65	-5.74
388.62	-2.43
394.97	-6.38
401.32	-5.87

HEADER DEFINITIONS FOR PPR2

$\delta^{18}O$(‰)	=	Isotopic composition of water with respect to O^{18}/O^{16} ratio
d_i(cm)	=	depth intervals
θ	=	volumetric water content
$\theta * d_i$	=	contribution of water per depth interval
[Cl] (mg/kg)	=	chloride concentration by mass
[Cl] mg/cm^2	=	chloride concentration per unit area
[Cl] (mg/L)	=	chloride concentration unit volume
δD_m (‰)	=	δD measured from mass spectometer
δD_c (‰)	=	δD corrected using daily correction equation

DATA FOR PPR2

Depth (cm)	d_i	θ	θ * d_i	[Cl] (mg/L)	[Cl] (mg/kg)	Time (years)	Cumulative		
							Time (years)	θ * d_i	[Cl] mg/cm²
2.54	5.08	0.004	0.020	2352	6.60	4	4	0.020	0.05
7.62	5.08	0.004	0.018	1390	3.60	2	6	0.038	0.07
12.70	5.08	0.005	0.025	1807	6.50	4	10	0.064	0.12
17.78	5.08	0.083	0.422	295	17.60	10	20	0.485	0.24
22.86	5.08	0.011	0.056	1516	12.00	7	27	0.541	0.33
27.94	5.08	0.013	0.064	1820	16.50	10	37	0.605	0.44
33.02	5.08	0.013	0.064	1657	14.90	9	46	0.669	0.55
38.10	5.08	0.013	0.068	1777	17.00	10	56	0.736	0.67
43.18	5.08	0.013	0.064	2135	19.20	11	67	0.800	0.80
48.26	5.08	0.013	0.066	3567	33.10	19	87	0.865	1.04
53.34	5.08	0.010	0.049	559	3.90	2	89	0.914	1.07
58.42	5.08	0.010	0.050	632	4.50	3	91	0.965	1.10
63.50	5.08	0.010	0.049	652	4.50	3	94	1.013	1.13
68.58	5.08	0.008	0.042	1022	6.10	4	98	1.056	1.17
73.66	5.08	0.010	0.049	1218	8.50	5	103	1.105	1.23
78.74	5.08	0.009	0.045	2077	13.30	8	111	1.150	1.33
83.82	5.08	0.009	0.047	3112	20.60	12	123	1.197	1.47
92.71	12.70	0.009	0.118	1569	10.50	15	138	1.315	1.66

Depth (cm)	d_i	θ	$\theta * d_i$	[Cl] (mg/L)	[Cl] (mg/kg)	Time (years)	Cumulative		
							Time (years)	$\theta * d_i$	[Cl] mg/cm^2
104.14	10.16	0.009	0.091	896	5.80	7	145	1.406	1.74
111.76	5.08	0.010	0.049	2207	15.40	9	154	1.456	1.85
119.38	10.16	0.010	0.097	936	6.40	8	162	1.552	1.94
129.54	10.16	0.010	0.106	1096	8.20	10	171	1.658	2.05
139.70	10.16	0.011	0.114	2333	18.80	22	193	1.772	2.32
149.86	10.16	0.011	0.116	1512	12.40	15	208	1.887	2.49
160.02	10.16	0.012	0.124	1572	13.80	16	224	2.011	2.69
168.91	7.62	0.012	0.091	3927	33.90	30	254	2.103	3.05
177.80	10.16	0.013	0.133	2016	19.00	22	276	2.236	3.32
186.69	7.62	0.013	0.101	1822	17.30	15	292	2.337	3.50
195.58	10.16	0.014	0.138	1318	12.90	15	307	2.475	3.68
204.47	7.62	0.013	0.098	754	7.00	6	313	2.573	3.76

DEPTH VERSUS δD AND $\delta^{18}O$ FOR PPR2

Depth (cm)	δD_m (‰)	δD_c (‰)	$\delta^{18}O$ (‰)
2.54			7.14
7.62	-40		9.68
12.7	-5		16.73
17.78	1		16.13
22.86	8		11.33
27.94	1		7.66
33.02	-7		5.35
38.1	-13		2.57
43.18	-24		2.13
48.26	-24		1.46
53.34	-46		1
58.42	-59		-0.75
63.5	-49		0.49
68.58	-53		0.05
73.66	-50		-1.75
78.74	-47		-0.63
83.82	-47		0.53
92.71	-42		-1.1
104.14	-47		
111.76	-40		1.61
119.38	-38		-1.79
129.54	-43		-1.4
139.7	-37		
149.86	-37		-2.42
160.02	-39		-2.55
168.91	-39		-1.41
177.8	-39		-2.89
186.69	-47		-2.87
195.58	-42		-2.24
204.47	-40		-3.28
212.09	-40	-52	-1.04
240.03	-44	-56	
259.08	-45	-56	
304.8	-43	-55	-2.703
351.79	-40	-52	-2.264
364.49	-45	-56	2.706

HEADER DEFINITIONS FOR PPR3

$\delta D(‰)$	=	Isotopic composition of water with respect to H^2/H^1 ratio
$\delta^{18}O(‰)$	=	Isotopic composition of water with respect to O^{16}/O^{18} ratio
$d_i(cm)$	=	depth intervals
θ	=	volumetric water content
[Cl] (mg/kg)	=	chloride concentration by mass
[Cl] mg/cm^2	=	chloride concentration per unit area

DEPTH VERSUS δD, $\delta^{18}O$, AND CHLORIDE CONCENTRATIONS FOR PPR3

Depth (cm)	δD	$\delta^{18}O$ ‰	d_i	θ	[Cl] (mg/kg)	Time (years)	[Cl] (mg/cm^2)	Cumulative Time (years)	Cumulative [Cl] (mg/cm^2)	Cumulative θ
2.54	-68		5.08	0.018	6.00	4	0.04	4	0.04	0.018
7.62	-54	-4.48	5.08	0.011	4.40	3	0.03	6	0.07	0.028
12.70	-33	7.11	5.08	0.007	2.40	1	0.02	8	0.09	0.035
17.78	-22	10.96	5.08	0.007	3.80	2	0.03	10	0.12	0.043
22.86	-16	13.31	5.08	0.007	1.60	1	0.01	11	0.13	0.050
27.94	-8		5.08	0.008	1.70	1	0.01	12	0.14	0.057
33.02	-10	13.36	5.08	0.096	3.20	2	0.02	14	0.16	0.153
38.10	-9	3.88	5.08	0.013	2.50	1	0.02	15	0.18	0.166
43.18	-13	2.68	5.08	0.025	1.90	1	0.01	16	0.19	0.192
48.26	-17	3.25	5.08	0.033	13.70	8	0.10	24	0.29	0.225
53.34	-34	0.54	5.08	0.029	8.70	5	0.06	29	0.35	0.253
58.24	-28	-1.28	5.08	0.019	7.60	4	0.05	34	0.41	0.273
63.50	-43	-1.16	5.08	0.018	12.40	7	0.09	41	0.49	0.291
68.58	-36	-2.03	5.08	0.018	10.50	6	0.07	47	0.57	0.309
73.66	-35	-3.17	5.08	0.017	8.80	5	0.06	52	0.63	0.326
83.82	-40	-3.47	15.24	0.018	17.90	32	0.38	84	1.01	0.344
97.79	-40	-3.56	12.70	0.019	13.80	20	0.24	104	1.25	0.363

Depth (cm)	δD	$\delta^{18}O$ ‰	d_i	θ	[Cl] (mg/kg)	Time (years)	[Cl] (mg/cm^2)	Cumulative		
								Time (years)	[Cl] (mg/cm^2)	θ
107.95	-40	-4.97	8.62	0.020	11.70	10	0.12	115	1.38	0.383
116.84	-41	-4.58	10.16	0.020	21.40	25	0.30	139	1.68	0.402
125.73	-46	-5.12	7.62	0.019	16.60	15	0.18	155	1.85	0.421
133.35	-46	-5.21	7.62	0.019	16.60	15	0.18	169	2.03	0.440
142.24	-47	-4.15	10.16	0.020	29.80	35	0.42	204	2.45	0.460
151.13	-42	-5.23	7.62	0.019	18.00	16	0.19	220	2.64	0.479
161.29	-40	-6.84	12.70	0.019	30.10	44	0.53	264	3.17	0.498
170.18	-39	-1.37	5.08	0.019	14.30	8	0.10	273	3.27	0.517
176.53	-39	-6.30	7.62	0.020	19.20	17	0.20	290	3.48	0.538
185.42	-39	-4.89	10.16	0.020	18.40	22	0.26	311	3.74	0.558
194.31	-35	-4.02	7.62	0.022	34.40	30	0.36	342	4.10	0.580
201.93	-39	0.47	7.62	0.022	23.60	21	0.25	363	4.35	0.601
209.55	-47	-5.94	7.62	0.021	22.20	20	0.24	382	4.59	0.622
218.44	-44	-6.06	10.16	0.035	27.00	32	0.38	414	4.97	0.657
228.60	-47	-6.07	10.16	0.022	17.60	21	0.25	435	5.22	0.679
238.76	-47	-6.81	10.16	0.024	10.50	12	0.15	447	5.37	0.703
248.92	-46	-5.42	10.16	0.020	17.80	21	0.25	468	5.62	0.723
304.80	-47	-2.97	101.60	0.023	12.50	147	1.77	615	7.38	0.746
269.24	-41		10.16	0.022	9.40	11	0.13	626	7.51	0.768

Depth (cm)	δD	$\delta^{18}O$ ‰	d_i	θ	[Cl] (mg/kg)	Time (years)	[Cl] (mg/cm^2)	Cumulative		
								Time (years)	[Cl] (mg/cm^2)	θ
279.40	-33	-2.20	10.16	0.029	17.00	20	0.24	646	7.75	0.797
289.56	-40	-2.69	10.16	0.027	8.60	10	0.12	656	7.88	0.824
299.72	-34	-2.69	10.16	0.030	8.00	9	0.11	666	7.99	0.854
309.88	-39	-2.69	10.16	0.029	14.70	17	0.21	683	8.20	0.883
318.77	-35	-6.54	7.62	0.031	7.80	7	0.08	690	8.28	0.915
328.93	-36	-6.73	12.70	0.032	6.90	10	0.12	700	8.40	0.946
339.09	-36	-6.49	7.62	0.032	5.40	5	0.06	705	8.46	0.978
349.25	-35	-6.78	12.70	0.033	3.20	5	0.06	710	8.51	1.011
360.68	-37	-7.01	10.16	0.032	2.30	3	0.03	712	8.55	1.042
370.84	-39	-6.18	10.16	0.036	7.00	8	0.10	721	8.65	1.078
381.00	-49	-7.73	10.16	0.034	3.80	4	0.05	725	8.70	1.112
391.16	-47	-7.44	10.16	0.037	3.20	4	0.05	729	8.74	1.149
401.32	-50	-7.82	10.16	0.034	9.10	11	0.13	739	8.87	1.182
411.48	-47	-7.66	10.16	0.034	5.20	6	0.07	746	8.95	1.216
421.64	-43	-9.37	10.16	0.033	4.60	5	0.06	751	9.01	1.249
431.80	-42	-7.03	10.16	0.035	8.50	10	0.12	761	9.13	1.284
443.23	-42	-7.06	12.70	0.034	6.00	9	0.11	770	9.24	1.317
453.39	-41	-7.28	7.62	0.033	4.10	4	0.04	773	9.28	1.350
463.55	-45	-6.61	12.70	0.033	4.10	6	0.07	779	9.35	1.383

Depth (cm)	δD	$\delta^{18}O$ ‰	d_i	θ	[Cl] (mg/kg)	Time (years)	[Cl] (mg/cm^2)	Cumulative		
								Time (years)	[Cl] (mg/cm^2)	θ
473.71	-43	-6.99	7.62	0.032	2.60	2	0.03	782	9.38	1.415
482.60	-39	-7.11	10.16	0.045	2.20	3	0.03	784	9.41	1.460
492.76	-39	-8.29	10.16	0.032	5.20	6	0.07	790	9.49	1.492
502.92	-41	-7.29	10.16	0.029	6.30	7	0.09	798	9.57	1.521
511.81	-53	-7.98	7.62	0.037	2.80	2	0.03	800	9.60	1.558
520.70	-52	-7.96	10.16	0.045	3.50	4	0.05	804	9.65	1.603
530.86	-45	-7.11	10.16	0.040	3.70	4	0.05	809	9.71	1.643
539.75	-46	-8.57	7.62	0.044	3.80	3	0.04	812	9.75	1.687
547.37	-49	-13.24	7.62	0.045	8.60	8	0.09	820	9.84	1.732
556.26	-58	-8.11	10.16	0.049	5.30	6	0.07	826	9.91	1.780
566.42	-48	-8.80	10.16	0.045	5.50	6	0.08	832	9.99	1.825
576.58	-48		10.16	0.080	5.40	6	0.08	839	10.07	1.905
585.47	-47	-8.95	7.62	0.057	12.50	11	0.13	850	10.20	1.962

HEADER DEFINITIONS FOR PPR4

$\delta D(‰)$	=	Isotopic composition of water with respect to hydrogen/denterium ratio
$\delta^{18}O(‰)$	=	Isotopic composition of water with respect to hydrogen/denterium ratio
$d_i(cm)$	=	depth intervals
θ	=	volumetric water content
$\theta * d_i$	=	contributions of water per a depth interval
[Cl] (mg/kg)	=	chloride concentration by mass
[Cl] (mg/cm^2)	=	chloride concentration per unit area
[Cl] (mg/L)	=	chloride concentration per unit volume
$\delta^{18}O$ (‰)	=	isotopic composition corrected for laboratory error
δD_r (‰)	=	δD composition rerun
δD_{rc} (‰)	=	δD composition rerun, corrected using daily correction equation
δD_m (‰)	=	δD composition measured on mass spectrometer
δD_c (‰)	=	δD composition corrected using daily correction equation

DATA FOR PPR4

Depth (cm)	d_i	θ	$\theta * d_i$	[Cl] (mg/L)	[Cl] (mg/kg)	Time (years)	Cumulative		
							Time (years)	θ	[Cl] (mg/cm²)
2.50	5.00	0.03	0.13	762	13.70	8	8	0.13	0.10
6.50	3.00	0.02	0.07	708	11.00	4	12	0.19	0.14
9.00	2.00	0.04	0.08	543	14.60	3	15	0.27	0.18
11.50	3.00	0.05	0.14	656	21.30	7	23	0.40	0.27
15.50	5.00	0.06	0.30	697	29.70	17	40	0.70	0.48
19.00	2.00	0.07	0.15	965	51.10	12	52	0.84	0.62
22.00	4.00	0.11	0.45	681	55.60	26	77	1.30	0.93
27.00	6.00	0.11	0.67	626	50.30	35	112	1.97	1.35
30.75	1.50	0.10	0.15	557	40.00	7	119	2.12	1.43
33.25	3.50	0.09	0.31	419	26.90	11	130	2.43	1.56
38.25	5.00	0.07	0.35	538	27.00	16	146	2.78	1.75
47.50	12.00	0.06	0.72	526	22.70	32	177	3.50	2.13
59.00	11.00	0.04	0.46	872	26.10	33	211	3.96	2.53
69.50	10.00	0.06	0.56	630	25.40	29	240	4.52	2.88
79.00	9.00	0.06	0.51	962	38.90	41	281	5.02	3.37
87.50	8.00	0.05	0.41	935	34.10	32	312	5.43	3.75
96.00	9.00	0.05	0.44	739	26.00	27	339	5.87	4.07

Depth (cm)	d_i	θ	$\theta * d_i$	[Cl] (mg/L)	[Cl] (mg/kg)	Time (years)	Cumulative Time (years)	Cumulative θ	Cumulative [Cl] (mg/cm²)
104.50	8.00	0.05	0.36	762	24.40	23	362	6.22	4.34
112.50	8.00	0.04	0.33	589	17.50	16	378	6.55	4.54
120.00	7.00	0.04	0.30	455	13.80	11	389	6.85	4.67
130.00	12.00	0.04	0.46	478	13.30	19	408	7.31	4.89
142.00	11.00	0.04	0.40	381	10.00	13	421	7.71	5.05
148.50	2.00	0.04	0.09	370	11.40	3	423	7.80	5.08
155.50	12.00	0.04	0.52	375	11.70	16	439	8.32	5.27
167.00	11.00	0.05	0.51	239	8.00	10	450	8.83	5.40
178.50	12.00	0.04	0.46	255	7.00	10	459	9.29	5.51
207.25	12.00	0.03	0.33	258	5.10	7	466	9.62	5.60
220.00	13.00	0.03	0.35	292	5.70	9	475	9.97	5.70
232.25	11.50	0.05	0.52	166	5.40	7	482	10.49	5.79
243.00	10.00	0.04	0.41	152	4.50	5	487	10.90	5.85
253.50	11.00	0.05	0.50	173	5.70	7	495	11.41	5.94
264.50	11.00	0.05	0.50	120	3.90	5	500	11.90	6.00
276.00	12.00	0.05	0.57	114	3.90	5	505	12.47	6.06
287.00	10.00	0.05	0.51	123	4.50	5	510	12.98	6.12
298.50	13.00	0.04	0.51	169	4.80	7	518	13.49	6.21
310.50	11.00	0.03	0.31	209	4.20	5	523	13.80	6.27

Depth (cm)	d_i	θ	$\theta * d_i$	[Cl] (mg/L)	[Cl] (mg/kg)	Time (years)	Cumulative		
							Time (years)	θ	[Cl] (mg/cm^3)
321.50	11.00	0.03	0.31	179	3.60	5	528	14.11	6.33
333.50	13.00	0.03	0.44	141	3.45	5	533	14.55	6.39
345.00	10.00	0.03	0.34	136	3.30	4	537	14.89	6.44
355.00	10.00	0.03	0.29	187	3.90	5	514	15.18	6.49
365.00	10.00	0.05	0.48	130	4.50	5	546	15.66	6.55
377.00	14.00	0.03	0.42	164	3.55	6	552	16.08	6.62
389.00	10.00	0.04	0.44	115	3.60	4	556	16.52	6.67
397.00	14.00	0.02	0.31	259	4.10	7	563	16.83	6.75
415.00	6.00	0.02	0.11	337	4.60	3	566	16.94	6.79
421.50	7.00	0.02	0.13	417	5.40	4	570	17.07	6.84
438.50	9.00	0.04	0.33	237	6.20	7	577	17.39	6.92

DATA FOR PPR4

Depth (cm)	$\delta^{18}O$	δD_m (‰)	δD_c (‰)	δD_r (‰)	δD_{rc} (‰)
2.50	6.98	-61	-45	-55	-44
6.50	8.65	-45	-28	-44	-32
9.00	14.17	-36	-19	-30	-17
11.50	13.39	-33	-15	-35	-22
15.50	13.44	-35	-18	-34	-21
19.00	9.51	-41	-24	-35	-22
22.00	7.32	-45	-28		
27.00	5.51	-41	-24	-36	-24
30.75	5.00	-38	-21	-46	-34
33.25		-46	-29	-39	-27
38.25	4.45	-32	-14	-48	-36
47.50	3.24	-27	-9	-52	-40
59.00	2.04	-30	-13	-53	-41
69.50	1.82	-36	-18	-50	-38
79.00	0.87	-39	-22	-56	-44
87.50	1.41	-33	-15	-54	-42
96.00	0.38	-40	-23	-52	-40
104.50	0.07	-49	-33		-41
112.50	-0.47	-44	-27		-46
120.00	-0.15				-48
130.00		-48	-32		-49
142.00	-1.07	-47	-31		-45
148.50	-2.08	-90	-77		-41
155.50	-1.15	-50	-34		-49
167.00	-1.17	-52	-36	-53	-41
178.50	-1.16	-68	-53		-49
207.25	-1.57	-57	-41	-50	-38

Depth (cm)	$\delta^{18}O$	δD_m (‰)	δD_c (‰)	δD_r (‰)	δD_{rc} (‰)
220.00	-0.93	-64	-42		-44
232.25	-1.03	-61	-39	-50	-38
243.00	-1.42	-68	-47	-54	-42
253.50	-1.57	-66	-45		-43
264.50	-1.60	-66	-45	-57	-46
276.00	-1.63	-64	-42		-48
287.00	-1.47	-65	-43	-53	-41
298.50	-1.47	-76	-55		-42
310.50	-1.03			-54	-40
321.50	-1.67	-67	-46		-52
333.50	-1.76			-58	-47
345.00	-1.68	-69	-47		-46
355.00	-1.52				-50
365.00	-1.17	-64	-42	-53	-42
377.00	-1.61	-63	-41		-46
389.00	-1.51	-67	-45	-56	-45
397.00	-1.34	-69	-48		-47
415.00	-0.90	-69	-48		-46
421.50	-1.80	-56	-34		-57
438.50	-1.67			-55	-44

HEADER DEFINITIONS FOR PPRR5 AND PPR5b

$\delta D(‰)$	=	Isotopic composition of water with respect to H^2/H^1 ratio
$\delta^{18}O(‰)$	=	Isotopic composition of water with respect to O^{18}/O^{16} ratio
$d_i(cm)$	=	depth intervals
θ	=	volumetric water content
$\theta * d_i$	=	contribution of water per depth interval
[Cl] (mg/kg)	=	chloride concentration by mass
[Cl] mg/cm^2	=	chloride concentration per unit area
δD_c (‰)	=	δD composition corrected using daily correction equation
δD_r (‰)	=	δD composition rerun
δD_{rc} (‰)	=	δD composition rerun, corrected using daily correction equation

DATA FOR PPR5

Depth (cm)	d_i	θ	θ * d_i	[Cl] mg/L	[Cl] mg/kg	Time (years)	Cumulative		
							Time (years)	θ	[Cl] (mg/cm^2)
5.00	3.00	0.01	0.02	1364	5.30	2	2	0.02	0.02
8.00	3.00	0.01	0.02	1317	5.40	2	4	0.03	0.04
11.50	2.50	0.01	0.02	1431	7.00	2	6	0.05	0.07
15.75	3.50	0.01	0.03	1390	8.00	3	9	0.08	0.11
19.25	3.50	0.01	0.03	818	5.00	2	11	0.11	0.13
22.25	2.50	0.01	0.03	723	5.10	1	12	0.13	0.15
24.75	2.50	0.01	0.03	501	4.40	1	14	0.16	0.17
29.00	6.00	0.02	0.11	365	4.70	3	17	0.27	0.20
34.00	4.00	0.02	0.09	613	9.70	4	22	0.36	0.26
38.25	4.50	0.02	0.10	388	6.40	3	25	0.46	0.30
41.75	2.50	0.02	0.05	277	4.20	1	26	0.51	0.31
51.50	11.00	0.03	0.04	179	4.10	5	31	0.86	0.38
63.50	13.00	0.04	0.47	163	4.20	6	38	1.33	0.45
75.00	10.00	0.03	0.31	283	6.40	7	45	1.64	0.54
85.00	10.00	0.03	0.31	226	5.10	6	51	1.96	0.61
94.50	9.00	0.03	0.25	196	3.90	4	55	2.21	0.66
107.50	9.00	0.04	0.33	150	3.90	4	59	2.53	0.71

Depth (cm)	d_i	θ	θ * d_i	[Cl] mg/L	[Cl] mg/kg	Time (years)	Cumulative		
							Time (years)	θ	[Cl] (mg/cm^3)
114.50	5.00	0.04	0.19	122	3.30	2	61	2.72	0.73
117.50	1.00	0.09	0.09	49	3.00	0	61	2.81	0.74
119.00	2.00	0.10	0.20	71	5.10	1	63	3.01	0.75
124.00	8.00	0.12	0.94	67	5.70	5	68	3.95	0.81
132.00	8.00	0.14	1.08	40	3.90	4	71	5.03	0.86
141.00	10.00	0.14	1.44	47	4.90	6	77	6.47	0.93
150.50	9.00	0.14	1.23	46	4.50	5	82	7.70	0.98
157.50	5.00	0.15	0.75	48	5.10	3	85	8.45	1.02
164.00	8.00	0.13	1.02	90	8.30	8	92	9.47	1.11
172.50	9.00	0.13	1.15	89	8.20	9	101	10.61	1.21
180.50	7.00	0.12	0.84	72	6.20	5	106	11.45	1.27
187.00	6.00	0.13	0.76	46	4.20	3	109	12.21	1.31
194.50	9.00	0.21	1.85	47	7.00	7	116	14.06	1.39

DATA FOR PPR5

Depth (cm)	$\delta^{18}O$ (‰)	δD (‰)	δD_c (‰)	δD_r (‰)	δD_{rc} (‰)
5.00	-0.76	-70	-50		
8.00	3.66	-60	-39		
11.50	8.66	-53	-32		-31
15.75		-41	-19		
19.25	10.43	-39	-17		
22.25		-36	-14	-42	-15
24.75	8.65	-48	-26	-50	-24
29.00	0.46	-46	-24		
34.00	3.82	-42	-20	-63	-37
38.25	0.65	-59	-38		
41.75		-66	-45		
44.50		-62	-41		
51.50		-68	-48		
63.50	-3.30	-64	-43	-67	-42
75.00		-56	-35		
85.00	-2.64	-59	-38	-66	-40
94.50		-65	-45		
107.50	-2.91	-62	-41	-64	-39
114.50	-1.80	-61	-40		
117.50	-2.29	-61	-41	-62	-36
119.00		-53	-27	-60	-34
124.00	-1.91	-57	-32	-59	-33
132.00		-51	-26		
141.00	-2.59	-60	-35		-35
150.50		-61	-36		
157.50	-3.16	-72	-49	-76	-51
164.00		-57	-32		

Depth (cm)	$\delta^{18}O$ (‰)	δD (‰)	δD_c (‰)	δD_r (‰)	δD_{rc} (‰)
172.50	-3.21	-62	-38		-47
180.50		-58	-33		
187.00	-3.43	-65	-41		
194.50		-60	-36		

PPR5b DATA

Depth (cm)	θ	δD (‰)	δD_c (‰)	$\delta^{18}O$ (‰)	δD_r (‰)
5.00	0.005				
8.00	0.006	-65	-43	3.45	
11.50	0.007	-61	-38	8.93	
15.75	0.008	-47	-24	10.91	
19.25	0.009	-38	-14	11.00	
22.25	0.010	-39	-15	10.54	-24
24.75	0.012	-44	-20	9.70	-24
29.00	0.018	-56	-33	7.21	-35
34.00	0.022	-50	-27	2.41	-36
38.25	0.023	-54	-32	0.28	
41.75	0.021	-59	-37	0.89	-41
44.50	0.029	-61	-39	-2.06	-44
51.50	0.318	-62	-40	-2.97	-50
62.50	0.036	-57	-35	-3.50	-42
75.00	0.031	-64	-42	-3.01	-42
85.00	0.031	-59	-37	-2.98	-37
94.50	0.028	-83	-62	-3.33	
107.50	0.036	-45	-20	-2.90	-39
114.50	0.038	-50	-26	-2.65	
117.50	0.085	-64	-41	-1.99	-39
119.00	0.100	-51	-26	-1.88	-35
124.00	0.118	-68	-45	-2.36	-40
132.00	0.136	-67	-44	-2.59	
141.00	0.144	-49	-25	-2.93	-34
150.50	0.137	-54	-30	-3.02	-41
157.50	0.149	-52	-28	-2.81	-48
164.00	0.128	-52	-27	-2.86	

Depth (cm)	θ	δD (‰)	δD_c (‰)	$\delta^{18}O$ (‰)	δD_t (‰)
172.50	0.127	-56	-32	-2.86	
180.50	0.119	-53	-28	-3.26	-43
157.00	0.127	-61	-44	-3.38	
194.50	0.206	-66	-43	-3.13	

HEADER DEFINITIONS FOR PPRR6

$\delta D(‰)$	=	Isotopic composition of water with respect to H^2/H^1 ratio
$\delta^{18}O(‰)$	=	Isotopic composition of water with respect to O^{18}/O^{16} ratio
$d_i(cm)$	=	depth intervals
θ	=	volumetric water content
$\theta * d_i$	=	contribution of water per depth interval
[Cl] (mg/kg)	=	chloride concentration by mass
[Cl] mg/cm^2	=	chloride concentration per unit area
δD_c (‰)	=	δD composition corrected using daily correction equation
δD_r (‰)	=	δD composition rerun
δD_{rc} (‰)	=	δD composition rerun, corrected using daily correction equation

Depth (cm)	d_i (cm)	θ	$\theta * d_i$	[Cl] mg/L	[Cl] mg/kg	Time (years)	Cumulative		
							Time (years)	θ	Cl (mg/cm^2)
117.00	11.00	0.036	0.396	181	4.70	6	79	4.787	0.95
126.50	8.00	0.043	0.344	259	8.00	7	87	5.131	1.04
136.00	11.00	0.044	0.484	398	12.60	16	103	5.615	1.23
145.50	8.00	0.046	0.368	426	14.10	13	116	5.983	1.39
155.00	7.00	0.049	0.343	218	7.70	6	122	6.326	1.46
162.50	8.00	0.044	0.350	204	6.40	6	128	6.676	1.53
169.00	9.00	0.061	0.549	130	5.70	6	134	7.225	1.61
176.50	8.00	0.049	0.392	199	7.00	6	140	7.617	1.68
185.00	11.00	0.067	0.737	172	8.30	11	151	8.354	1.81
194.50	10.00	0.055	0.550	210	8.30	10	160	8.904	1.93

DATA FOR PPR6

Depth (cm)	$\delta^{18}O$	δD_m	δD_r	δD_c
2.50	0.86	-66		
7.50	2.09	-58		
10.00	10.49	-32	-40	-15
14.50	10.18	-39		
30.25	9.22	-39	-53	-29
36.50	6.82	-76	-53	-29
44.00	1.97	-50	-53	-30
51.00	0.96	-45	-52	-28
55.50	-2.02	-56	-62	-38
59.50	-2.02	-63	-71	-48
68.00	-2.09	-56		
73.50	-2.52	-57	-62	-39
78.00	-2.59	-59	-59	-35
82.00	-2.64	-62	-62	-39
92.50	-2.51	-69	-64	-41
99.50	-2.90	-75	-69	-46
108.50	-2.07	-72		
117.00	-3.56	-69		
126.50	-4.18	-73	-67	-45
136.00	-2.98	-63	-64	-41
145.50	-2.98	-66	-76	-54
155.00	-3.67	-62	-65	-42
162.50	-4.36	-68	-77	-54
169.00		-66	-61	-38
176.50	-3.24	-62	-70	-48
185.00		-55	-65	-42
194.50	-4.83	-56	-72	-50